STANFORD
AERONAUTICS & ASTRONAUTICS

A Universal Velocity Profile for Wall Bounded Flows

Open Access links to the relevant references at JFM and Physics of Fluids are on my website at https://web.stanford.edu/~cantwell/

Brian Cantwell
Stanford University
May 19, 2025

Turbulent boundary layer wall variables y^+ and u^+ and the friction Reynolds number R_τ

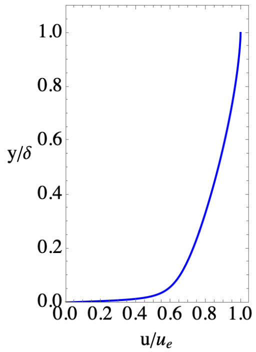

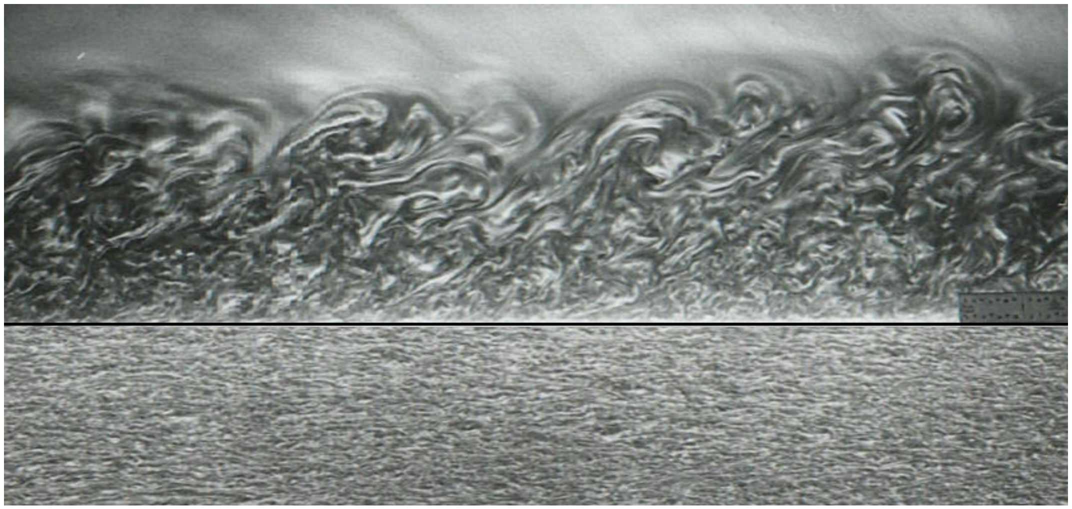

From: D. Chung and D.I. Pullin LES and wall modeling of turbulent channel flow. JFM vol 631, 2009 – Fig 2

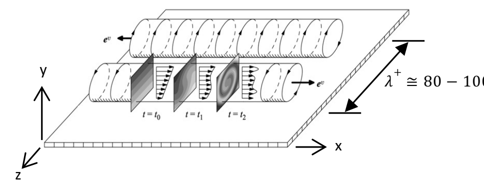

$$\tau_w = \mu \frac{\partial U}{\partial y}\bigg|_{y=0} \qquad u_\tau = \sqrt{\frac{\tau_w}{\rho}}$$

$$y^+ = \frac{y u_\tau}{\nu} \qquad u^+ = \frac{u}{u_\tau}$$

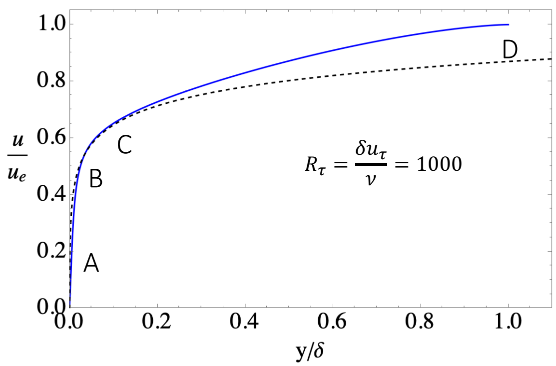

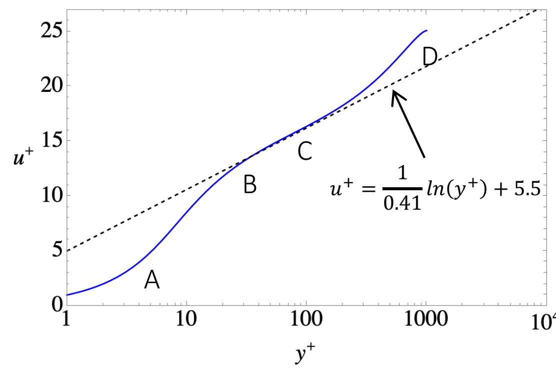

$$R_\tau = \frac{\delta u_\tau}{\nu} = \delta^+$$

$$\frac{y}{\delta} = \frac{y^+}{R_\tau}$$

Classical wall-wake formulation

Coles (1956) recommends
$W = 2\sin^2\left(\frac{\pi}{2}\frac{y}{\delta}\right)$
$\kappa = 0.41$, $C = 5.5$
for $dPe/dx = 0$, $\Pi = 0.62$

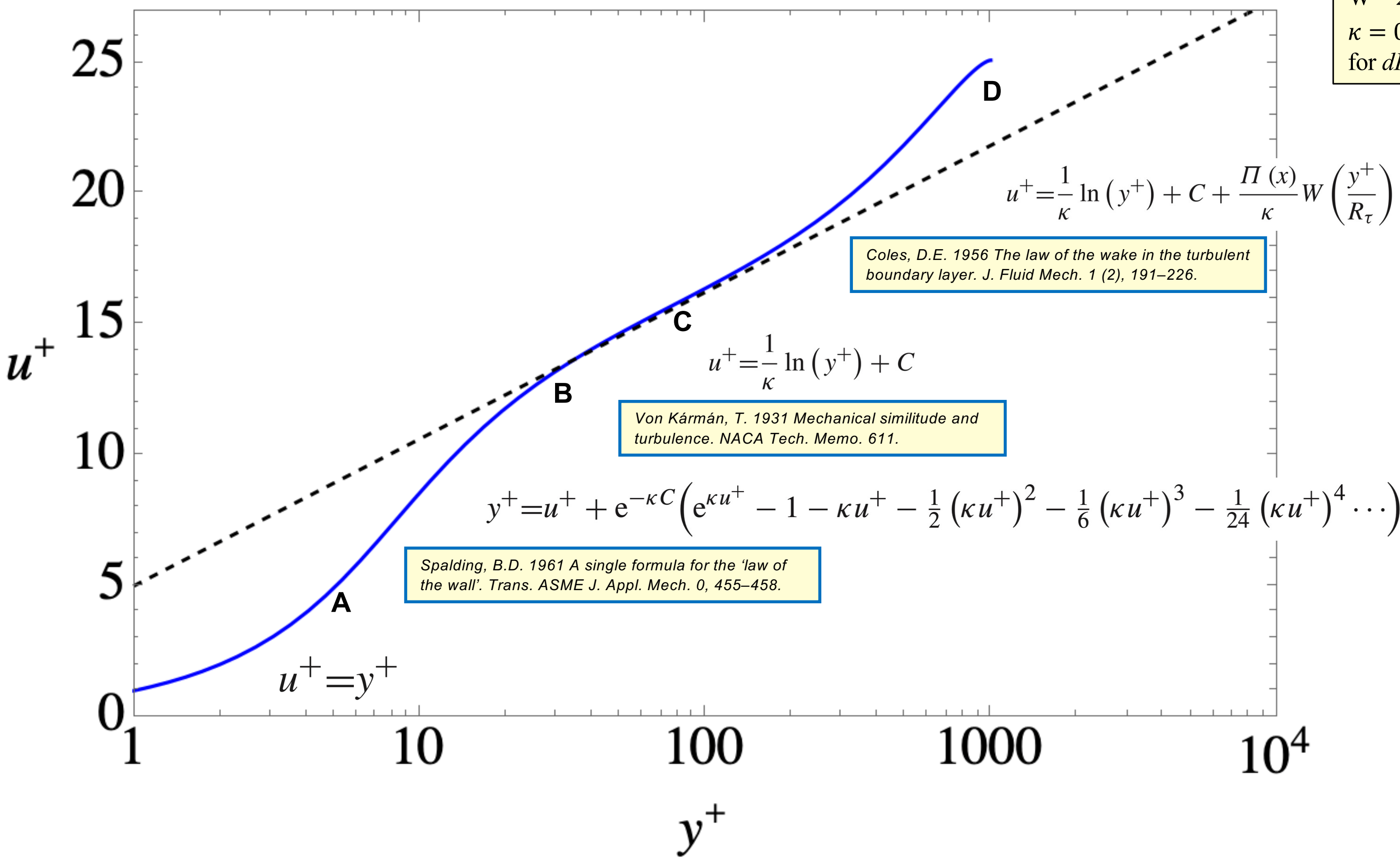

Pipe Flow – wall variables

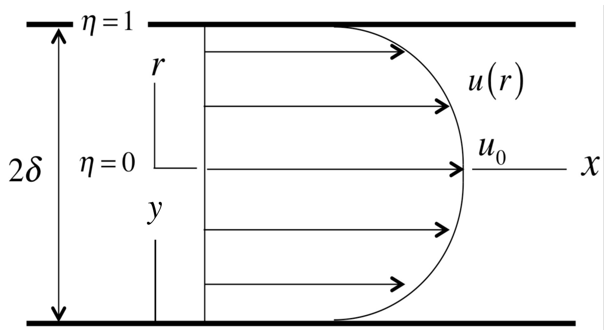

Laminar solution in wall variables

$$u^+_{laminar} = y^+\left(1 - \frac{y^+}{2R_\tau}\right)$$

$$C_{f_{laminar}} = \frac{8}{{R_\tau}^2}$$

$$u_\tau = \left(-\frac{\tau_w}{\rho}\right)^{1/2}$$

$$R_\tau = \frac{\delta u_\tau}{\nu}$$

Integrate the governing equation once and apply the centerline boundary condition *dU/dr = 0* at *r = 0*. Express the first order governing equation in terms of wall variables.

$$\tau^+ + \frac{du^+}{dy^+} - \left(1 - \frac{y^+}{R_\tau}\right) = 0$$

$$u^+ = \frac{u}{u_\tau} \qquad y^+ = \frac{y u_\tau}{\nu} \qquad \tau^+ = \frac{\overline{u'v'}}{u_\tau^2}$$

Note

$$\frac{u_0}{u_\tau} \equiv \frac{R_e}{R_\tau} \equiv \sqrt{\frac{2}{C_f}}$$

STANFORD AERONAUTICS & ASTRONAUTICS

Mixing length model for the turbulent shear stress

$$\tau^{+} = \left(\lambda(y^{+})\frac{\mathrm{d}u^{+}}{\mathrm{d}y^{+}}\right)^{2}$$

Prandtl 1934

The first order governing equation becomes a quadratic equation in the derivative of the mean velocity

$$\left(\frac{\mathrm{d}u^{+}}{\mathrm{d}y^{+}}\right)^{2} + \frac{1}{\lambda(y^{+})^{2}}\frac{\mathrm{d}u^{+}}{\mathrm{d}y^{+}} - \frac{1}{\lambda(y^{+})^{2}}\left(1-\frac{y^{+}}{R_{\tau}}\right) = 0$$

Take the positive root

$$\frac{\mathrm{d}u^{+}}{\mathrm{d}y^{+}} = -\frac{1}{2\lambda(y^{+})^{2}} + \frac{1}{2\lambda(y^{+})^{2}}\left(1+4\lambda(y^{+})^{2}\left(1-\frac{y^{+}}{R_{\tau}}\right)\right)^{1/2}$$

Remove the singularity at $\lambda = 0$

$$\frac{du^{+}}{dy^{+}} = \frac{2\left(1-\frac{y^{+}}{R_{\tau}}\right)}{1+\left(1+4\lambda\,(y^{+})^{2}\left(1-\frac{y^{+}}{R_{\tau}}\right)\right)^{1/2}}$$

STANFORD
AERONAUTICS & ASTRONAUTICS

Define a new mixing length function

$$\lambda(y^+) = \frac{k y^+ \left(1 - e^{-(y^+/a)^m}\right)}{\left(1 + \left(\frac{y^+}{bR_\tau}\right)^n\right)^{1/n}}$$

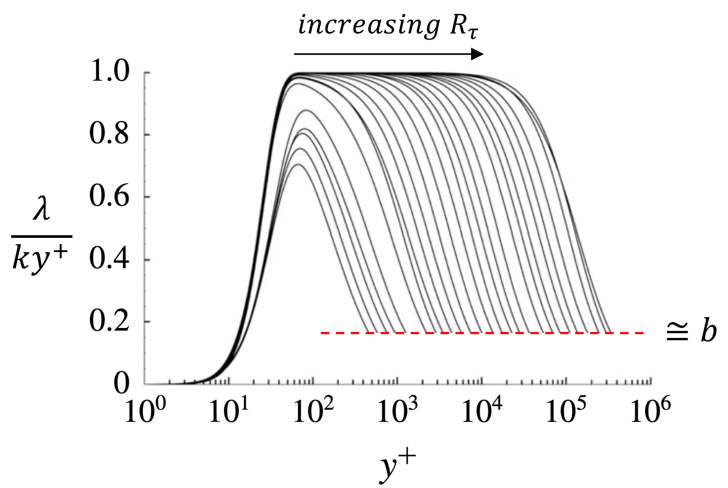

k - essentially the Karman constant.

a - wall damping length scale similar to the van Driest length.

m - exponent that, along with *a*, governs the shape and thickness of the near wall profile.

b - length scale proportional to the distance above the wall of the beginning of the outer layer.

n - exponent that, along with *b*, controls the transition of the profile to the wake function.

Later we will see that, for boundary layers, *b* and *n* can be related through a modified Clauser parameter β_c.

STANFORD AERONAUTICS & ASTRONAUTICS

The Universal Velocity Profile (UVP) - Integrate the velocity derivative from the wall

The velocity profile is uniformly valid from the wall to the pipe centerline at all Reynolds numbers.

$$u^+(k,a,m,b,n,R_\tau,y^+) = \int_0^{y^+} \frac{2\left(1-\frac{s}{R_\tau}\right)}{1+\left(1+4\lambda^2\left(1-\frac{s}{R_\tau}\right)\right)^{1/2}}ds$$

$$\lambda(y^+) = \frac{ky^+\left(1-\mathrm{e}^{-(y^+/a)^m}\right)}{\left(1+\left(\frac{y^+}{bR_\tau}\right)^n\right)^{1/n}}$$

The boundary layer friction law is generated by evaluating the UVP at $y^+ = R_\tau$

$$\frac{u_e}{u_\tau} = \int_0^{R_\tau} \frac{2\left(1-\frac{s}{R_\tau}\right)}{1+\left(1+4\lambda^2\left(1-\frac{s}{R_\tau}\right)\right)^{1/2}}ds$$

The velocity profile reduces to the laminar solution in the limit of zero Reynolds number independent of the choice of λ.

$$\lim_{R_\tau\to 0}\int_0^{y^+} \frac{2\left(1-\frac{s}{R_\tau}\right)}{1+\left(1+4\lambda^2\left(1-\frac{s}{R_\tau}\right)\right)^{1/2}}ds = y^+\left(1-\frac{y^+}{2R_\tau}\right)$$

$$\lim_{R_\tau\to 0} C_f = \frac{2}{\left(\lim_{R_\tau\to 0}\int_0^{R_\tau} \frac{2\left(1-\frac{s}{R_\tau}\right)}{1+\left(1+4\lambda^2\left(1-\frac{s}{R_\tau}\right)\right)^{1/2}}ds\right)^2} = \frac{8}{{R_\tau}^2}$$

STANFORD
AERONAUTICS & ASTRONAUTICS

The Princeton Superpipe (PSP) Facility

Zagarola, M. V. & Smits, A. J. 1998 Mean-flow scaling of turbulent pipe flow. J. Fluid Mech. 373, 33–79.

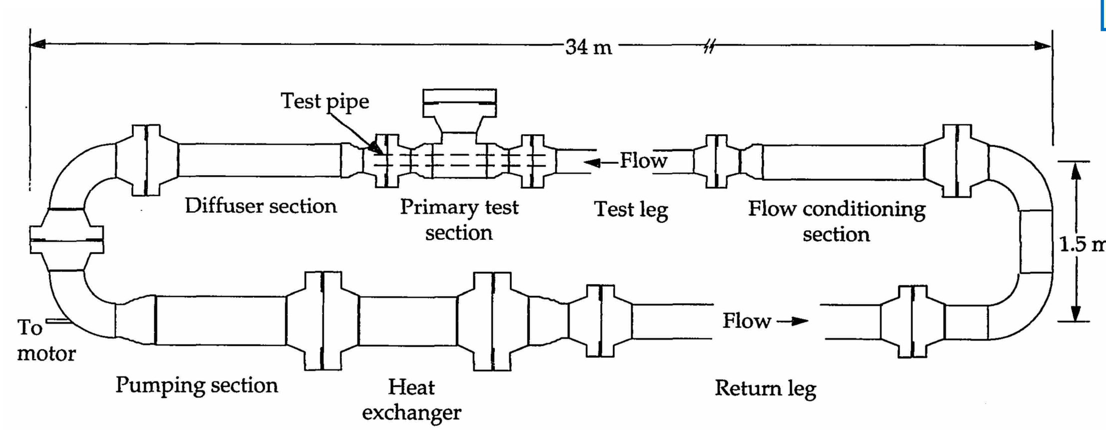

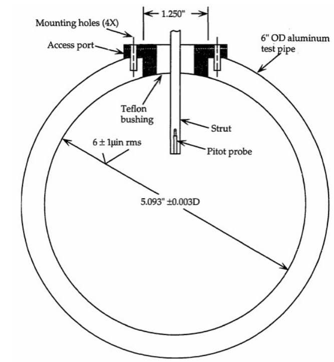

ZAGAROLA, M. V. 1996 Mean-flow scaling of turbulent pipe flow. Doctoral Dissertation, Princeton University.

MCKEON, B. J. 2003 High Reynolds number turbulent pipe flow. Doctoral Dissertation, Princeton University.

Pitot tube diameter = 0.9mm

Pitot tube diameter = 0.3mm

26 cases

$19639 < R_e < 20{,}088{,}000$

$851 < R_\tau < 530{,}000$

$23 < {}^{u_0}/_{u_\tau} < 38$

$$R_e = \frac{u_0 R}{\nu}$$

STANFORD
AERONAUTICS & ASTRONAUTICS

Determination of best fit model parameters

Minimize G with respect to k, a, m, b, n

$$G = \sum_{i=1}^{N} \left(u^{+}(k, a, m, b, n, y_i^{+}) - u_i^{+}(y_i^{+})\right)^2$$

UVP — PSP data

Flow conditions and optimal model parameters for all 26 velocity profiles

PSP #	p_d mm	u_τ	R_τ	R_e	$\bar{R}_e$	k	a	m	b	n	u_0/u_τ	$u^+_{rms\,error}$	$u^+_{max\,error}$	$u^+_{min\,error}$
1	0.9	0.2089	850.947	19639.	15789.	0.459526	25.801	1.28798	0.299588	1.23686	23.0788	0.152301	0.538874	−0.139258
2	0.9	0.2683	1090.56	25818.	20864.	0.45944	25.7568	1.28759	0.293575	1.24395	23.6738	0.116743	0.474895	−0.185527
3	0.9	0.3455	1430.26	34818.	28339.	0.457774	25.7518	1.28734	0.291299	1.24498	24.3436	0.0971337	0.371735	−0.184978
4	0.3	0.432	1824.72	45284.	37173.	0.455477	25.863	1.25214	0.295422	1.18658	24.8171	0.135614	0.344811	−0.128301
5	0.9	0.5641	2344.74	59872.	49406.	0.452669	25.6633	1.29994	0.297001	1.2471	25.5345	0.0807474	0.192072	−0.164053
6	0.3	0.7919	3327.37	87150.	72290.	0.403394	19.7637	1.4964	0.350243	1.33343	26.1918	0.211454	0.682335	−0.287154
7	0.9	1.0065	4124.89	110550.	92715.	0.403106	20.2094	1.61048	0.341454	1.51165	26.8018	0.107034	0.182098	−0.270575
8	0.3	0.4183	5108.56	139380.	116990.	0.400524	19.6565	1.55346	0.353091	1.37315	27.284	0.155725	0.666555	−0.185794
9	0.3	0.5437	6617.44	183270.	154820.	0.406081	19.682	1.61578	0.330602	1.48471	27.6954	0.112958	0.485734	−0.164828
10	0.3	0.7035	8536.62	242050.	205430.	0.405547	19.7355	1.63359	0.32875	1.51099	28.3537	0.0863432	0.387908	−0.137764
11	0.3	0.9003	10 914.4	314810.	268470.	0.406278	19.8188	1.6433	0.322005	1.61863	28.8432	0.0533497	0.155367	−0.114963
12	0.3	0.2423	14 848.9	439790.	376800.	0.405533	19.8187	1.63899	0.317069	1.64829	29.6175	0.0582442	0.0984979	−0.144372
13	0.3	0.323	19 778.3	599100.	515450.	0.405505	19.8541	1.64732	0.323093	1.66532	30.2907	0.0456737	0.0825095	−0.0989688
14	0.3	0.4136	25 278.1	780760.	673100.	0.406013	19.9893	1.6426	0.317063	1.75114	30.8868	0.0411267	0.0582979	−0.156567
15	0.3	0.5411	32 869.1	1038300.	897500.	0.40532	19.8023	1.65305	0.32421	1.66428	31.5881	0.0508534	0.118501	−0.14304
16	0.3	0.7001	42 293.5	1363000.	1181500.	0.406164	19.9961	1.62818	0.307786	1.71916	32.2268	0.0690966	0.175211	−0.12347
17	0.3	0.4721	54 530.6	1785500.	1552500.	0.407998	20.075	1.6311	0.30966	1.73322	32.743	0.0743128	0.259387	−0.106957
18	0.3	0.1759	76 479.8	2558700.	2231100.	0.40993	20.0117	1.65763	0.326951	1.68545	33.4563	0.0885882	0.262977	−0.281911
19	0.3	0.2358	102 200.	3500000.	3056400.	0.409934	19.9569	1.64637	0.317958	1.66433	34.2462	0.0779887	0.228758	−0.17882
20	0.3	0.2147	127 914.	4457300.	3903100.	0.410112	20.0706	1.63716	0.312475	1.64664	34.8458	0.074515	0.211301	−0.192975
21	0.3	0.2782	165 704.	5884200.	5157000.	0.410176	20.0915	1.64094	0.314927	1.6552	35.5102	0.0595818	0.214504	−0.122477
22	0.3	0.3652	216 979.	7813500.	6859500.	0.416118	20.6722	1.58559	0.293151	1.68512	36.0106	0.0706957	0.292235	−0.0989045
23	0.3	0.4821	284 254.	10392000.	9154000.	0.417539	20.673	1.59258	0.294283	1.67078	36.5586	0.058332	0.20287	−0.105169
24	0.9	0.6168	366 972.	13540000.	11989000.	0.418696	20.8983	1.62571	0.306356	1.75128	36.8963	0.0999892	0.155755	−0.269669
25	0.9	0.7571	452 380.	16888000.	14964000.	0.419289	20.8329	1.62031	0.303987	1.73244	37.3313	0.0669581	0.109743	−0.178982
26	0.3	0.9127	530 023.	20088000.	17862000.	0.418993	20.3797	1.64264	0.314469	1.49687	37.9002	0.096876	0.291624	−0.114251

STANFORD
AERONAUTICS &
ASTRONAUTICS

Comparison between PSP data and the universal velocity profile

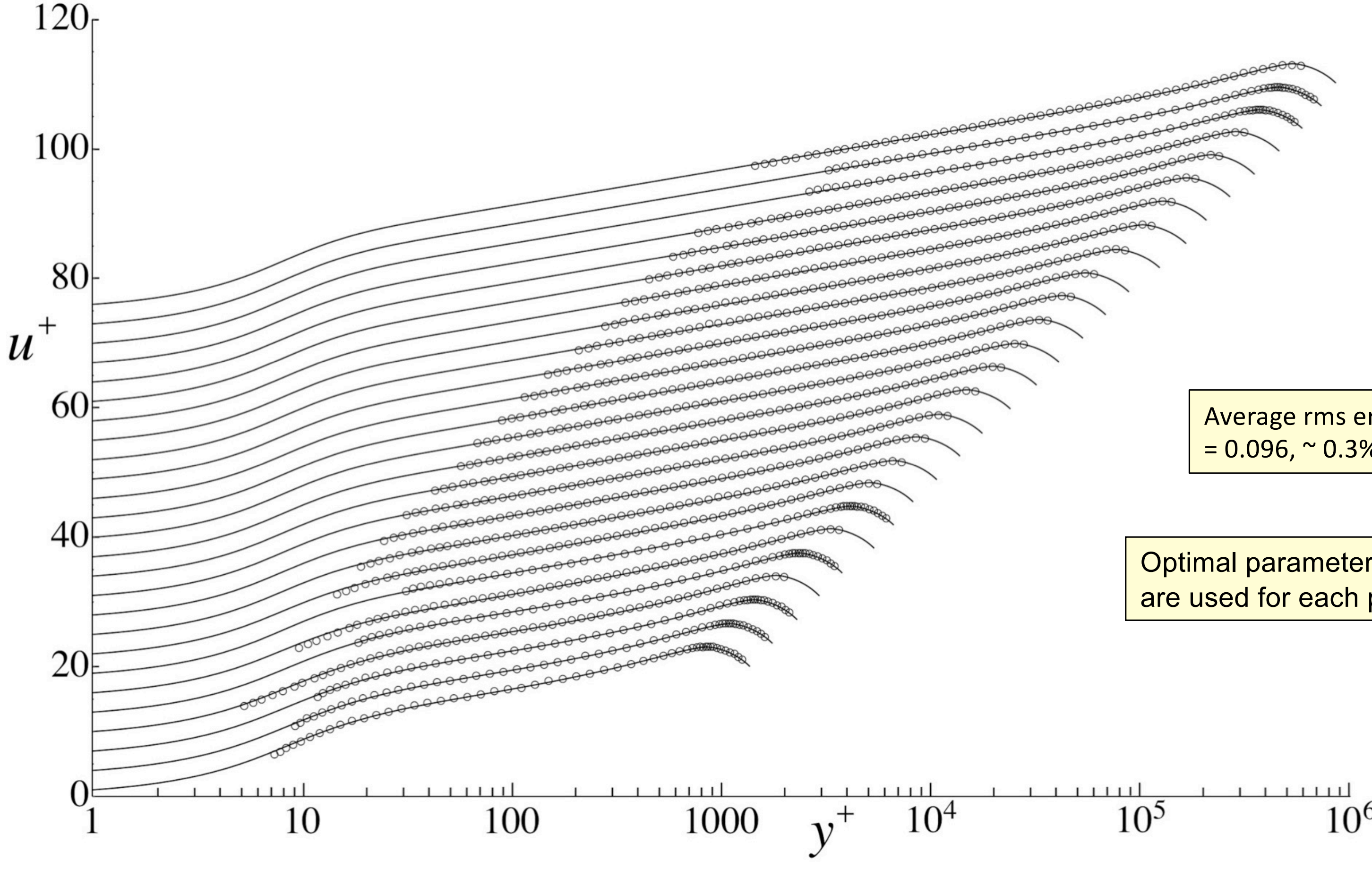

Average rms error = 0.096, ~ 0.3%

Optimal parameter values are used for each profile.

Optimal values of k and a

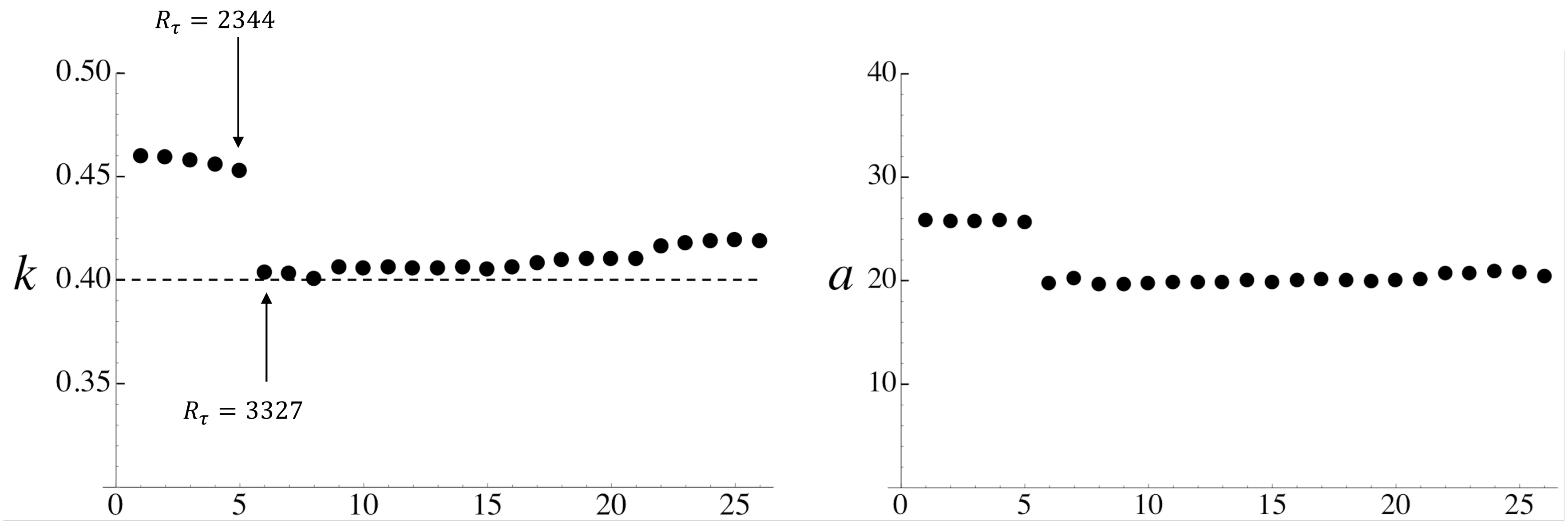

The minimization process is not convex. Alternate values of the model parameters can lead to the same accuracy. This seems to be the case at low and perhaps moderate Reynolds numbers but less so at Reynolds numbers above R_τ = 20,000 or so. Experience suggests that at high R_τ the minima may lie very close together in parameter space, but no analysis exists to show this.

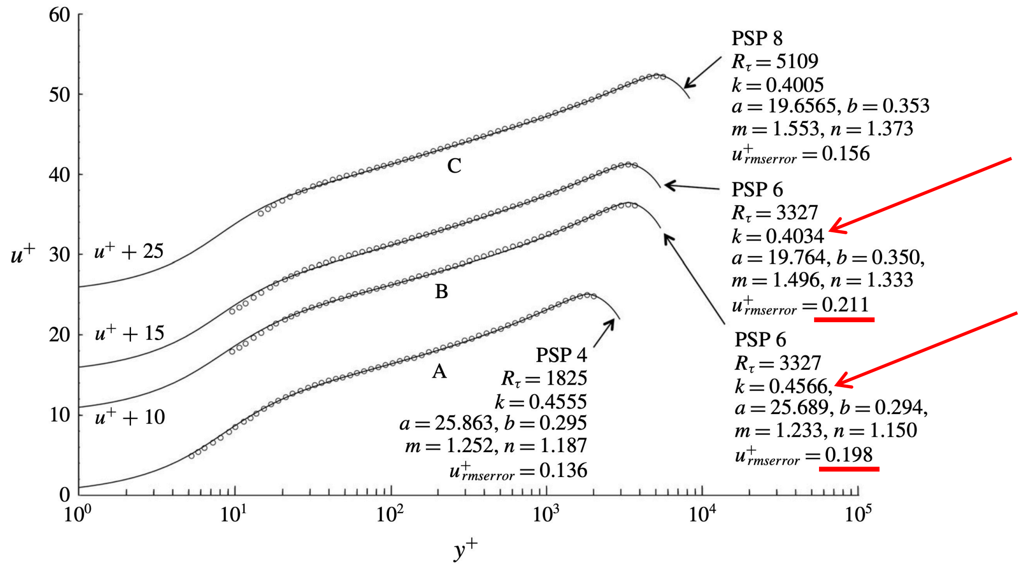

FIGURE 11. PSP 4, 6 and 8 velocity surveys are shown. The survey data (open circles ○) and comparison velocity profiles, equations (3.5) and (3.13), with optimal values of (k, a, m, b, n) are displaced 10, 15 and 25 units in u^+. PSP 6 is shown with two approximate profiles defined by two relatively different sets of optimal parameters. Each set of (k, a, m, b, n) values define a local minimum in $u^+_{rmserror}$ identified by the procedure described in § 5. Labels A, B and C identify the intermediate region of the profile generally associated with logarithmic behaviour.

Optimal values of ka, b, m and n

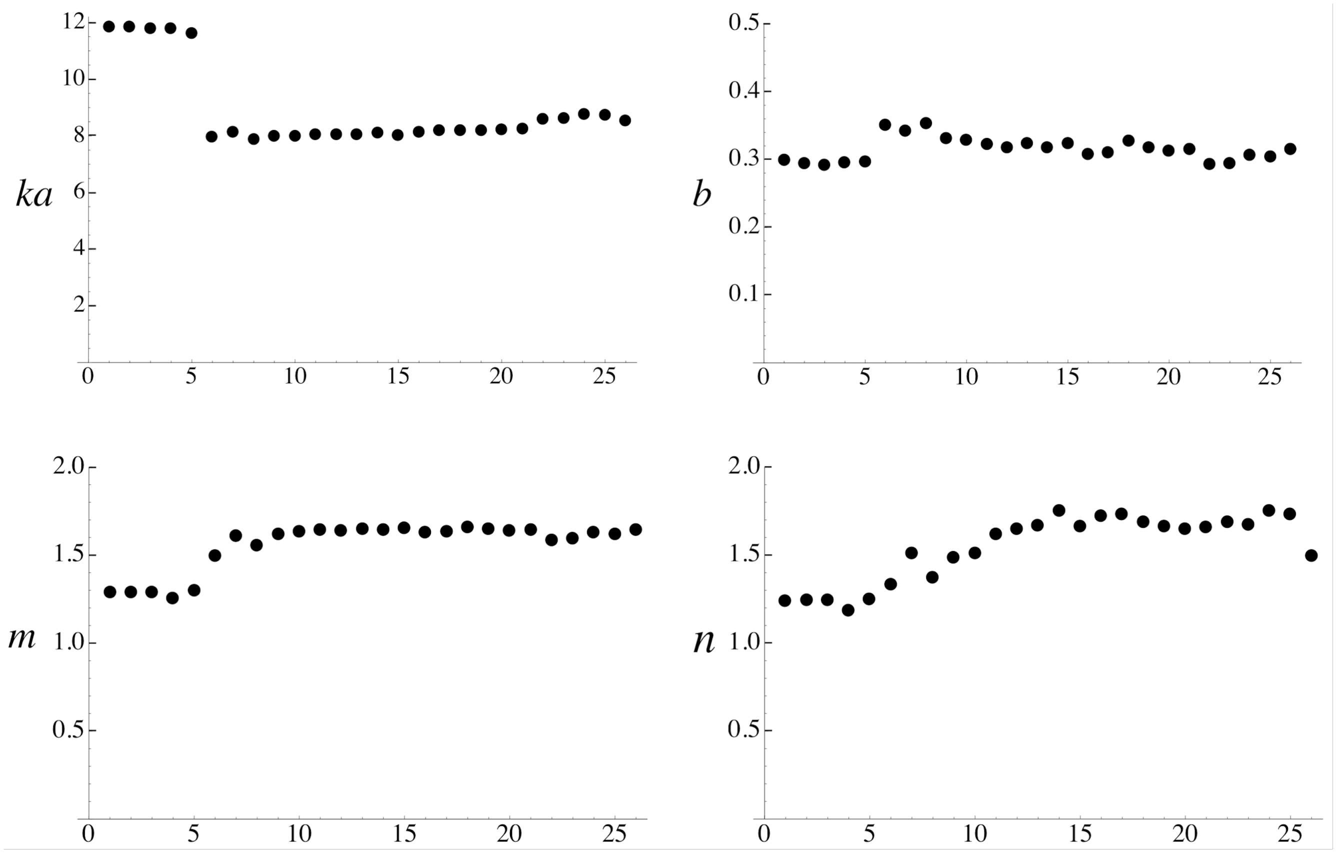

Error

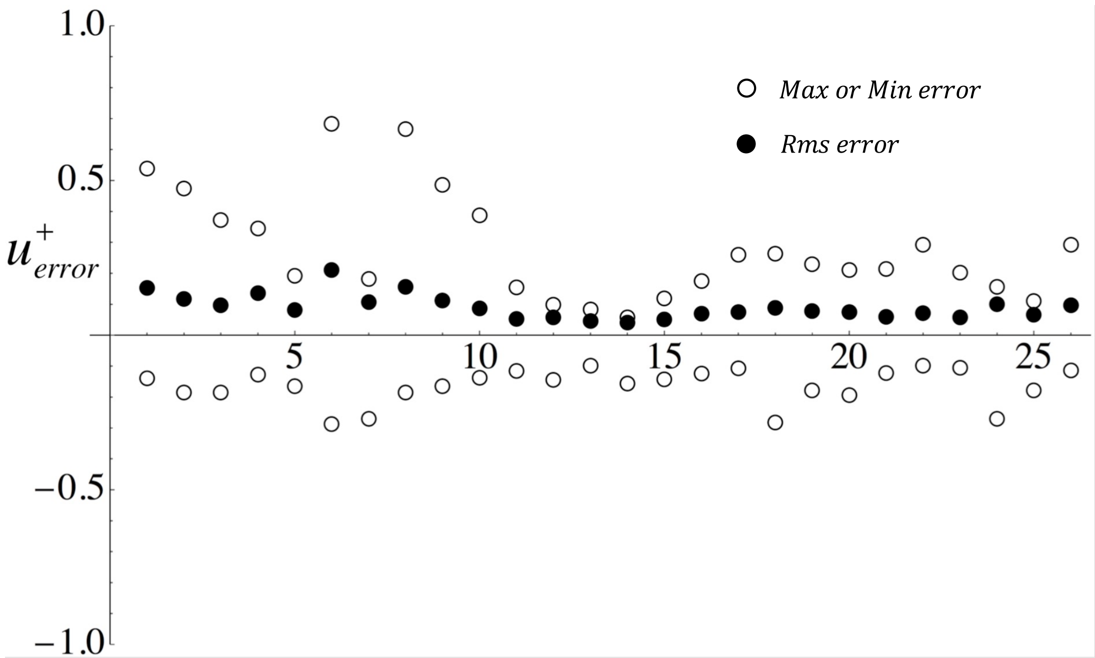

Average rms error = 0.096, ~ 0.3%

STANFORD
AERONAUTICS & ASTRONAUTICS

Log indicator function for the PSP data

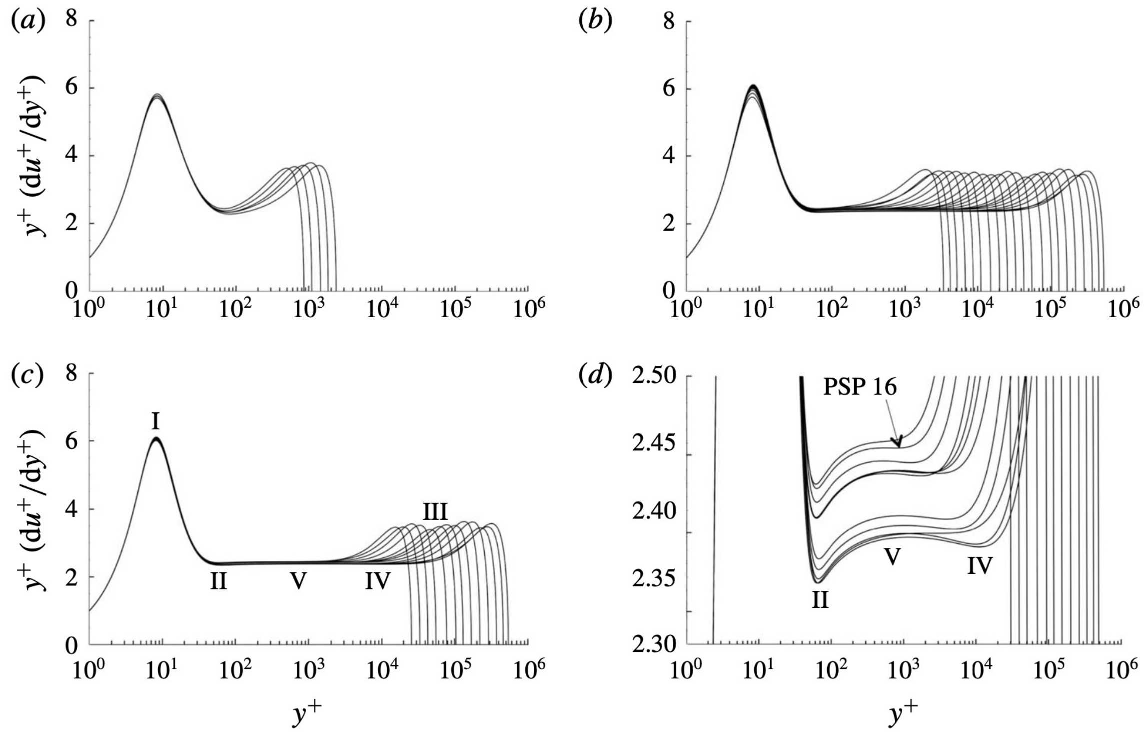

FIGURE 15. Comparison of the log-law indicator function for several sets of PSP model profiles. (*a*) PSP 1 to PSP 5, (*b*) PSP 6 to PSP 26, figure, (*c*) PSP 15 to 26. (*d*) Shows PSP profiles 15 to 26 on an expanded scale. Extrema of $y^+(du^+/dy^+)$ in (*c*) are identified by I, II, III, IV and V. The arrow in (*d*) indicates the lowest Reynolds number appearance of the minimum IV at PSP case 16.

PSP 16
$R_\tau = 42,294$

Channel Flow

STANFORD AERONAUTICS & ASTRONAUTICS

Channel Flow, $R_\tau = 550\ to\ 8016$

Average rms error = 0.044, ~ 0.18%

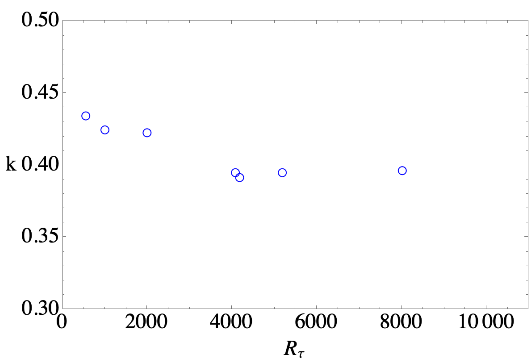

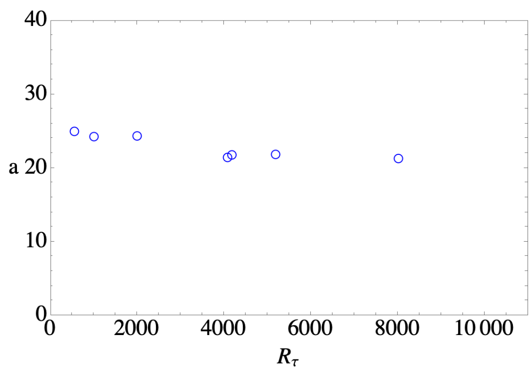

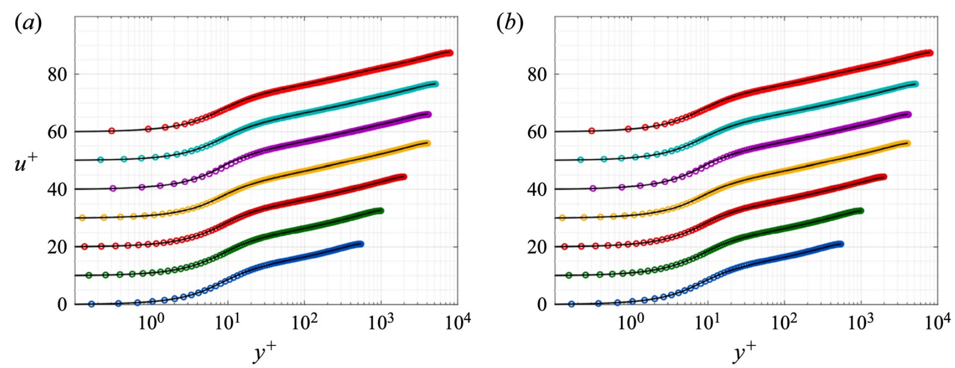

Figure 6. Channel flow velocity profiles from Lee & Moser (2015), Lozano-Durán & Jiménez (2014), Bernardini *et al.* (2014) and Yamamoto & Tsuji (2018) overlaid on the universal velocity profile with (*a*) optimal parameters from table 3 and (*b*) average parameter values from table 1 for $(\bar{k}, \bar{a}, \bar{m}, \bar{b}, \bar{n})$ at $R_\tau = 550$ (dark blue), 1001 (green), 1995 (dark red), 4079 (yellow), 4179 (purple), 5186 (light blue), 8016 (light red). Profiles are separated vertically by 10 units.

R_τ	$(u_e/u_\tau)_{data}$	$(u_e/u_\tau)_{uvp}$	k	a	m	b	n	u^+_{rms}
550	21.0008	21.0595	0.4344	24.9898	1.2504	0.4237	1.3395	0.055682
1001	22.5932	22.6511	0.4247	24.2801	1.2341	0.4289	1.3058	0.051927
1995	24.3959	24.4841	0.4227	24.3731	1.2164	0.4307	1.2588	0.043820
4079	25.9546	26.0605	0.3950	21.4550	1.2607	0.4654	1.4602	0.042982
4179	25.9565	26.1392	0.3916	21.7990	1.3035	0.5020	1.5284	0.038933
5186	26.5753	26.6803	0.3950	21.8670	1.2667	0.4472	1.5700	0.043438
8016	27.3808	27.5914	0.3964	21.3074	~~1.2828~~ 1.199	0.5558	1.3171	0.032911

Table 3. Reynolds number, optimal model parameters and root-mean-square (r.m.s.) error for channel flow datasets. Second column is extrapolation of u/u_τ data to channel centreline. Third column is u_e/u_τ calculated using the universal velocity profile (*uvp*).

Average parameter values are used for each profile on the right.

$$(\bar{k}, \bar{a}, \bar{m}, \bar{b}, \bar{n}) = (0.4086,\ 22.8673,\ 1.2569,\ 0.4649,\ 1.3972)$$

STANFORD
AERONAUTICS &
ASTRONAUTICS

Zero Pressure Gradient Turbulent Boundary Layer

ZPG Turbulent Boundary Layer experimental data, $R_\tau = 2109\ to\ 17207$

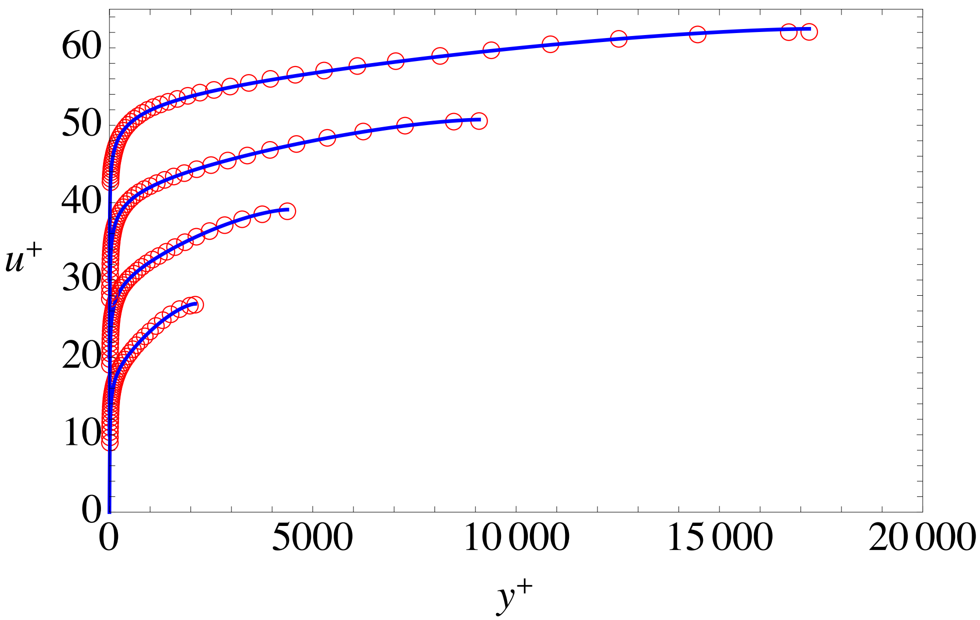

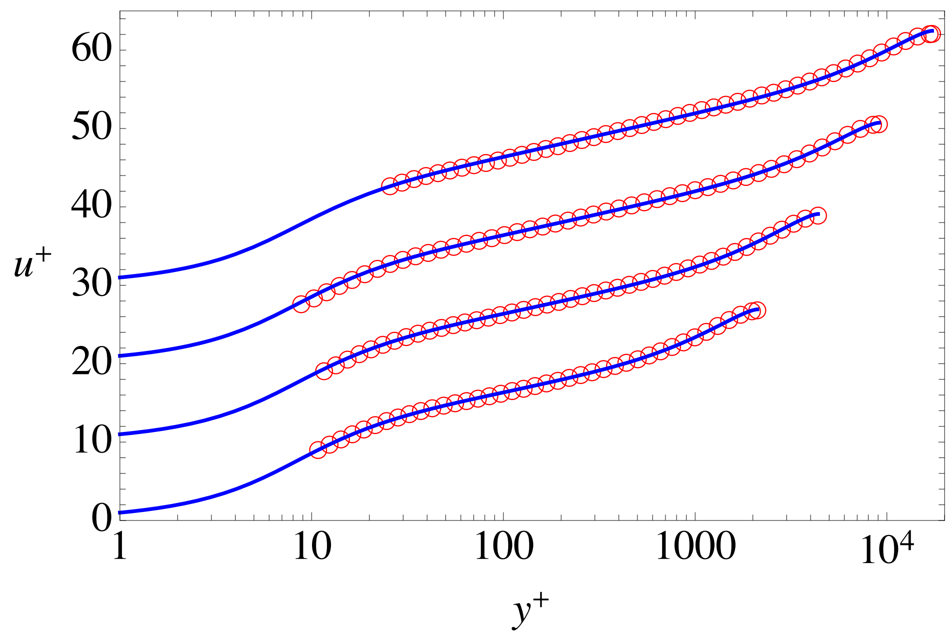

R. Baidya, J. Phillip, N. Hutchins, J.P. Monty & I. Marusic 2021 Spanwise velocity statistics in high-Reynolds-number turbulent boundary layers. *J. Fluid Mech.* 913, A35.

ZPG TBL computational data, $R_\tau = 1343\ to\ 2571$

Average rms error = 0.033, ~ 0.13%
δ_h=$\delta_{0.993}$- $\delta_{0.996}$

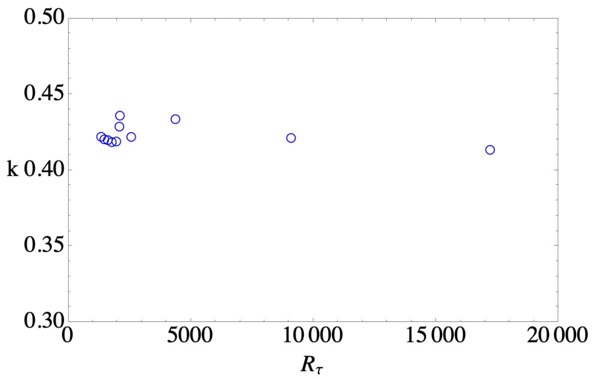

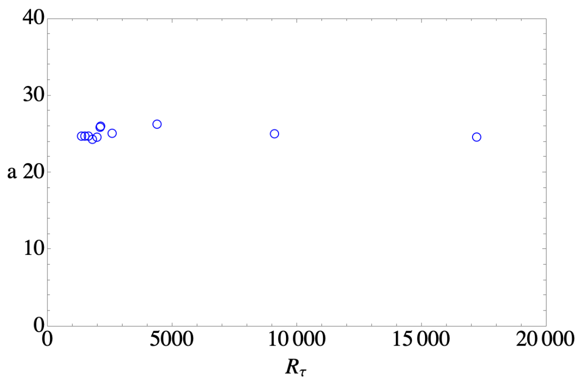

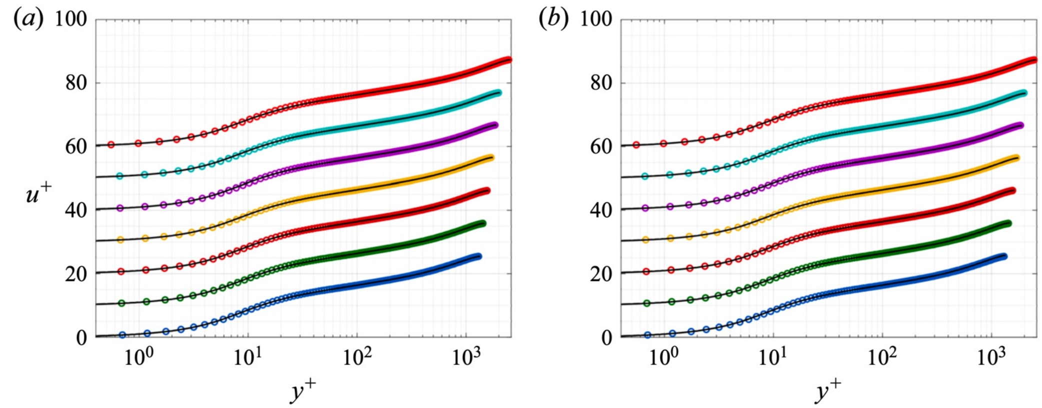

Figure 12. Turbulent boundary layer DNS data from Simens *et al.* (2009), Borrell *et al.* (2013), Sillero *et al.* (2013) and Eitel-Amor *et al.* (2014) at $R_\tau = 1343$ (dark blue), 1475 (green), 1616 (dark red), 1779 (yellow), 1962 (purple), 2088 (light blue) and 2571 (light red) compared with the universal velocity profile using (*a*) optimal parameters from table 4, (*b*) average parameters from 1. Profiles are separated vertically by 10 units.

Average parameter values are used for each profile on the right.

$$(\bar{k}, \bar{a}, \bar{m}, \bar{b}, \bar{n}) = (0.4233,\ 24.9583,\ 1.1473,\ 0.1752,\ 2.1707)$$

R_τ	$(u_e/u_\tau)_{data}$	$(u_e/u_\tau)_{uvp}$	k	a	m	b	n	u^+_{rms}	u_e/U
1343	25.5088	25.4939	0.4222	24.7756	1.1820	0.1828	2.3298	0.03617	0.993
1475	25.9305	25.8994	0.4205	24.7786	1.1732	0.1787	2.3622	0.03332	0.993
1616	26.2722	26.2365	0.4200	24.7834	1.1720	0.1764	2.3548	0.03390	0.993
1779	26.5926	26.5818	0.4187	24.3610	1.2032	0.1757	2.2932	0.03215	0.994
1962	26.8226	26.8512	0.4191	24.6388	1.1752	0.1747	2.2833	0.03298	0.994
2088	27.0332	27.0255	0.4289	25.9290	1.1480	0.1696	2.2516	0.03143	0.994
2571	27.4177	27.4073	0.4221	25.1424	1.1130	0.1724	2.3087	0.03150	0.993
2109	26.8104	26.9239	0.4361	26.0709	1.1410	0.1665	2.1993	0.05453	0.996
4374	28.8876	29.0940	0.4338	26.3286	1.1060	0.1664	1.8792	0.09473	0.996
9090	30.5483	30.7301	0.4214	25.0804	1.1216	0.1829	1.7753	0.13364	0.996
17 207	32.0670	32.4649	0.4136	24.6549	1.0846	0.1816	1.8397	0.16864	0.996

Turbulent Boundary Layer equivalent channel half height (overall thickness) δ_h

δ_h is defined as the thickness that minimizes the error between a specific data set and the UVP

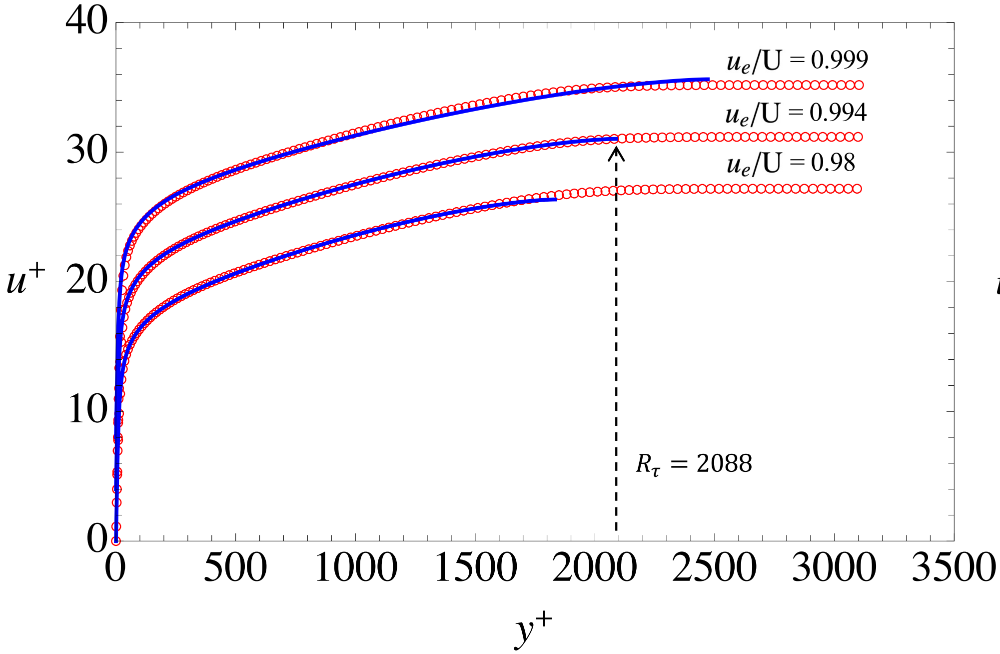

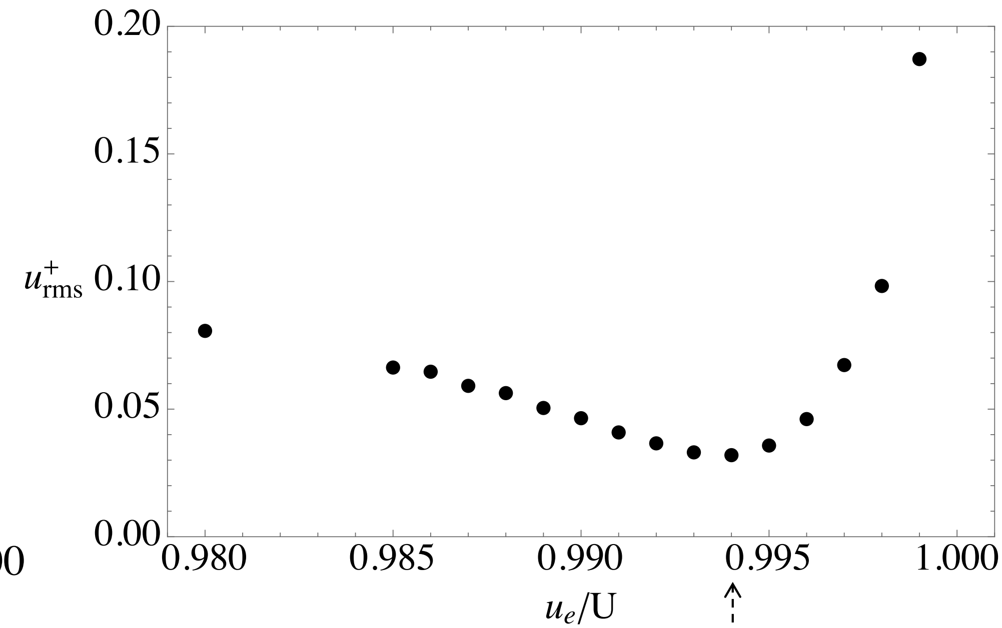

δ_h=$\delta_{0.994}$

DNS data is from

J. A. Sillero, J. Jimenez & R. D. Moser 2013 One-point statistics for turbulent wall-bounded flows at Reynolds numbers up to δ+ = 2000. *Phys. Fluids* 25 (10), 105102.

$R_\tau = 2652$ Velocity Profile Comparison

$$\lambda(y^+) = \frac{k y^+ \left(1 - e^{-(y^+/a)^m}\right)}{\left(1 + \left(\frac{y^+}{bR_\tau}\right)^n\right)^{1/n}}$$

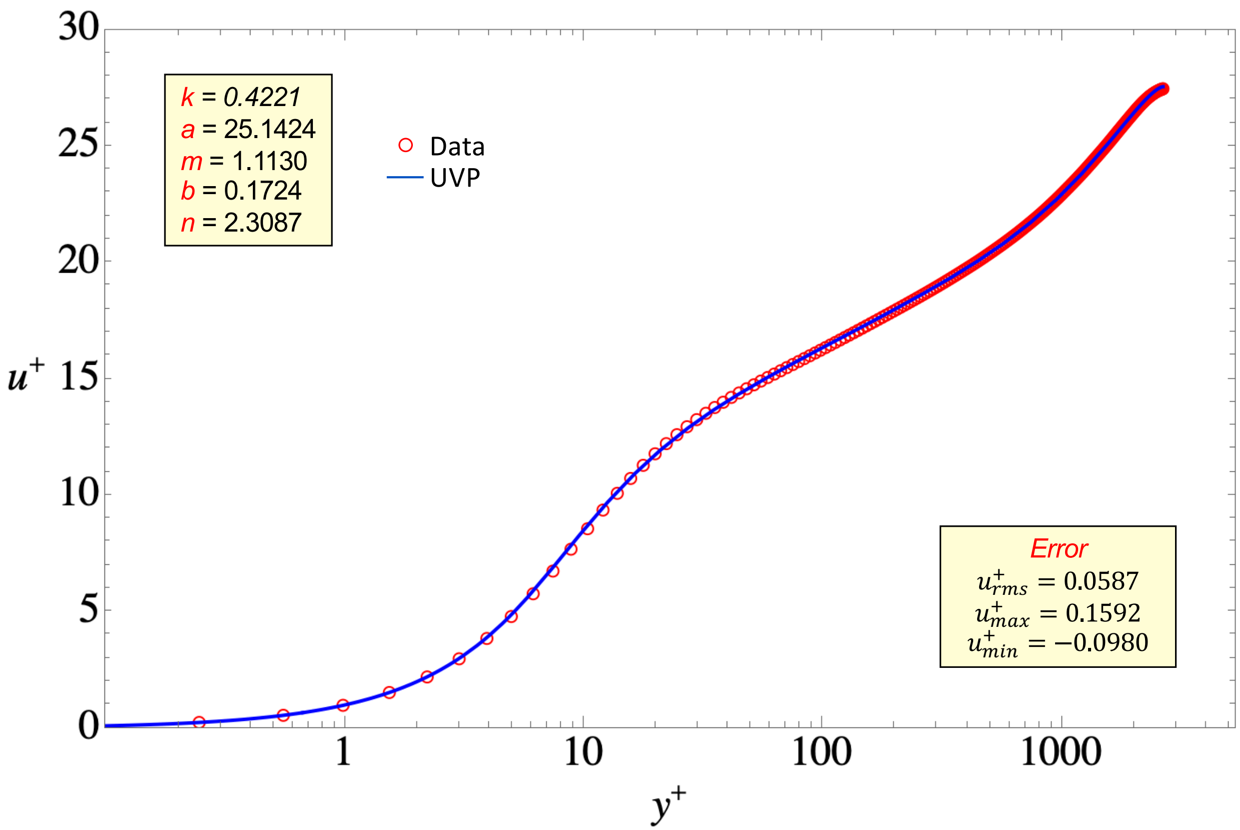

UVP Wall Damping Function

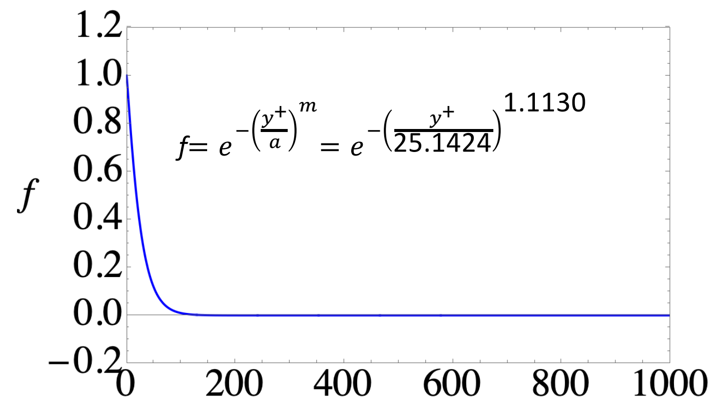

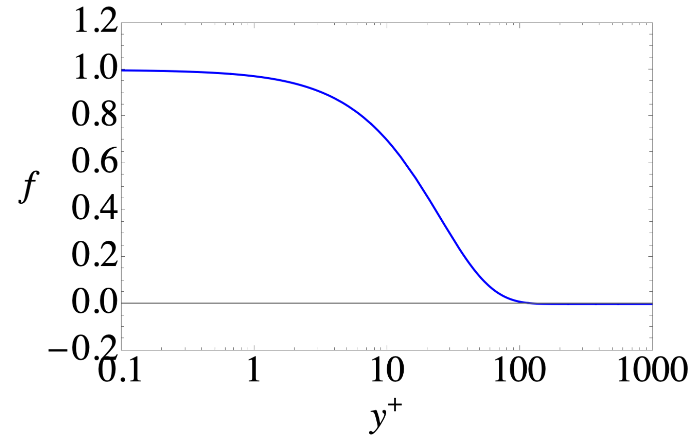

$R_\tau = 2652$ Velocity Derivative Comparison

Log Indicator Function y^+dU^+/dy^+

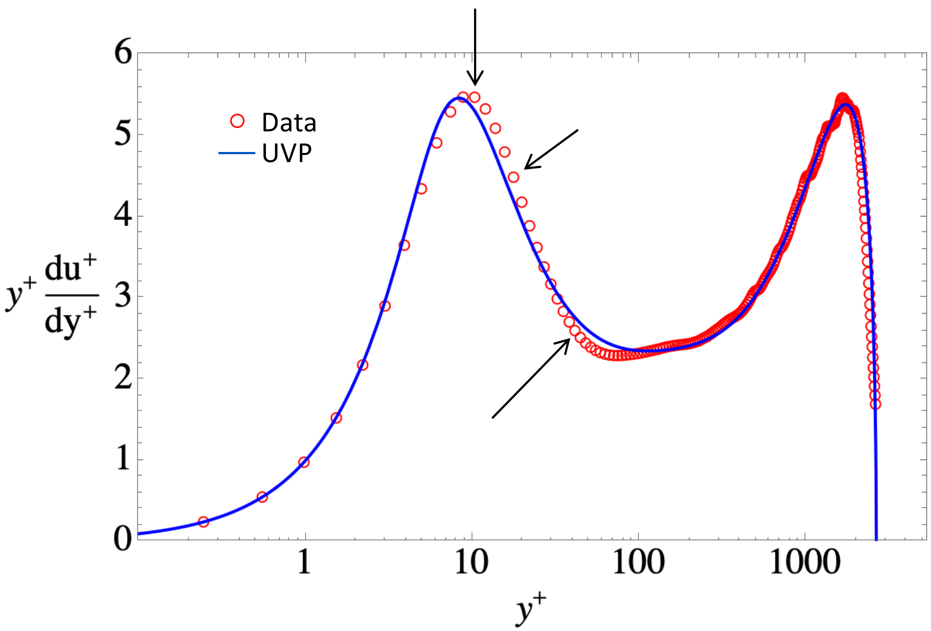

Velocity Derivative dU^+/dy^+

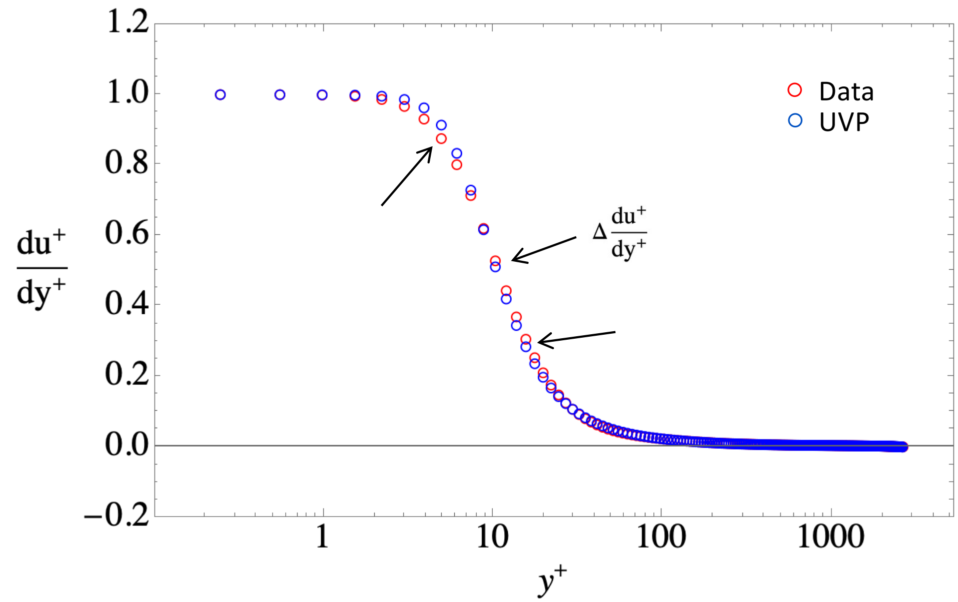

STANFORD AERONAUTICS & ASTRONAUTICS

Average parameter values for pipe, channel and ZPG boundary layer flows

TABLE I. Average model parameters with standard deviation for basic wall flows. Ranges of R_τ for each flow are as follows: Pipe (3327–530 023), Channel (550–8016), ZPG boundary layer (1343–17 207).

Flow	$\bar{k}$	σ_k	$\bar{a}$	σ_a	$\bar{m}$	σ_m	$\bar{b}$	σ_b	$\bar{n}$	σ_n
Pipe (21 profiles)	0.4092	0.0057	20.0950	0.381	1.6210	0.0379	0.3195	0.0157	1.6190	0.1204
Channel (7 profiles)	0.4086	0.0179	22.8673	1.599	1.2569	0.0292	0.4649	0.0485	1.3972	0.1213
ZPG boundary layer (11 profiles)	0.4233	0.0068	24.9583	0.663	1.1473	0.0373	0.1752	0.0060	2.1707	0.2238

STANFORD
AERONAUTICS &
ASTRONAUTICS

Turbulent Boundary Layer Flow with Pressure Gradient

STANFORD
AERONAUTICS & ASTRONAUTICS

Adverse pressure gradient Turbulent Boundary Layer experimental data, $R_\tau = 2461\ to\ 3587$

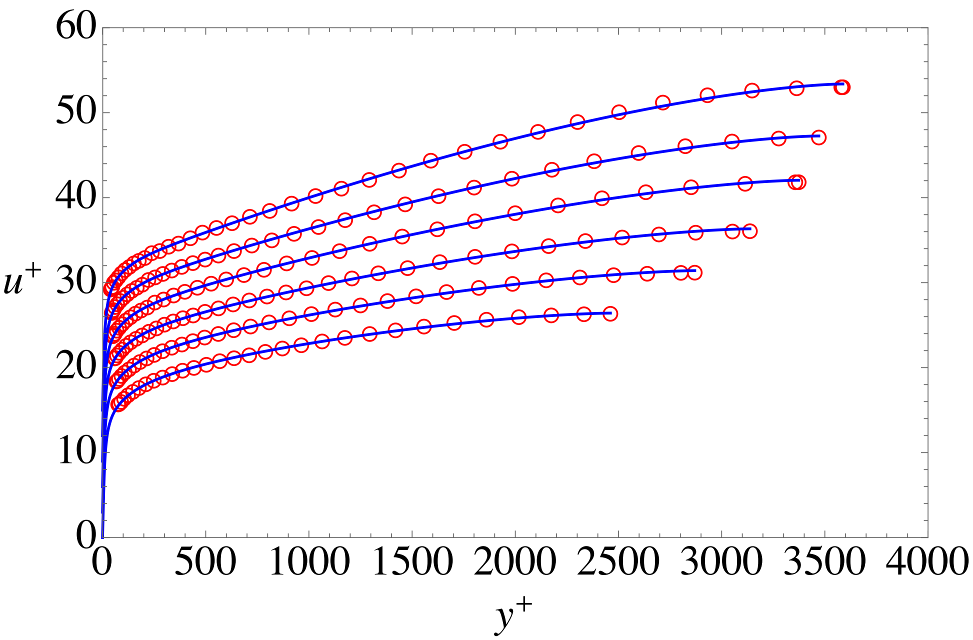

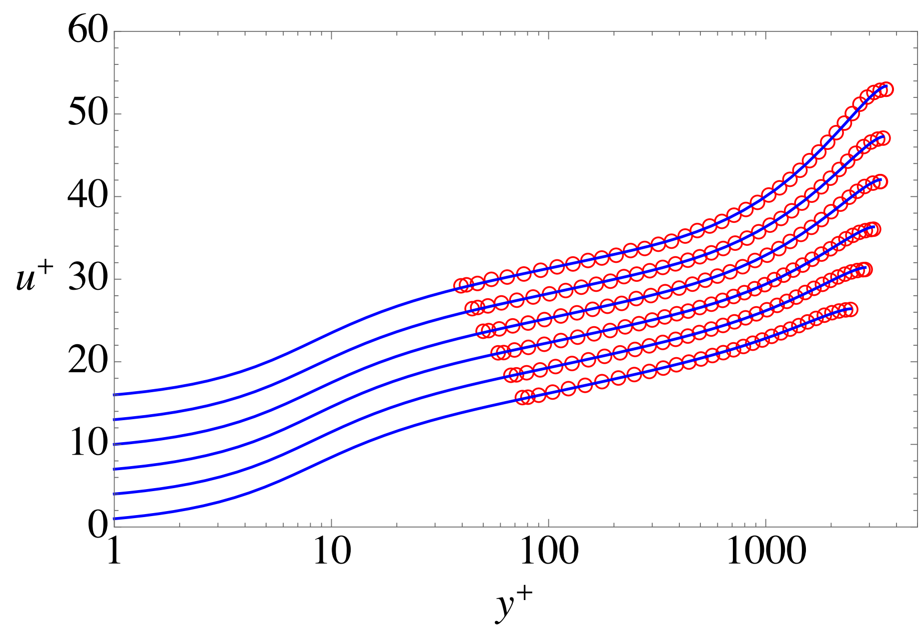

Perry, A.E. & Marusic, I. 1995 A wall-wake model for the turbulence structure of boundary layers. Part 1. Extension of the attached eddy hypothesis. *J. Fluid Mech.* 298, 361–388.

Average rms error = 0.148, ~ 0.46%
$\delta_h = \delta_{0.998}$

STANFORD
AERONAUTICS &
ASTRONAUTICS

Changes in boundary layer wall parameters (k, a, m) in an adverse pressure gradient are small.

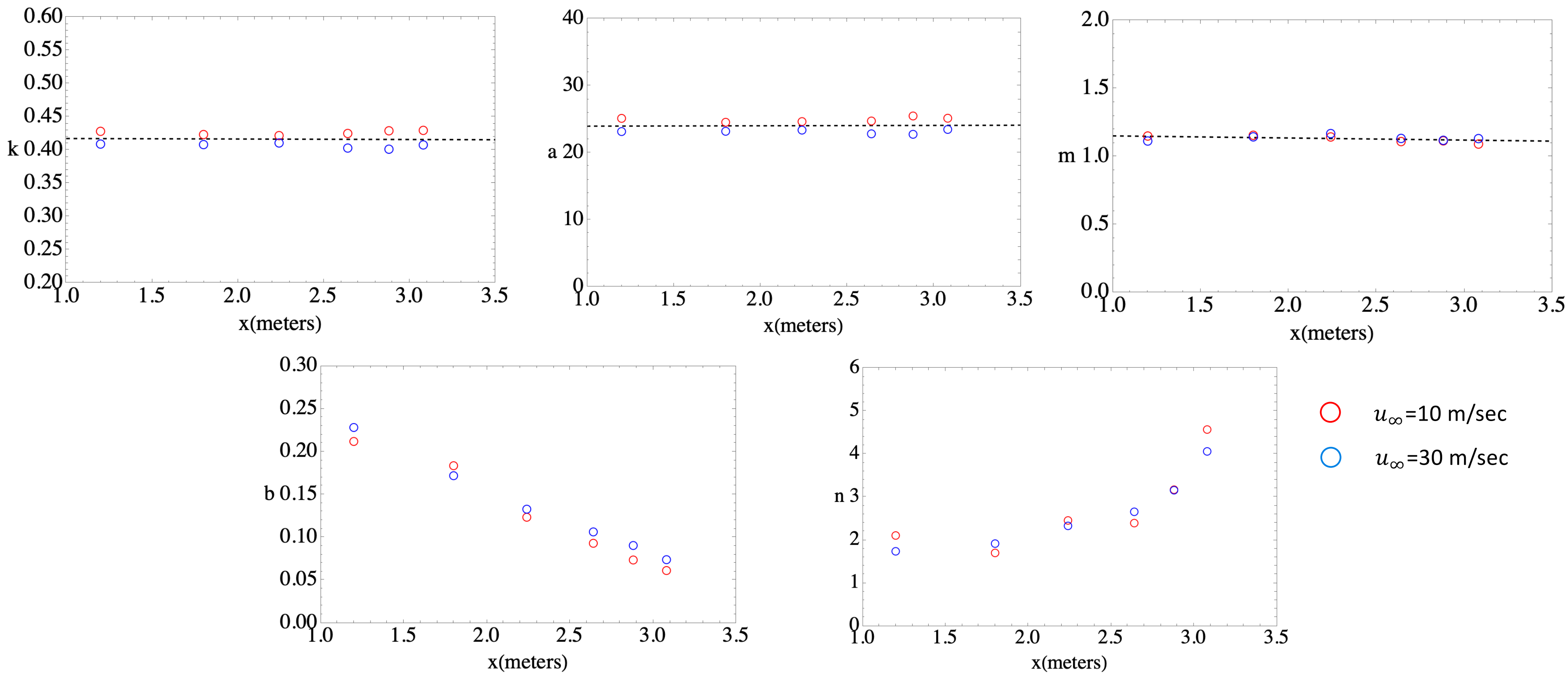

STANFORD AERONAUTICS & ASTRONAUTICS

Parameters for the adverse pressure gradient cases

TABLE II. Run data, Reynolds number, optimal model parameters, and RMS error for adverse pressure gradient boundary layer datasets from Perry and Marusic.[27] Initial free stream values are $u_\infty = 10$ and $u_\infty = 30$ m/s. Channel half height thickness for these data are at $u = 0.998u_e$; $\delta_h = \delta_{0.998}$. Reprinted with permission from Subrahmanyam *et al.*, J. Fluid Mech. **933**, A16 (2022). Copyright 2022 Author(s), licensed under a Creative Commons Attribution (CC BY) License.[17]

x (m)	$u_e\left(\frac{m}{s}\right)$	R_{δ_1}	R_{δ_2}	β	β_c	δ_{998} (m)	$R_{\delta_{998}}$	R_τ	$\left(\frac{u_e}{u_\tau}\right)$	k	a	m	b	n	u^+_{rms}
1.20	10.361	3 165	2 282	0.0	0.0	0.031 79	21 439	912	23.51	0.4287	25.18	1.1528	0.212 2	2.111	0.120
1.80	9.976	5 226	3 734	0.65	1.115	0.050 19	32 606	1285	25.37	0.4239	24.59	1.1583	0.183 9	1.705	0.253
2.24	9.256	6 410	4 342	1.45	2.432	0.055 43	33 456	1195	28.00	0.4223	24.70	1.1460	0.123 7	2.461	0.163
2.64	8.588	8 606	5 517	2.90	4.760	0.070 55	39 406	1252	31.47	0.4255	24.79	1.1121	0.093 31	2.399	0.152
2.88	8.155	11 235	6 879	4.48	7.223	0.086 34	46 043	1337	34.44	0.4296	25.54	1.1173	0.073 83	3.178	0.220
3.08	7.896	12 397	7 213	7.16	11.326	0.092 63	47 598	1248	38.13	0.4302	25.20	1.0938	0.061 51	4.578	0.231
1.20	30.704	8 772	6 564	0.0	0.0	0.033 53	64 807	2461	26.34	0.4095	23.21	1.1161	0.228 5	1.743	0.0705
1.80	29.054	12 401	9 073	0.71	1.230	0.044 15	80 849	2870	28.17	0.4088	23.25	1.1468	0.172 2	1.922	0.0895
2.24	27.035	16 307	11 587	1.39	2.378	0.055 26	94 275	3137	30.05	0.4112	23.42	1.1710	0.133 1	2.335	0.0942
2.64	25.150	21 634	14 736	2.74	4.606	0.069 68	110 700	3373	32.82	0.4035	22.87	1.1352	0.106 6	2.663	0.0984
2.88	23.885	25 854	17 020	3.96	6.567	0.080 54	121 760	3471	35.08	0.4018	22.80	1.1213	0.090 7	3.164	0.1183
3.08	22.908	31 767	20 052	6.07	9.901	0.093 73	136 290	3587	37.99	0.4083	23.53	1.1339	0.074 2	4.069	0.1673

Favorable pressure gradient Turbulent Boundary Layer experimental data, $R_\tau = 429\ to\ 1746$.

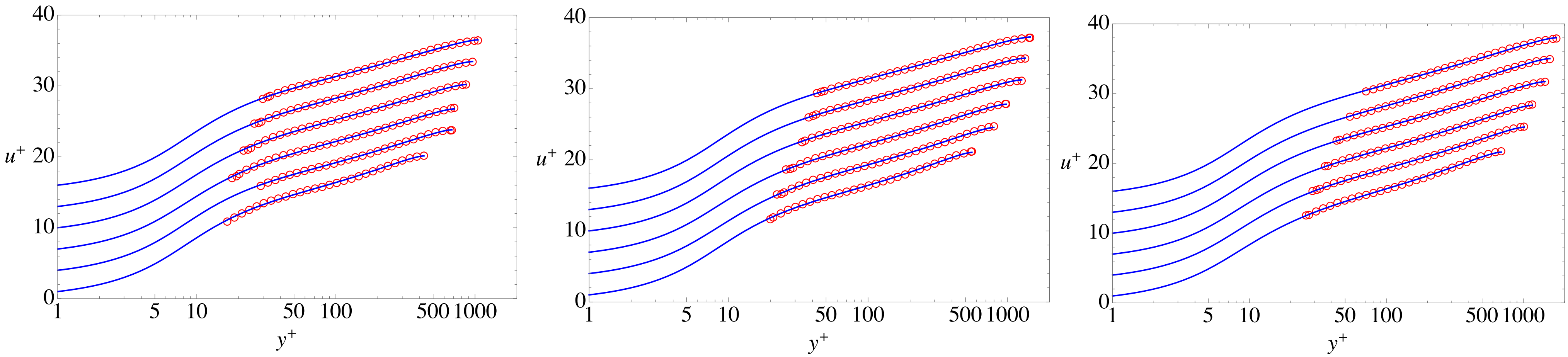

M. Jones, I. Marusic, and A. E. Perry, "Evolution and structure of sink-flow turbulent boundary layers," Journal of Fluid Mechanics 428, 1 – 27 (2001).

Average rms error = 0.075, ~ 0.36%
δ_h=$\delta_{0.996}$

STANFORD
AERONAUTICS & ASTRONAUTICS

Changes in boundary layer wall parameters (k, a, m) in a <u>favorable</u> pressure gradient are modest.

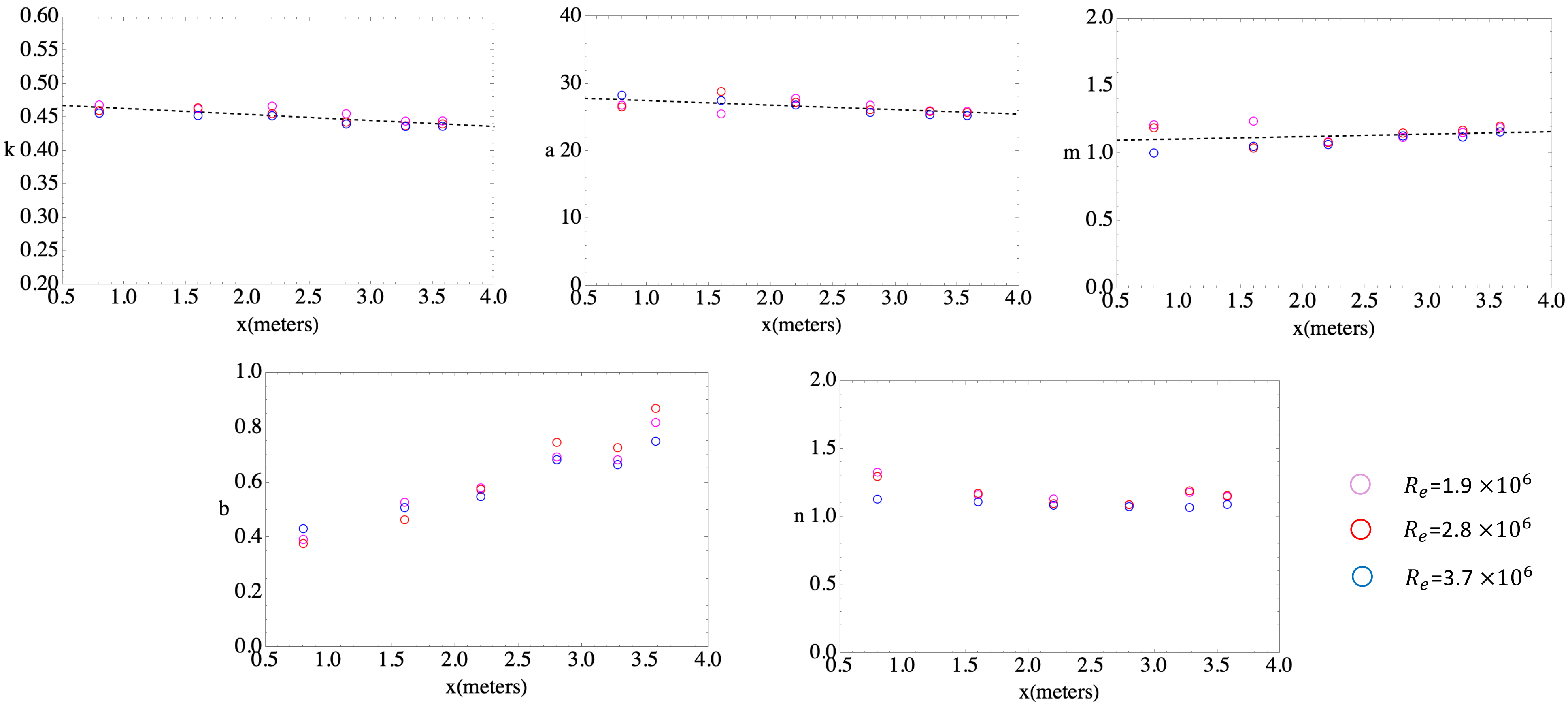

STANFORD AERONAUTICS & ASTRONAUTICS

Parameters for the favorable pressure gradient cases

TABLE III. Run data, Reynolds number, optimal model parameters, and RMS error for favorable pressure gradient boundary layer datasets from Jones *et al.*[28] Converging channel entry velocities are $u_0 = 5.0, 7.5$ and 10.0 m/s. Channel half height thickness for these data are at $u = 0.996u_e$; $\delta_h = \delta_{0.996}$. Kinematic viscosity is $\nu = 1.51 \times 10^{-5}$m/s^2. Note, according to Jones *et al.*,[28] $u_e/u_0 = 1/(1 - x/L)$ and the calibrated sink length is $L = 5.60$m.

$K \times 10^7$	x (mm)	$u_0\left(\frac{m}{s}\right)$	R_{δ_1}	R_{δ_2}	$-\beta$	$-\beta_c$	$R_{\delta_{996}}$	R_τ	$\left(\frac{u_e}{u_\tau}\right)$	k	a	m	b	n	u^+_{rms}
5.39	800	5.0	1112	780	0.2436	0.4145	8656	429	20.16	0.4686	26.88	1.2136	0.3931	1.3295	0.098
5.39	1600	5.0	1629	1192	0.3780	0.6548	14 130	681	20.75	0.4630	25.58	1.2408	0.5284	1.1644	0.068
5.39	2200	5.0	1648	1209	0.3880	0.6726	14 806	709	20.90	0.4670	27.89	1.0869	0.5806	1.1343	0.105
5.39	2800	5.0	1946	1449	0.4713	0.8222	18 244	861	21.20	0.4555	26.89	1.1196	0.6934	1.0908	0.089
5.39	3280	5.0	2138	1606	0.5276	0.9241	20 549	960	21.40	0.4445	26.04	1.1563	0.6831	1.1818	0.067
5.39	3580	5.0	2226	1687	0.5500	0.9671	22 468	1049	21.41	0.4448	25.96	1.1920	0.8189	1.1514	0.068
3.59	800	7.5	1496	1069	0.3613	0.4125	11 752	555	21.17	0.4602	26.62	1.1906	0.3738	1.2986	0.092
3.59	1600	7.5	2000	1470	0.3382	0.5868	17 325	798	21.70	0.4644	28.91	1.0413	0.4647	1.1745	0.085
3.59	2200	7.5	2350	1755	0.4030	0.7040	21 366	977	21.86	0.4557	27.30	1.0822	0.5752	1.0988	0.060
3.59	2800	7.5	2827	2155	0.4850	0.8748	27 899	1262	22.12	0.4431	26.19	1.1527	0.7463	1.0917	0.065
3.59	3280	7.5	2928	2245	0.5202	0.9191	29 762	1338	22.25	0.4374	25.93	1.1726	0.7271	1.1931	0.055
3.59	3580	7.5	3027	2339	0.5344	0.9473	32 204	1452	22.17	0.4403	25.78	1.2037	0.8700	1.1579	0.062
2.70	800	10.0	1862	1343	0.3161	0.4092	15 001	690	21.74	0.4564	28.35	1.0045	0.4324	1.1316	0.097
2.70	1600	10.0	2555	1904	0.3421	0.5969	22 546	1013	22.27	0.4529	27.56	1.0538	0.5090	1.1120	0.074
2.70	2200	10.0	2873	2160	0.3908	0.6846	26 114	1164	22.44	0.4525	26.90	1.0669	0.5491	1.0864	0.047
2.70	2800	10.0	3372	2577	0.4689	0.8273	32 769	1444	22.70	0.4402	25.79	1.1307	0.6833	1.0766	0.047
2.70	3280	10.0	3725	2851	0.5297	0.9351	35 899	1564	22.95	0.4364	25.45	1.1227	0.6653	1.0704	0.073
2.70	3580	10.0	3936	3044	0.5575	0.9888	39 990	1746	22.91	0.4368	25.31	1.1607	0.7504	1.0923	0.095

STANFORD
AERONAUTICS &
ASTRONAUTICS

A New Wall Damping Function for Pipe, Channel and Boundary Layer Flows.

STANFORD AERONAUTICS & ASTRONAUTICS

$R_\tau = 2652$ Velocity Profile Comparison

$$\lambda(y^+) = \frac{ky^+\left(1 - e^{-(y^+/a)^m}\right)}{\left(1 + \left(\frac{y^+}{bR_\tau}\right)^n\right)^{1/n}}$$

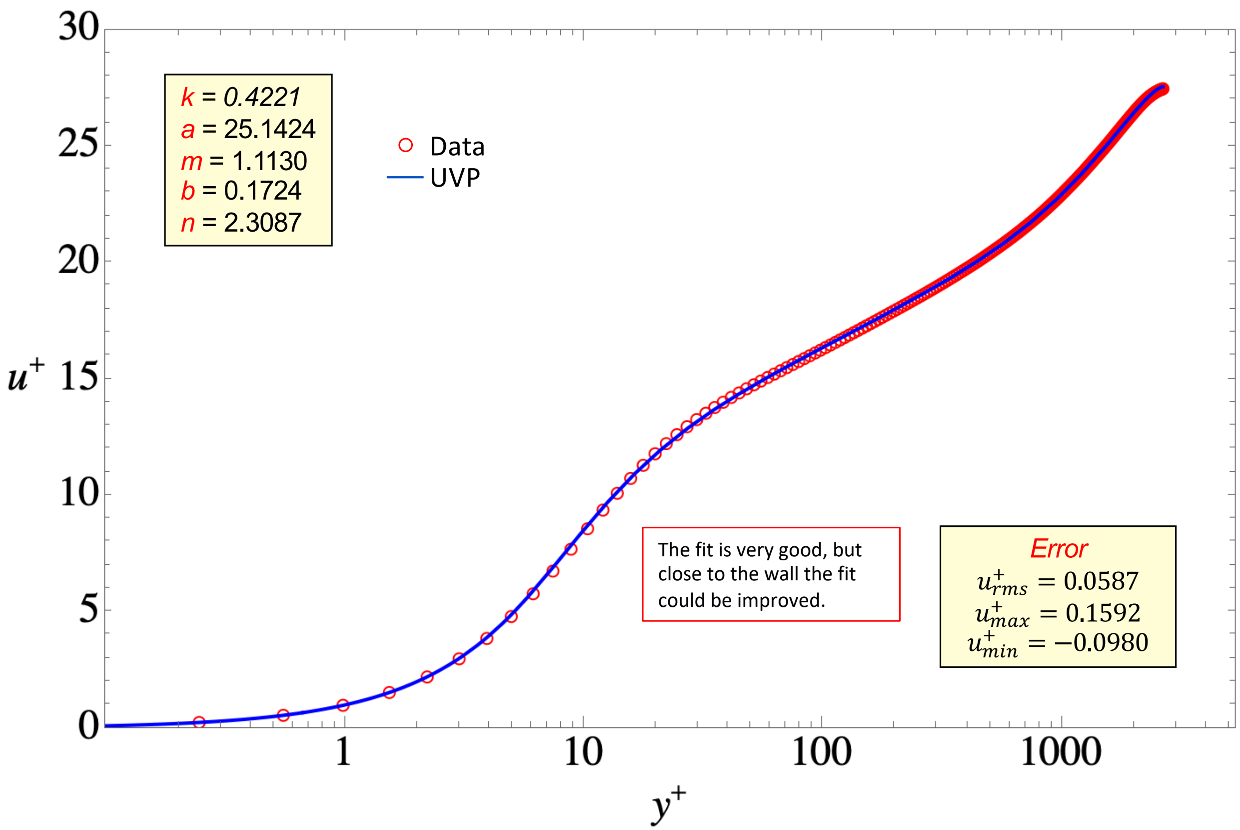

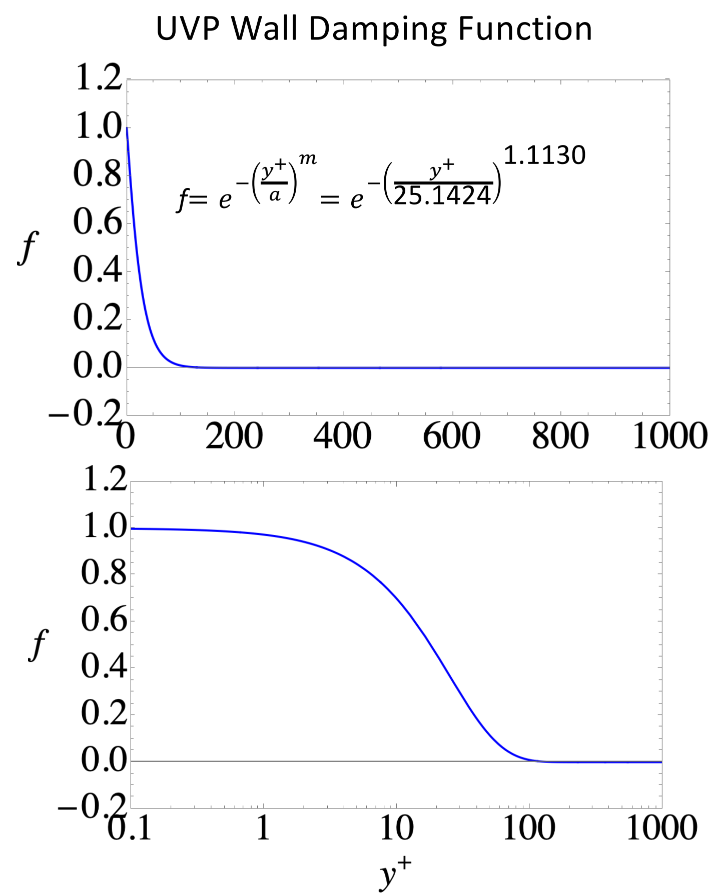

$R_\tau = 2652$ Velocity Derivative Comparison

Log Indicator Function y^+dU^+/dy^+

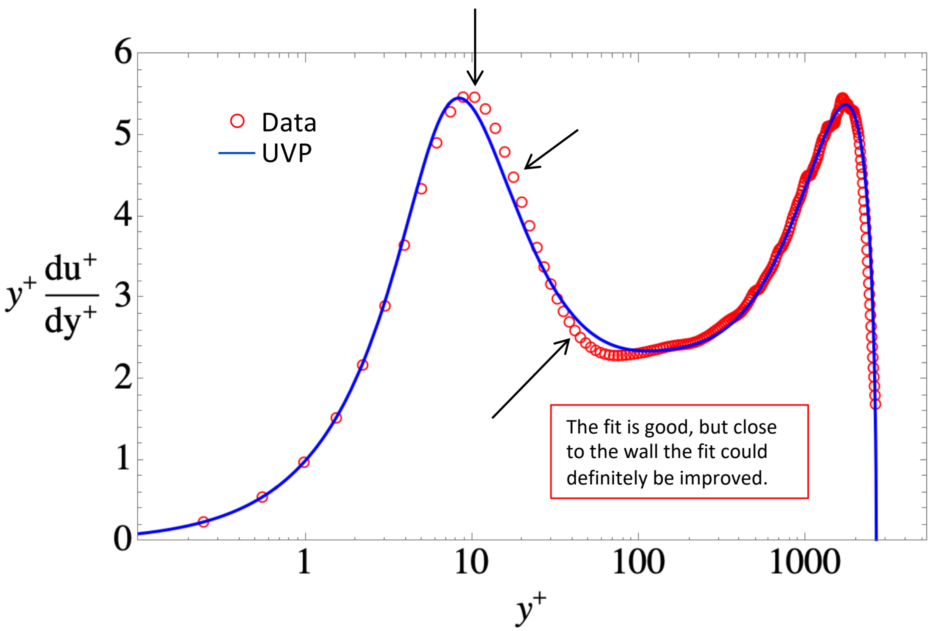

Velocity Derivative dU^+/dy^+

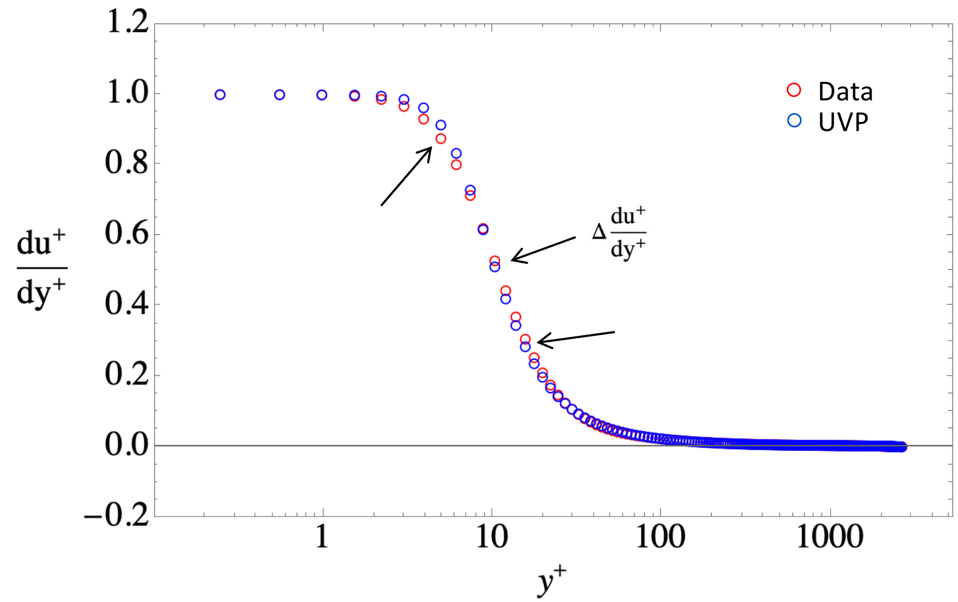

Error in the $R_\tau = 2652$ velocity derivative

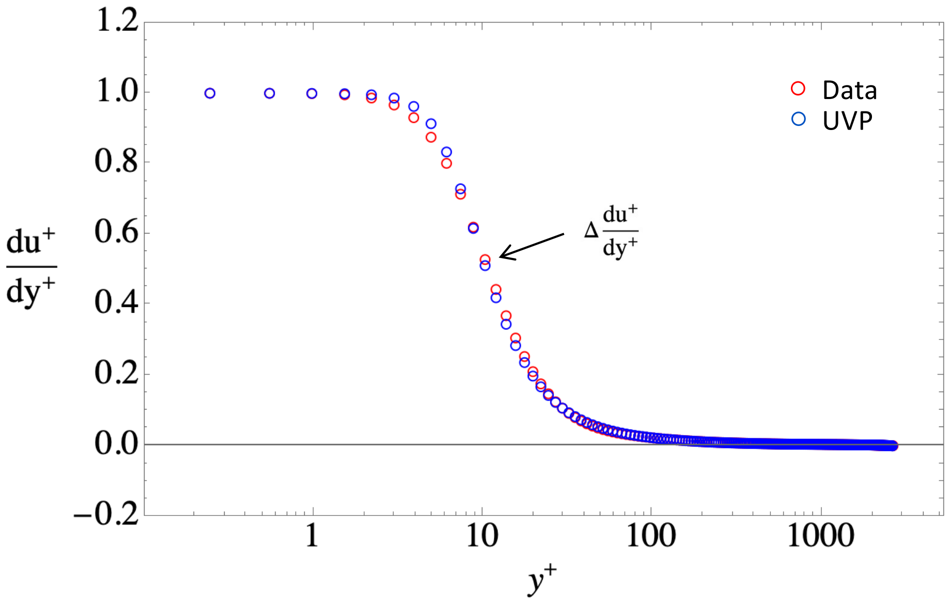

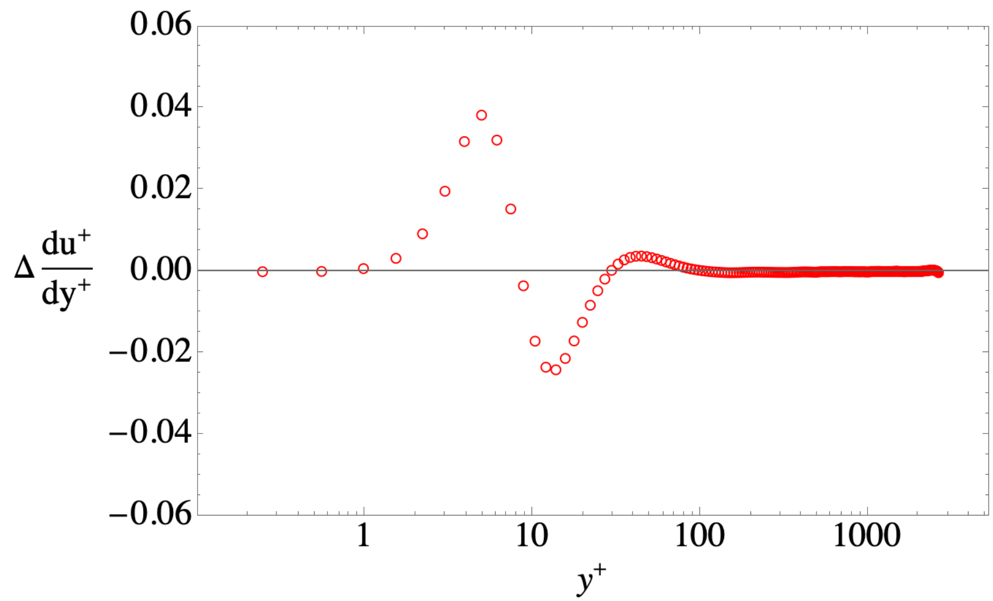

STANFORD
AERONAUTICS &
ASTRONAUTICS

UVP damping function

$$\lambda(y^+) = \frac{ky^+\left(1 - e^{-(y^+/a)^m}\right)}{\left(1 + \left(\frac{y^+}{bR_\tau}\right)^n\right)^{1/n}}$$

Ask:
What damping function would enable the UVP to match the $R_\tau = 2652$ data exactly?

Consider a generalized Wall Damping Function $\sigma(y^+/a)$. In effect, replace the two parameters, a and m in the function, $e^{-(y^+/a)^m}$, with just a damping length scale. The new damping length scale will still be designated *a*.

$$\lambda(y^+) = \frac{ky^+\left(1-\sigma\left(\frac{y^+}{a}\right)\right)}{\left(1+\left(\frac{y^+}{bR_\tau}\right)^n\right)^{1/n}}$$

What should we use for $\sigma(y^+/a)$?

$$\frac{du^+}{dy^+} = \frac{2\left(1-\frac{y^+}{R_\tau}\right)}{1+\left(1+4\left(\frac{ky^+\left(1-\sigma\left(\frac{y^+}{a}\right)\right)}{\left(1+\left(\frac{y^+}{bR_\tau}\right)^n\right)^{1/n}}\right)^2\left(1-\frac{y^+}{R_\tau}\right)\right)^{1/2}}$$

$$u^+(y^+) = \int_0^{y^+}\left[\frac{2\left(1-\frac{y^+}{R_\tau}\right)}{1+\left(1+4\left(\frac{ky^+\left(1-\sigma\left(\frac{y^+}{a}\right)\right)}{\left(1+\left(\frac{y^+}{bR_\tau}\right)^n\right)^{1/n}}\right)^2\left(1-\frac{y^+}{R_\tau}\right)\right)^{1/2}}\right]ds$$

STANFORD AERONAUTICS & ASTRONAUTICS

At each y_i^+ solve for the wall damping value, σ_i , in the UVP that exactly matches the derivative given by the data.

What should we use for $\sigma(y^+/a)$?

k = 0.4221, b = 0.1724, n = 2.3087

At each y_i^+ solve for σ_i.

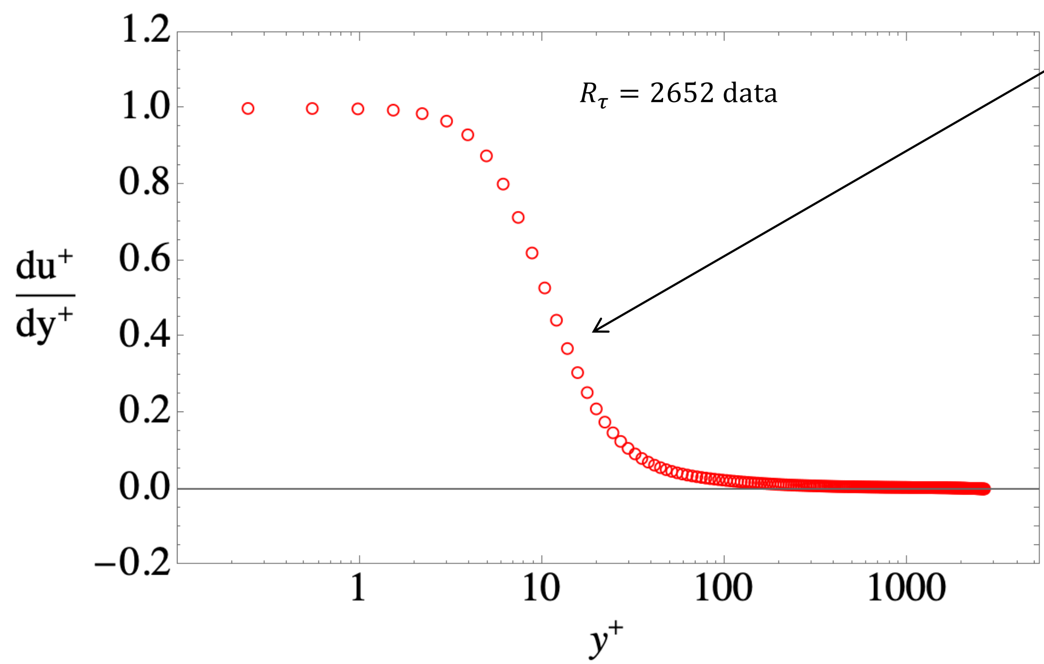

$$\left(\frac{du^+}{dy^+}\right)_i = \frac{2\left(1-\frac{y_i^+}{R_\tau}\right)}{1+\left(1+4\left(\frac{k y_i^+(1-\sigma_i)}{\left(1+\left(\frac{y_i^+}{bR_\tau}\right)^n\right)^{1/n}}\right)^2\left(1-\frac{y_i^+}{R_\tau}\right)\right)^{1/2}}$$

From data

The result is an exact match between the UVP and the data

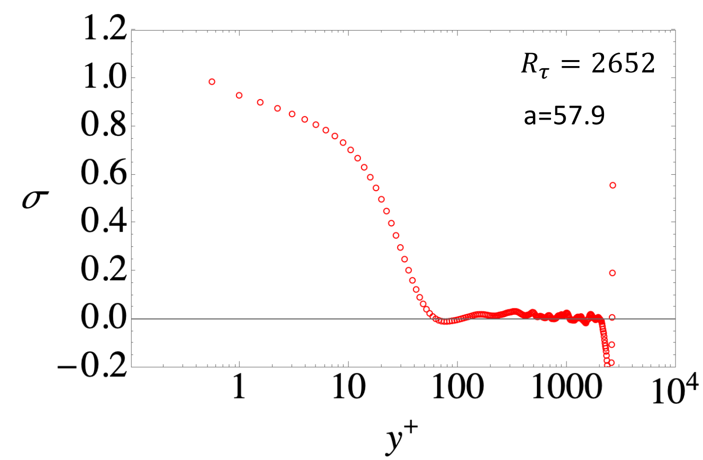

Comparison of old and new wall damping functions

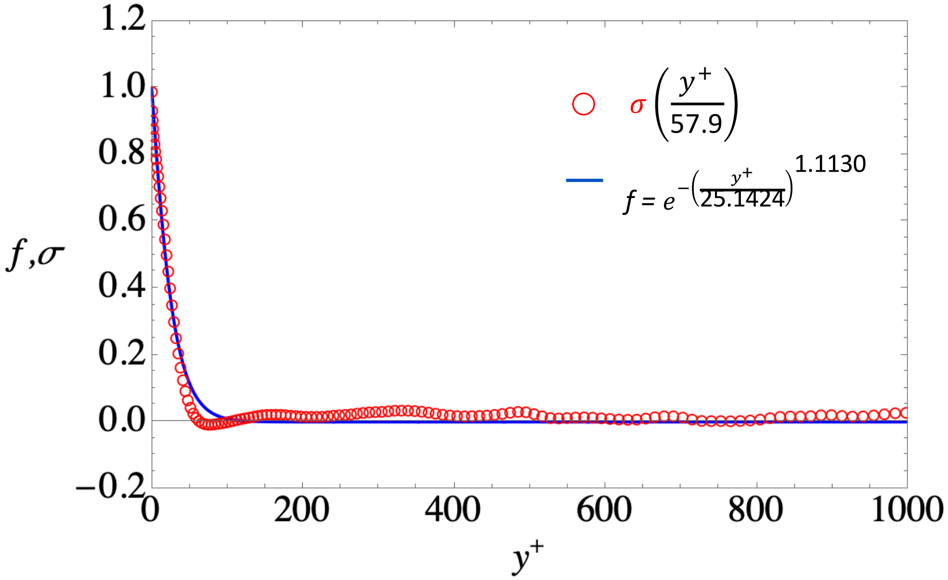

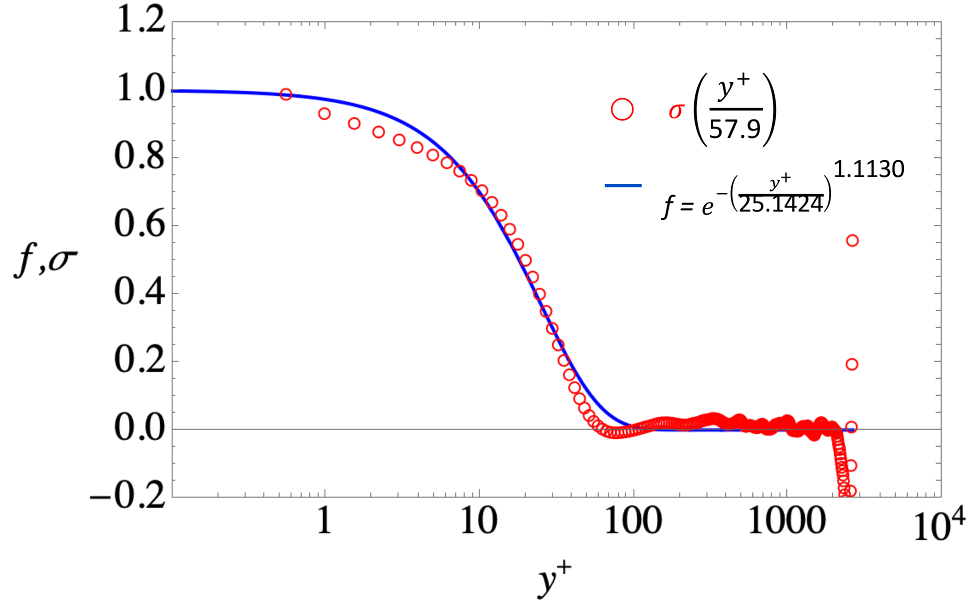

The new damping function decays faster than the van Driest-type exponential and it oscillates about zero several times.

STANFORD
AERONAUTICS & ASTRONAUTICS

Normalize the individual damping functions of 11 cases and average. Assume the average is a *Universal Wall Damping Function*.

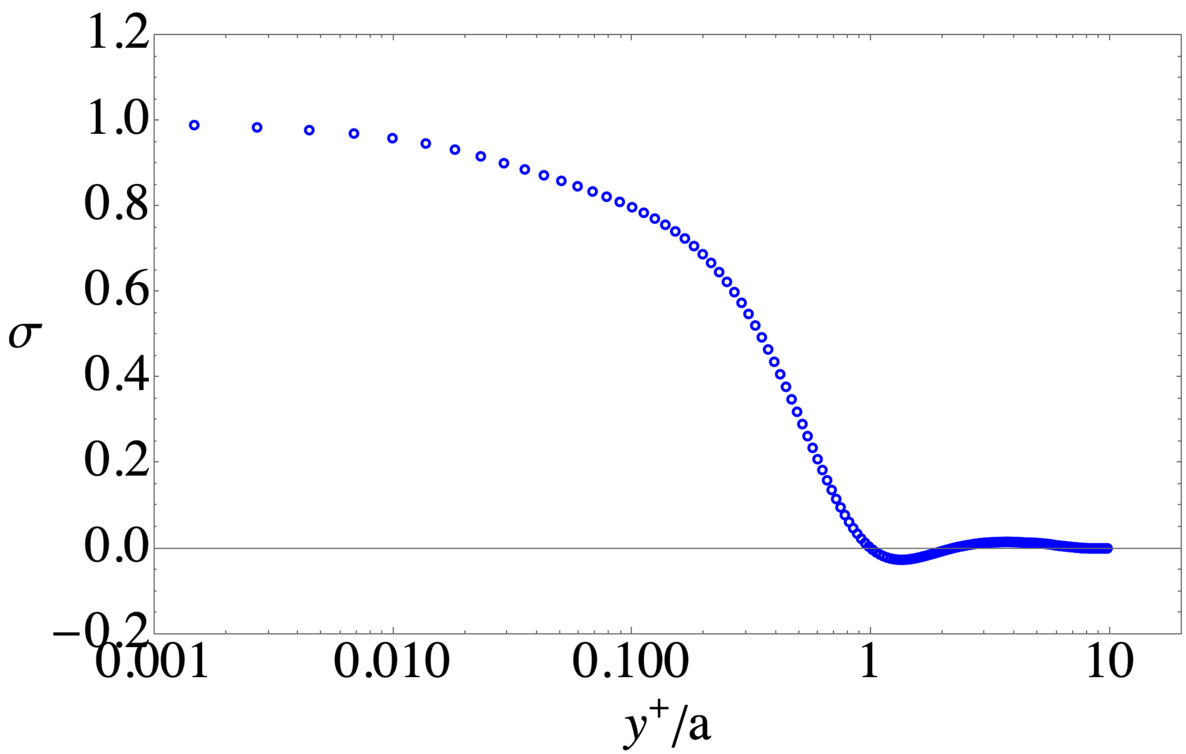

STANFORD
AERONAUTICS & ASTRONAUTICS

$R_\tau = 2652$ wall damping function compared to the Universal Wall Damping Function.

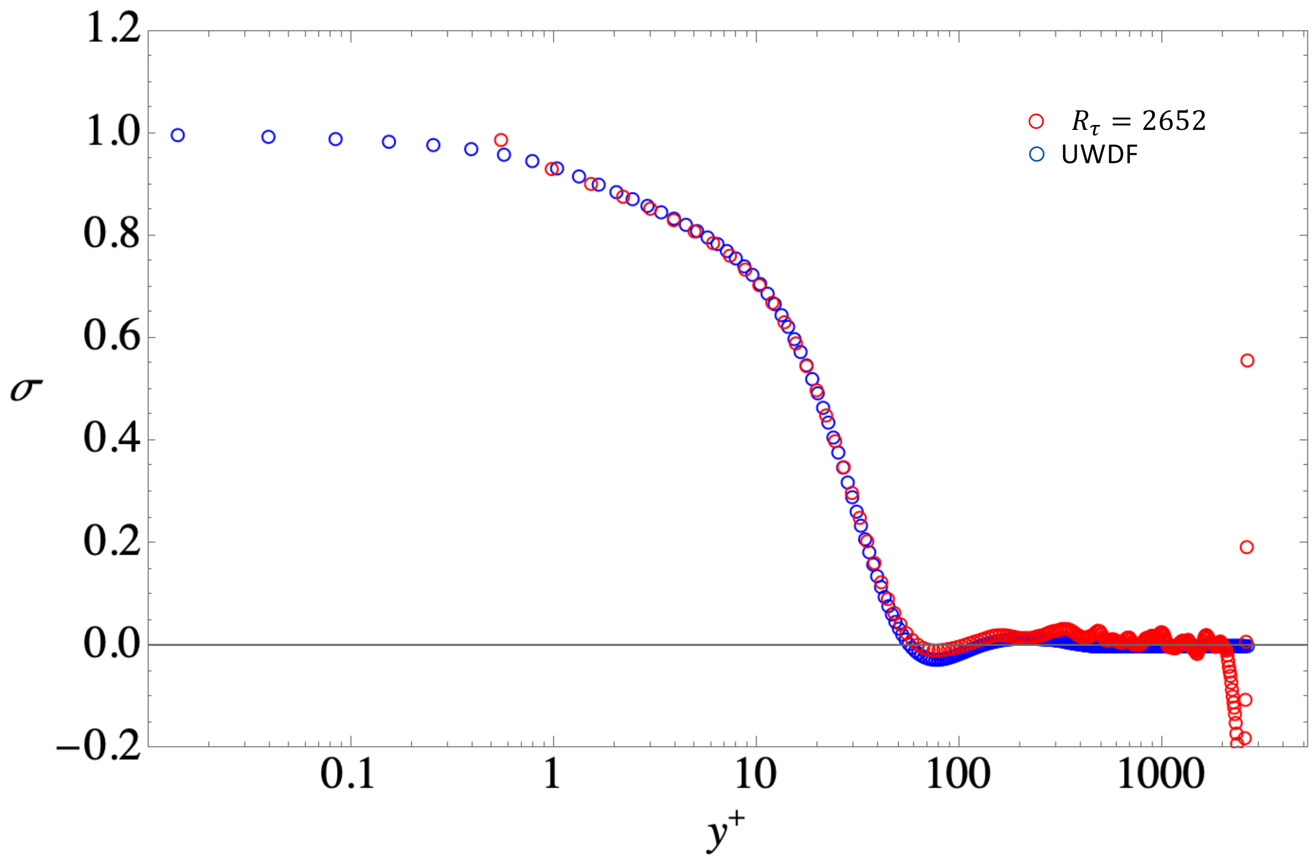

$R_\tau = 2652$ reduction in the velocity derivative error using $\sigma(y^+/a)$.

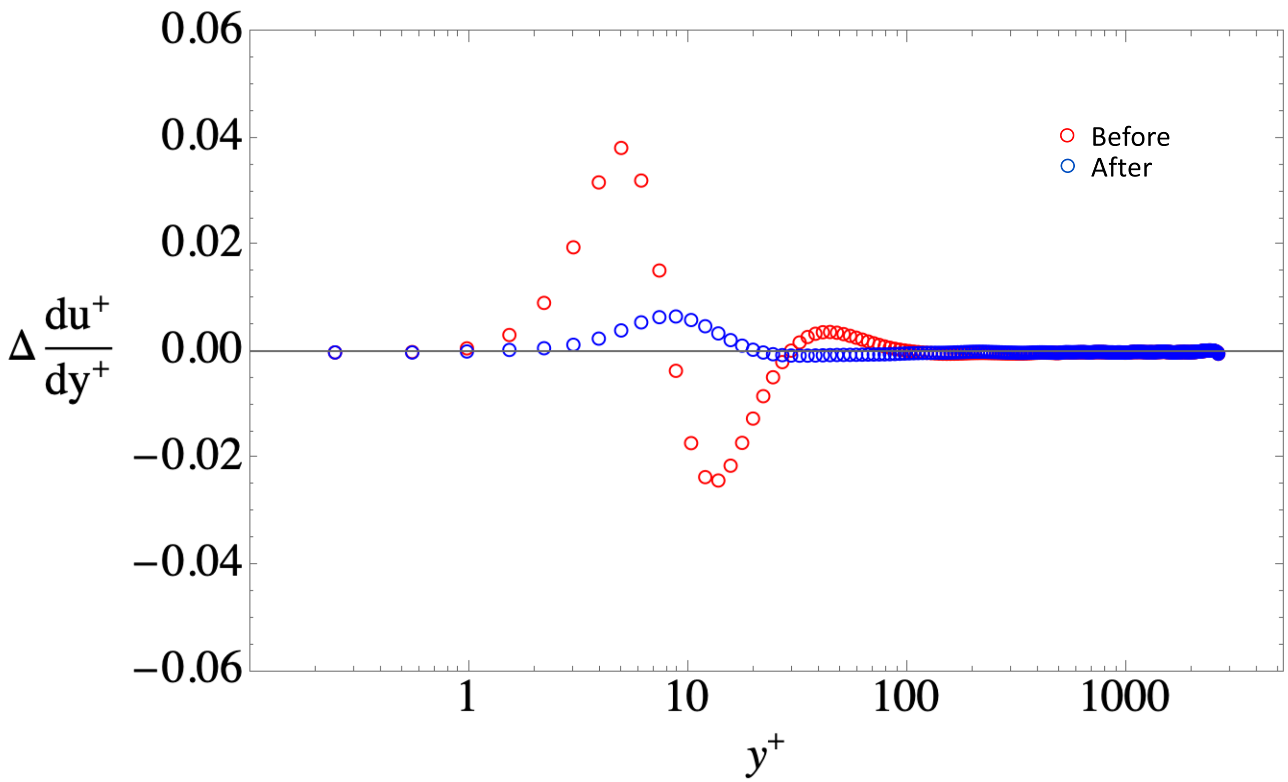

New mixing length function, λ/ky^+ versus R_τ using parameters from $R_\tau = 2652$ data

The new λ/ku^+ has a peak of 1.027 at $y^+ = 77.54$

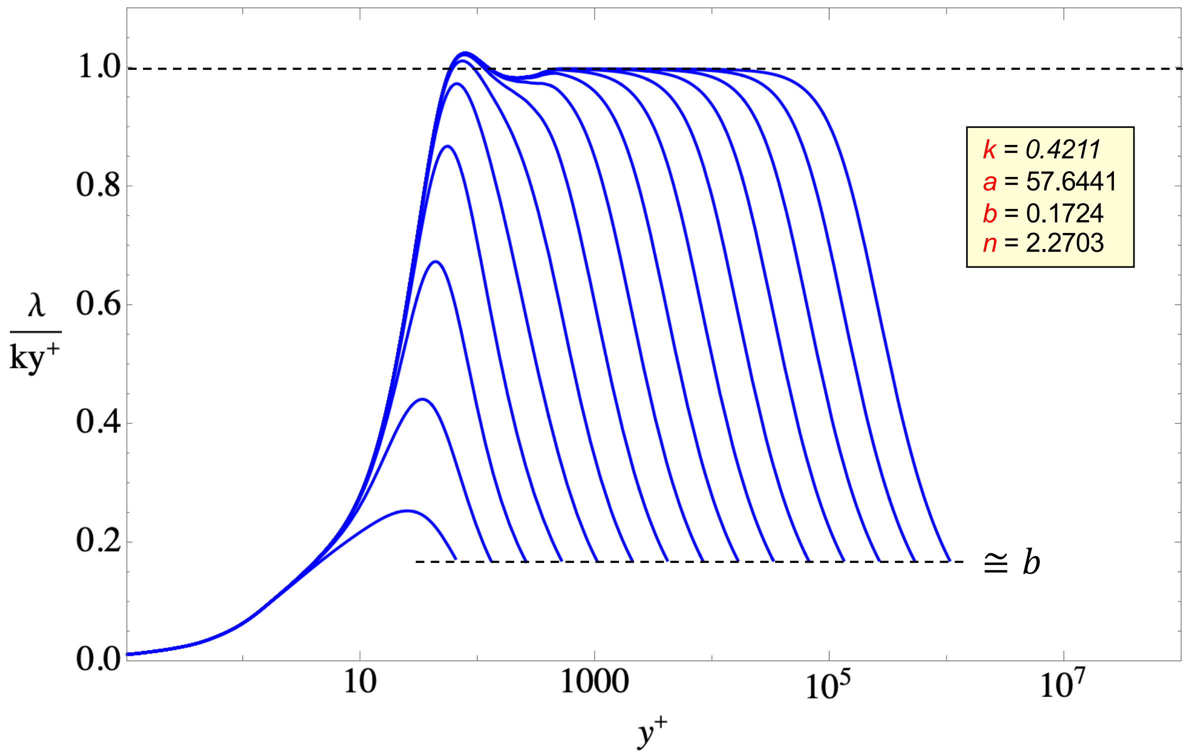

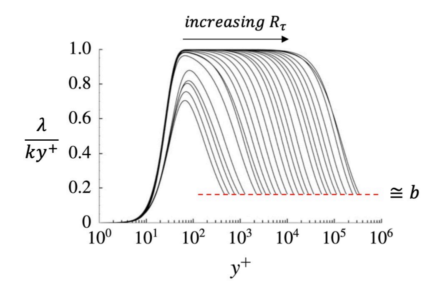

$R_\tau =$ 64, 128, 256, 512, 1024, 2048, 4096, 8192, 16384, 32768, 65536, 131072, 262144, 524288, 1,048576

Determination of best fit model parameters

Minimize G with respect to k, a, b, n

$$G = \sum_{i=1}^{N} \left(u^{+}(k, a, \not{m}, b, n, y_i^{+}) - u_i^{+}(y_i^{+})\right)^2$$

UVP with new damping function

DNS data

Finding the minimum is much easier with 4 parameters than with 5!

STANFORD AERONAUTICS & ASTRONAUTICS

$R_\tau = 2652$ reduction in the velocity error using $\sigma(y^+/a)$.

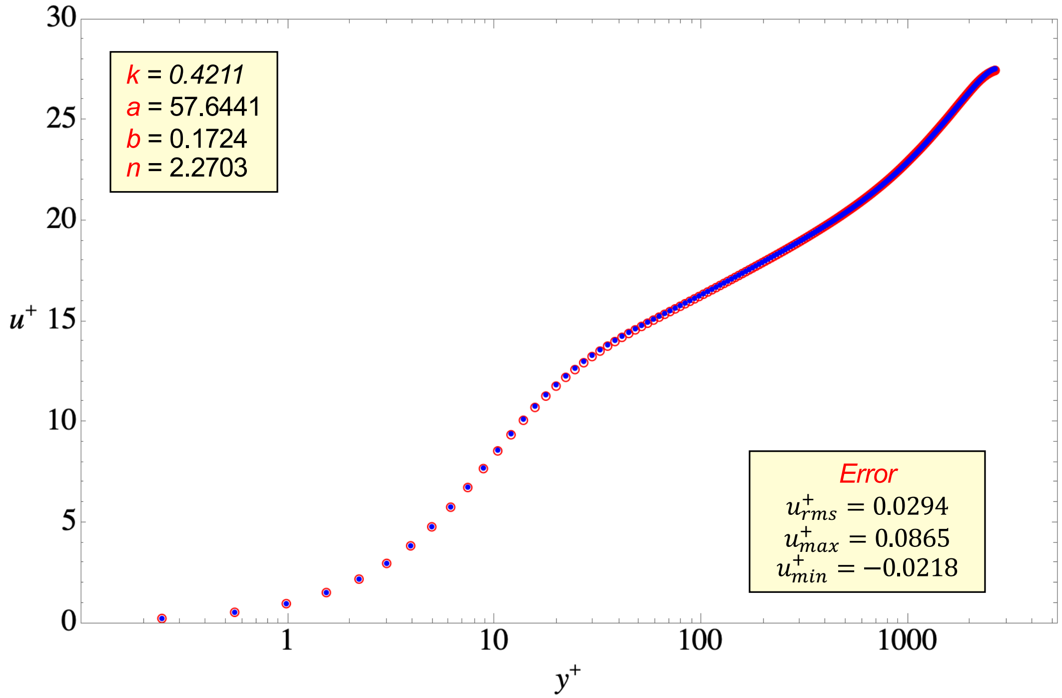

Optimum values of k, b and n remain about the same.

$k = 0.4221$
$a = 25.1424$
$m = 1.1130$
$b = 0.1724$
$n = 2.3087$

Previous error using the exponential damping function

Error
$u^+_{rms} = 0.0587$
$u^+_{max} = 0.1592$
$u^+_{min} = -0.0980$

$$u^+(y^+) = \int_0^{y^+} \left[\frac{2\left(1 - \frac{y^+}{R_\tau}\right)}{1 + \left(1 + 4\left(\frac{ky^+\left(1 - \sigma\left(\frac{y^+}{a}\right)\right)}{\left(1 + \left(\frac{y^+}{bR_\tau}\right)^n\right)^{1/n}}\right)^2 \left(1 - \frac{y^+}{R_\tau}\right)\right)^{1/2}} \right] ds$$

STANFORD AERONAUTICS & ASTRONAUTICS

$R_\tau = 2652,$ reduced error in the log indicator function.

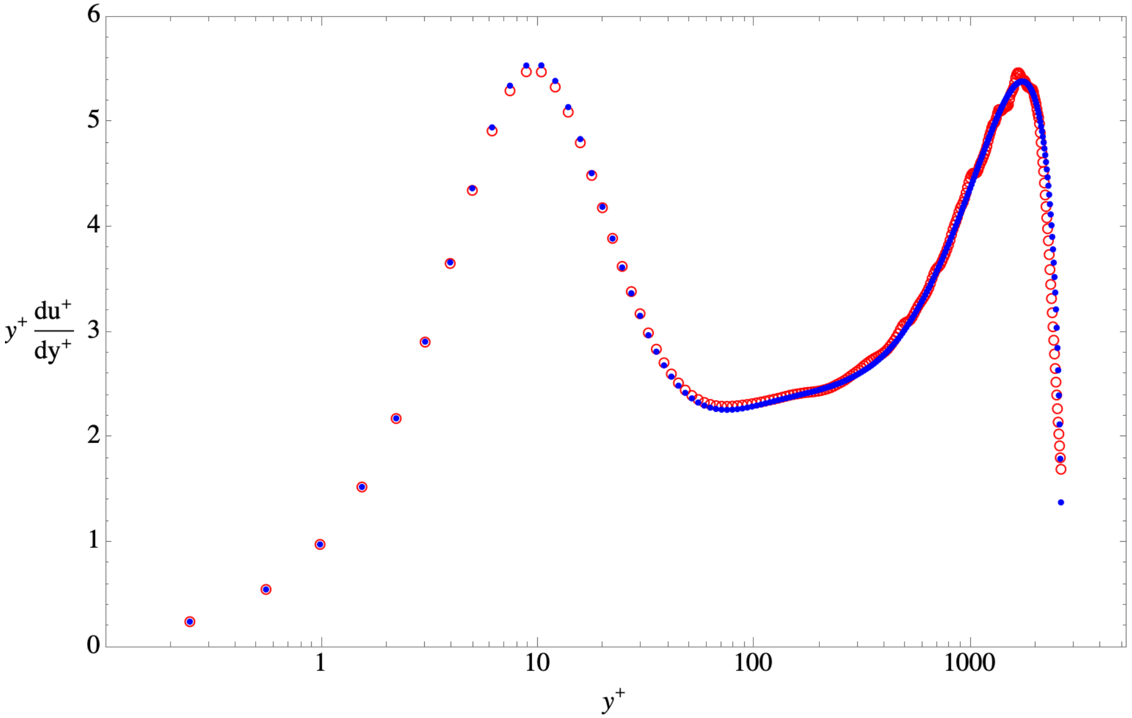

With exponential damping

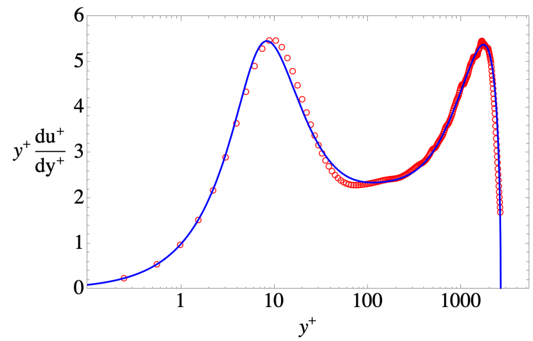

At low Reynolds number, when the error is small, further reducing the error to reach a minimum might not produce the most accurate value of the friction.

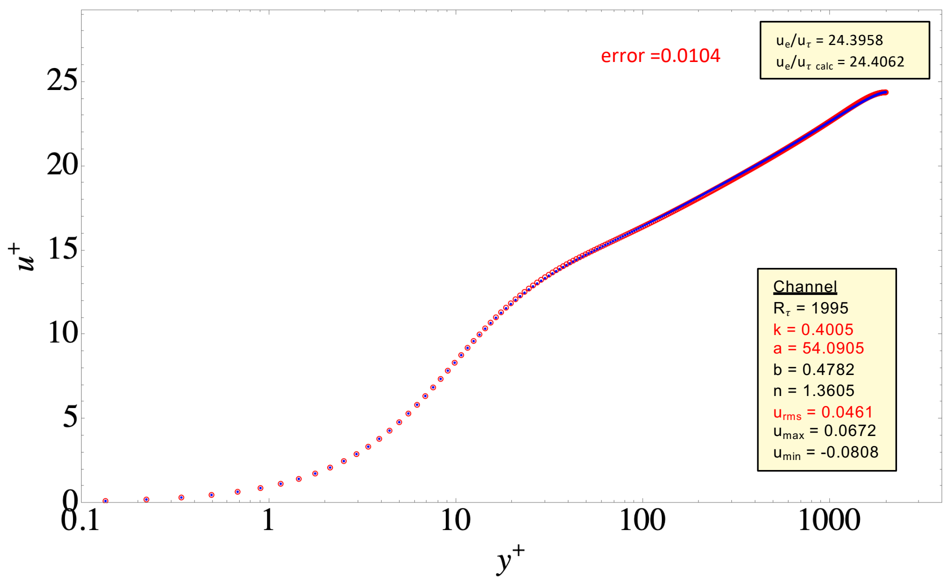

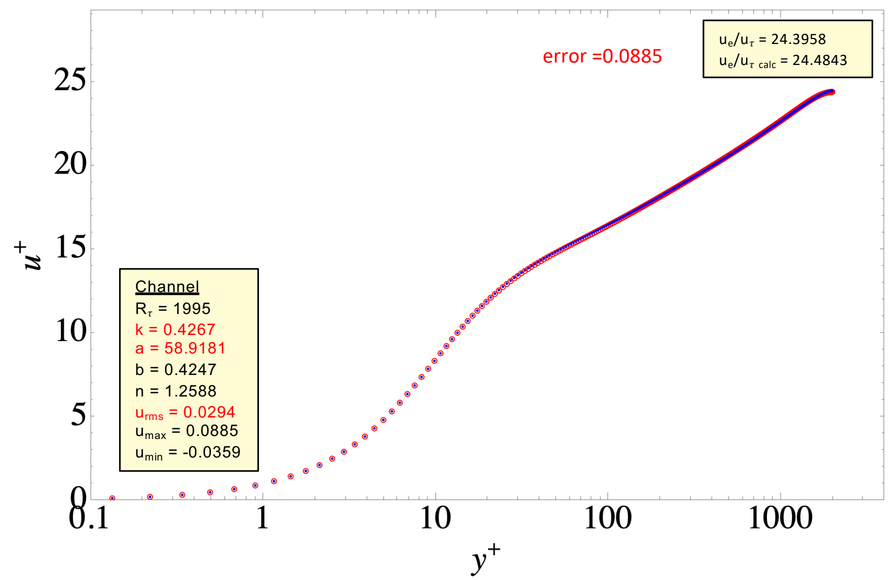

By not requiring the most extreme level of accuracy, a 'soft constraint' can be applied to *k* and *a* when minimizing the error. This may not be true at high Reynolds number, R_τ > 20,000. Experience suggests that for large R_τ the minima in parameter space may lie very close to one another.

STANFORD
AERONAUTICS & ASTRONAUTICS

R_τ	$\frac{u_e}{u_\tau}_{data}$	$\frac{u_e}{u_\tau}_{uvp}$	k	a	b	n	u^+_{rms}	u^+_{max}	u^+_{min}
543.500	21.0003	21.0081	0.4020	54.9869	0.5112	1.3415	0.0554	0.0760	-0.1141
1000.51	22.5929	22.5875	0.4010	54.5329	0.5002	1.3525	0.0583	0.0922	-0.0797
1995.00	24.3958	24.4062	0.4005	54.0905	0.4782	1.3605	0.0461	0.0672	-0.0808
4078.86	25.9545	26.0442	0.4030	54.0763	0.4474	1.4582	0.0429	0.0897	-0.0549
4178.88	25.9565	25.9685	0.3956	53.5765	0.5180	1.5004	0.0419	0.0980	-0.0738
5185.90	26.5753	26.6711	0.3970	53.3417	0.4441	1.5680	0.0333	0.0958	-0.0380
7996.01	27.3808	27.4701	0.3964	50.3149	0.5578	1.3171	0.0286	0.0320	-0.1510

Channel

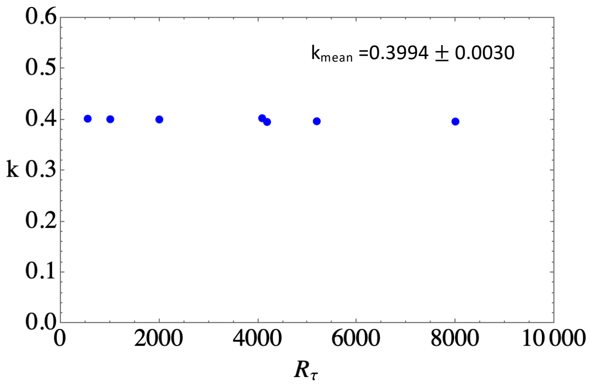

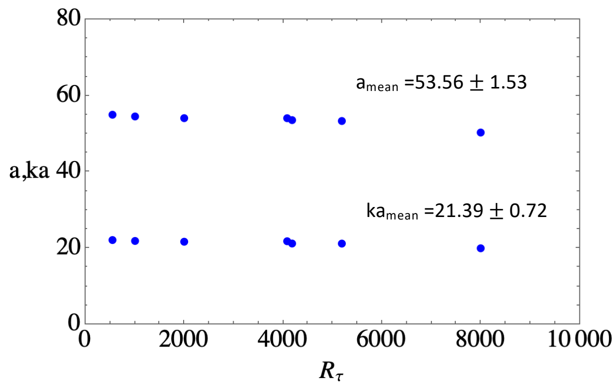

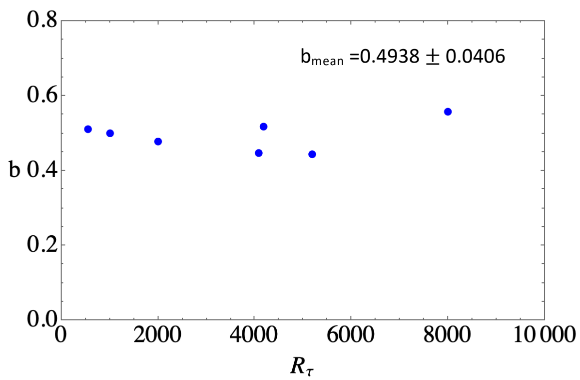

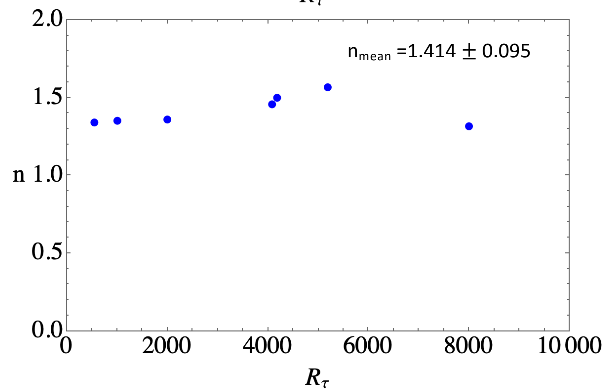

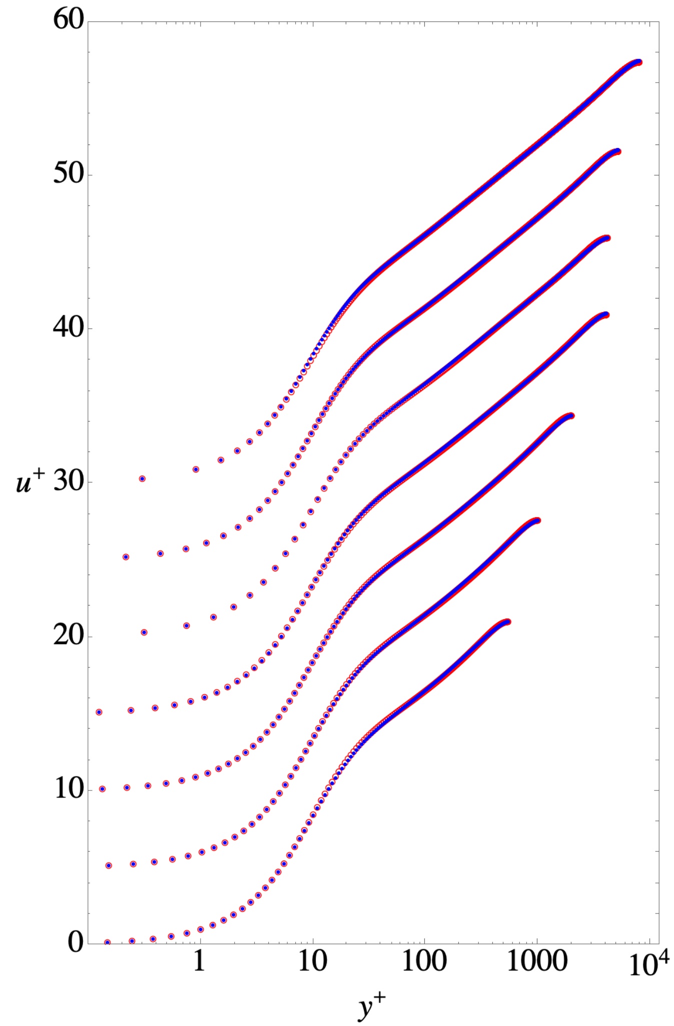

STANFORD AERONAUTICS & ASTRONAUTICS

Channel turbulence from simulations

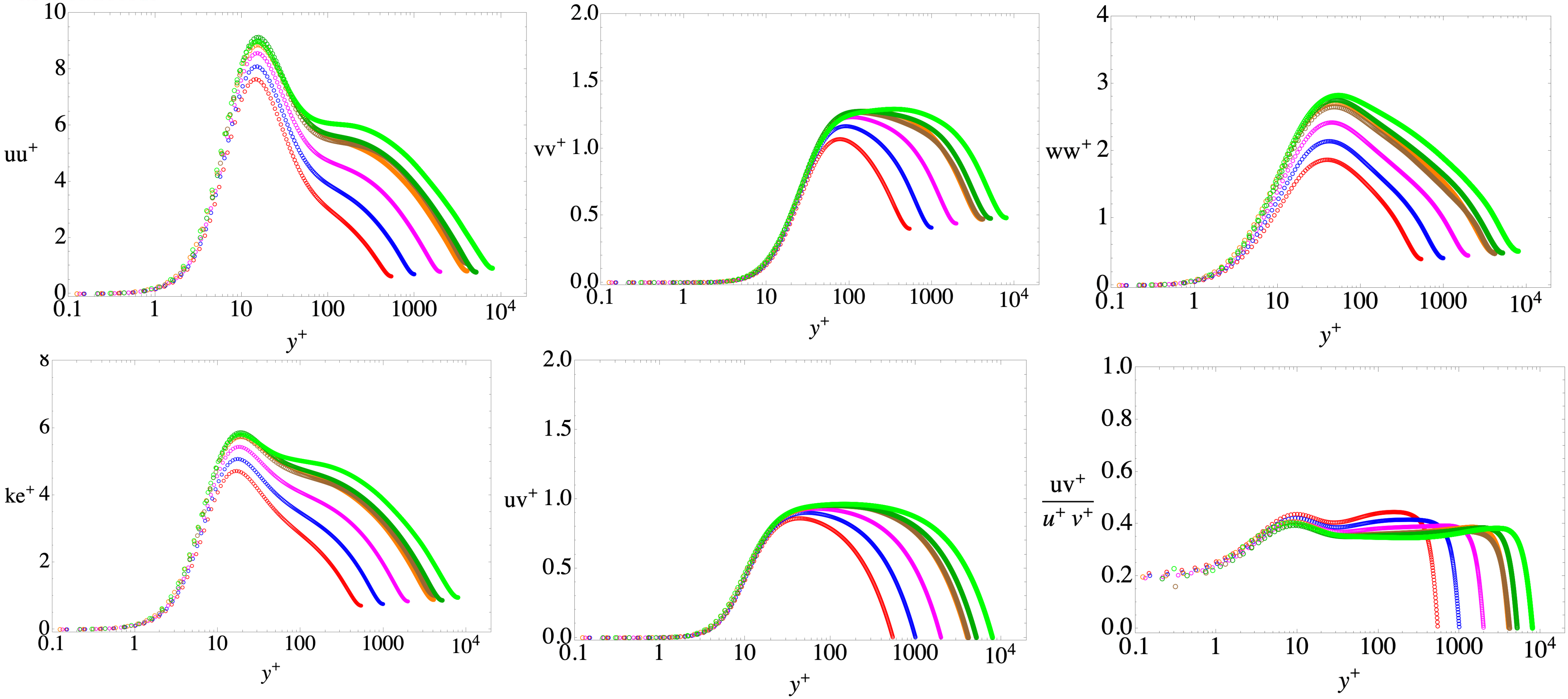

$R_\tau =$ 544, 1001, 1995, 4079, 4179, 5186, 7996

STANFORD
AERONAUTICS & ASTRONAUTICS

PSP Pipe

$PSP\#$	R_τ	$\frac{u_e}{u_\tau}_{data}$	$\frac{u_e}{u_\tau}_{uvp}$	k	a	b	n	u^+_{rms}	u^+_{max}	u^+_{min}
1	850.947	23.0788	23.0187	0.4054	55.3277	0.3692	1.3354	0.1402	0.3014	-0.3515
2	1090.56	23.6738	23.6043	0.4034	54.3234	0.3672	1.3494	0.1646	0.2090	-0.3306
3	1430.26	24.3436	24.2704	0.4034	54.1727	0.3702	1.3414	0.1672	0.2907	-0.3662
4	1824.72	24.9410	24.9194	0.4034	54.1146	0.3652	1.3434	0.0858	0.2004	-0.1615
5	2344.74	25.5345	25.4860	0.4054	54.3996	0.3642	1.3474	0.1488	0.2040	-0.3920
6	3327.37	26.1918	26.2473	0.4034	52.0356	0.3652	1.3354	0.1041	0.3163	-0.2044
7	4124.89	26.8018	26.8141	0.4031	54.5318	0.3405	1.5196	0.1070	0.1782	-0.2879
8	5108.56	27.2840	27.3753	0.4005	52.3625	0.3651	1.3751	0.0810	0.3327	-0.1265
9	6617.44	27.6954	27.8247	0.4061	53.2176	0.3436	1.4587	0.0644	0.2168	-0.1345
10	8536.62	28.3537	28.4962	0.4055	53.4499	0.3367	1.4930	0.0644	0.2306	-0.1264
11	10914.38	28.8432	28.9788	0.4062	53.8116	0.3260	1.6086	0.0484	0.1355	-0.1115
12	14848.87	29.6175	29.7748	0.4055	53.7105	0.3201	1.6423	0.0570	0.1574	-0.1430
13	19778.30	30.2906	30.4074	0.4055	53.8858	0.3271	1.6513	0.0441	0.1167	-0.1035
14	25278.07	30.8868	30.9618	0.4060	54.4156	0.3191	1.7531	0.0417	0.0750	-0.1466
15	32869.08	31.5881	31.6753	0.4053	53.6086	0.3212	1.6723	0.0538	0.0872	-0.1675
16	42293.51	32.2268	32.3582	0.4062	54.0781	0.3098	1.7132	0.0647	0.1427	-0.1257
17	54530.62	32.7430	32.8613	0.4080	54.3395	0.3127	1.7132	0.0714	0.2227	-0.1163
18	76479.83	33.4563	33.4893	0.4099	54.7671	0.3250	1.7014	0.0860	0.2524	-0.2771
19	102200.19	34.2462	34.2870	0.4099	54.4778	0.3180	1.6763	0.0774	0.2345	-0.1674
20	127913.55	34.8458	34.9315	0.4101	54.6843	0.3135	1.6546	0.0755	0.2213	-0.1830
21	165704.41	35.5102	35.5322	0.4102	54.7826	0.3159	1.6586	0.0597	0.2218	-0.1154
22	216978.54	36.0106	36.0936	0.4161	55.7691	0.2962	1.6731	0.0707	0.2942	-0.0967
23	284254.01	36.5586	36.6758	0.4175	55.8720	0.2953	1.6668	0.0596	0.1996	-0.1084
24	366972.50	36.8963	37.0508	0.4187	57.2946	0.3054	1.7693	0.1015	0.1574	-0.2655
25	452379.62	37.3313	37.5257	0.4193	57.0466	0.3060	1.7364	0.0740	0.1944	-0.1704
26	530023.42	37.9002	38.1287	0.4190	55.7425	0.3215	1.4689	0.0974	0.2794	-0.1186

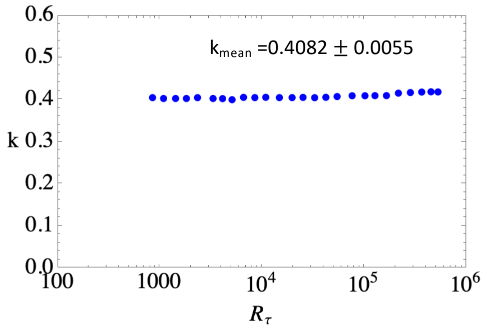

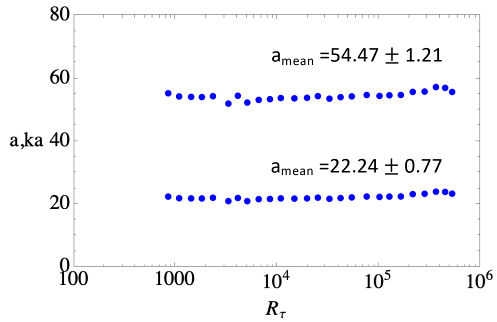

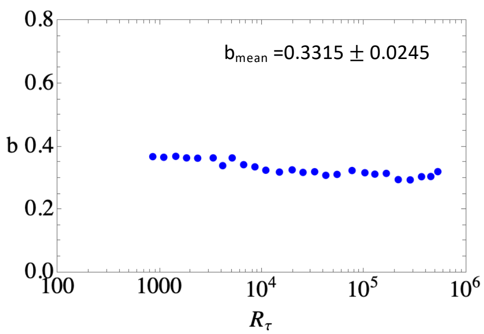

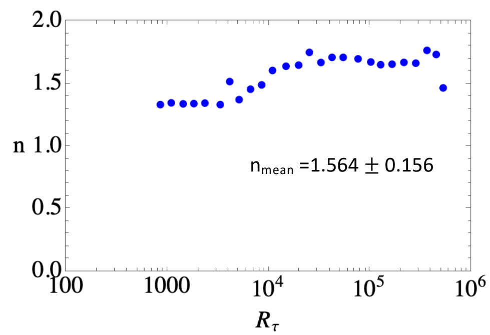

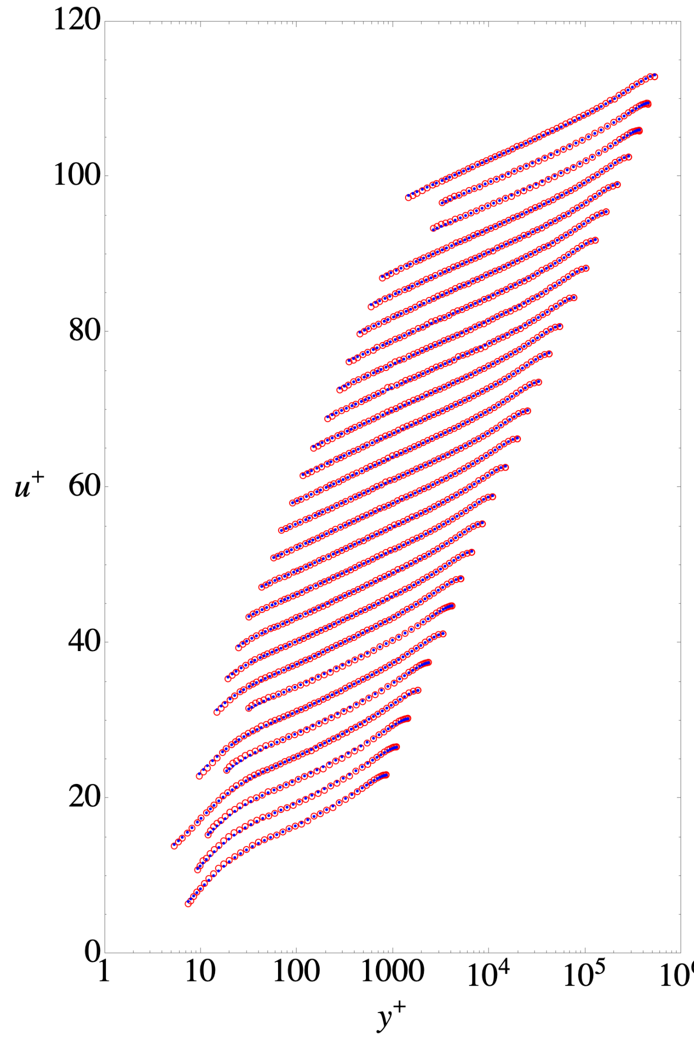

STANFORD
AERONAUTICS & ASTRONAUTICS

ZPGTBL

R_τ	$\frac{u_e}{u_\tau}_{data}$	$\frac{u_e}{u_\tau}_{uvp}$	k	a	b	n	u^+_{rms}	u^+_{max}	u^+_{min}	$\frac{u_e}{U}$
1383.36	25.5602	25.6151	0.4202	58.6033	0.1828	2.3718	0.0294	0.0655	-0.0381	0.995
1516.99	25.9827	25.9999	0.4205	58.9419	0.1787	2.3842	0.0327	0.0635	-0.0420	0.995
1660.91	26.3251	26.3489	0.4200	58.7051	0.1764	2.3328	0.0237	0.0410	-0.0339	0.995
1806.16	26.6193	26.6304	0.4207	58.7189	0.1757	2.2392	0.0197	0.0402	-0.0337	0.995
1955.32	26.8496	26.8544	0.4211	58.8018	0.1747	2.2373	0.0184	0.0356	-0.0385	0.995
2104.15	27.0464	27.0652	0.4211	58.8125	0.1727	2.2933	0.0150	0.0383	-0.0167	0.995
2651.82	27.4729	27.5508	0.4211	57.6441	0.1724	2.2703	0.0294	0.0218	-0.0865	0.995
2077.23	26.7834	26.7838	0.4207	57.4787	0.1775	2.2416	0.0494	0.0782	-0.1488	0.995
4199.96	28.8297	28.8929	0.4205	57.3455	0.1685	2.1976	0.0850	0.1971	-0.1379	0.995
8708.43	30.5176	30.6446	0.4205	57.7037	0.1715	2.1045	0.1476	0.3032	-0.2258	0.995
16711.52	32.0348	32.2518	0.4191	57.0626	0.1856	1.7177	0.1780	0.2853	-0.2620	0.995

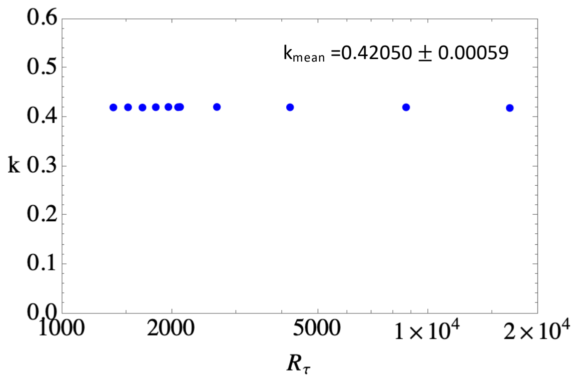

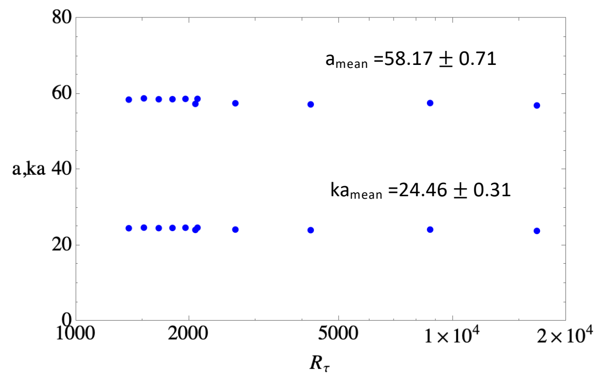

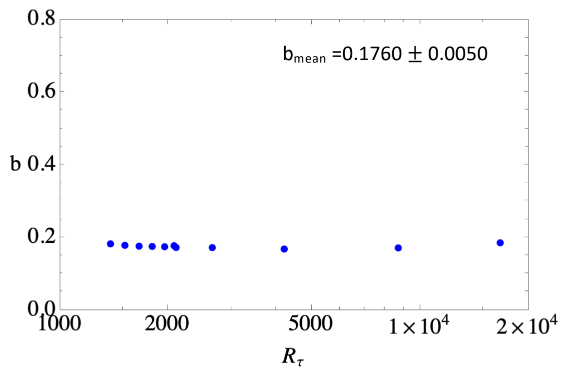

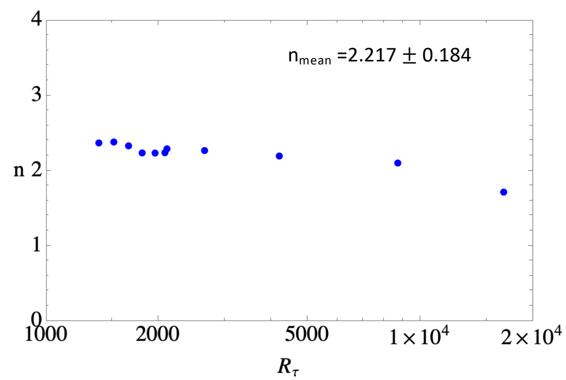

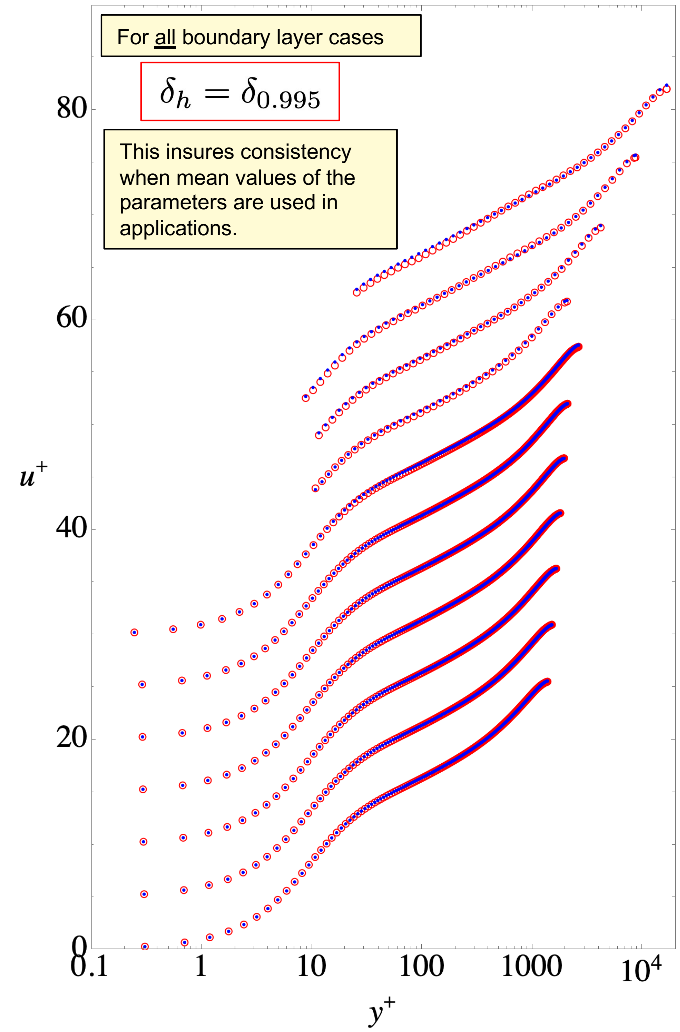

STANFORD AERONAUTICS & ASTRONAUTICS

ZPGTBL turbulence from simulations

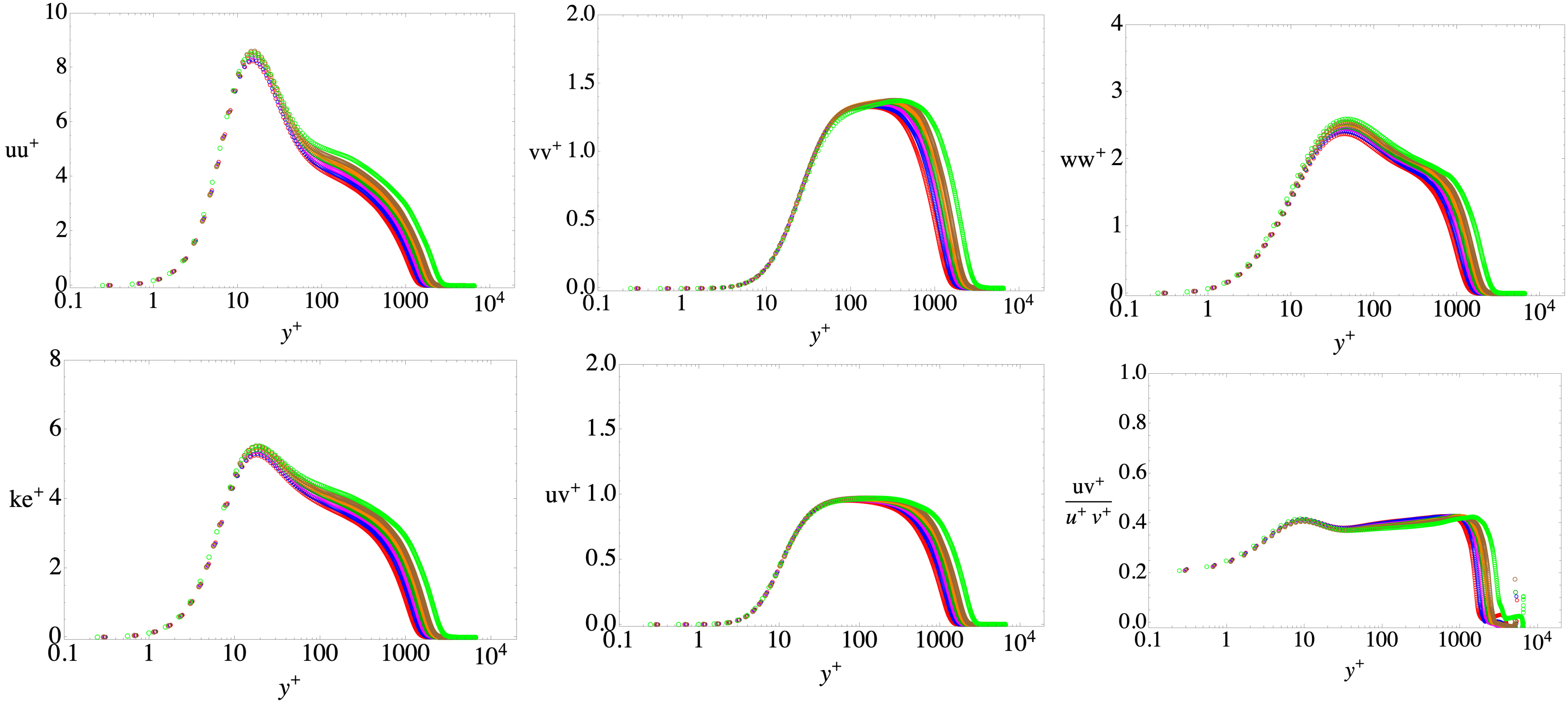

$R_\tau =$ 1383, 1517, 1661, 1806, 1955, 2104, 2652

STANFORD AERONAUTICS & ASTRONAUTICS

R_τ	$\frac{u_e}{u_\tau}_{data}$	$\frac{u_e}{u_\tau}_{uvp}$	k	a	b	n	u^+_{rms}	u^+_{max}	u^+_{min}	$\frac{u_e}{U}$
840.788	23.4405	23.5363	0.4215	56.7993	0.1992	2.5400	0.0796	0.1111	-0.1701	0.995
1082.73	25.2970	25.3327	0.4225	56.5478	0.1836	1.8138	0.1024	0.1403	-0.2467	0.995
1128.48	27.9189	27.9205	0.4223	57.3206	0.1237	2.7091	0.0964	0.2086	-0.2439	0.995
1188.00	31.3791	31.0872	0.4195	55.3516	0.0983	2.2553	0.1771	0.2975	-0.2918	0.995
1233.35	34.3316	34.1980	0.4225	56.6264	0.0770	3.7015	0.1667	0.2862	-0.3337	0.995
1199.70	38.0131	37.5798	0.4201	56.0683	0.0641	4.6239	0.2884	0.5872	-0.4433	0.995
2294.49	26.2558	26.2637	0.4195	54.8484	0.2180	1.7118	0.0819	0.1196	-0.1950	0.995
2693.75	28.0896	28.1486	0.4212	55.8802	0.1696	1.7915	0.0384	0.0741	-0.1007	0.995
2972.75	29.9626	30.0105	0.4214	56.0065	0.1334	2.0693	0.0516	0.0636	-0.1271	0.995
3204.70	32.7188	32.6572	0.4214	55.8777	0.1042	2.3448	0.0805	0.1439	-0.1591	0.995
3289.93	34.9745	34.6631	0.4211	56.2013	0.0897	2.6032	0.1590	0.2544	-0.3208	0.995
3370.72	37.8787	37.6014	0.4183	56.5134	0.0747	3.8665	0.1707	0.2846	-0.4330	0.995

AdvPGTBL

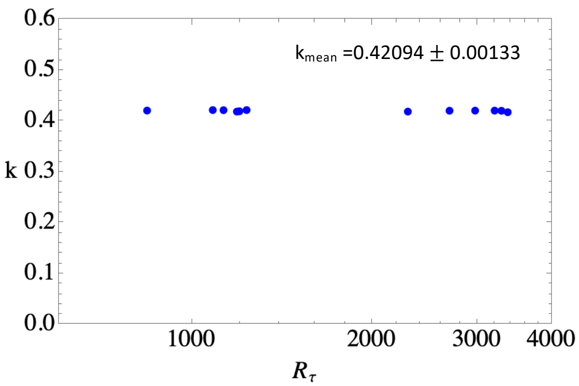

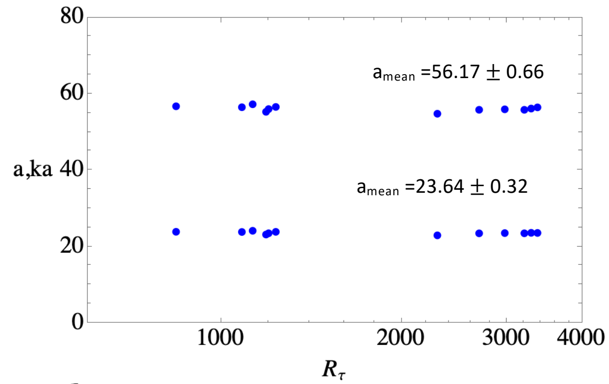

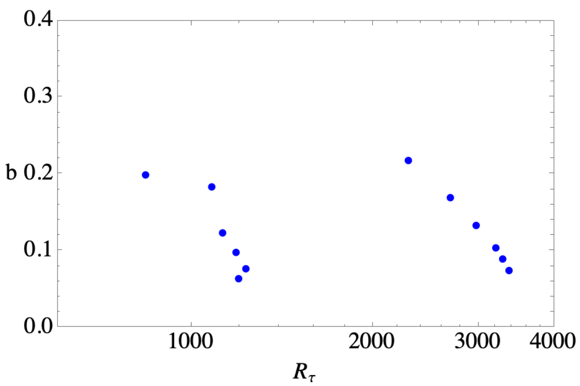

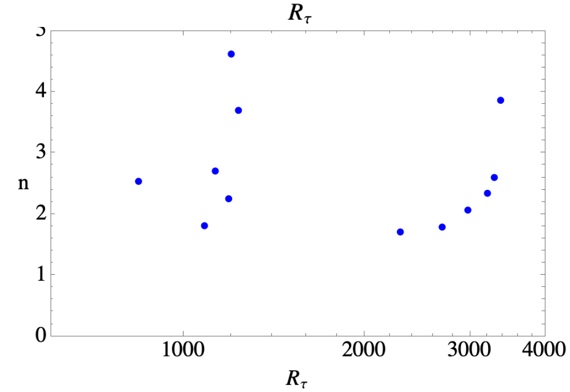

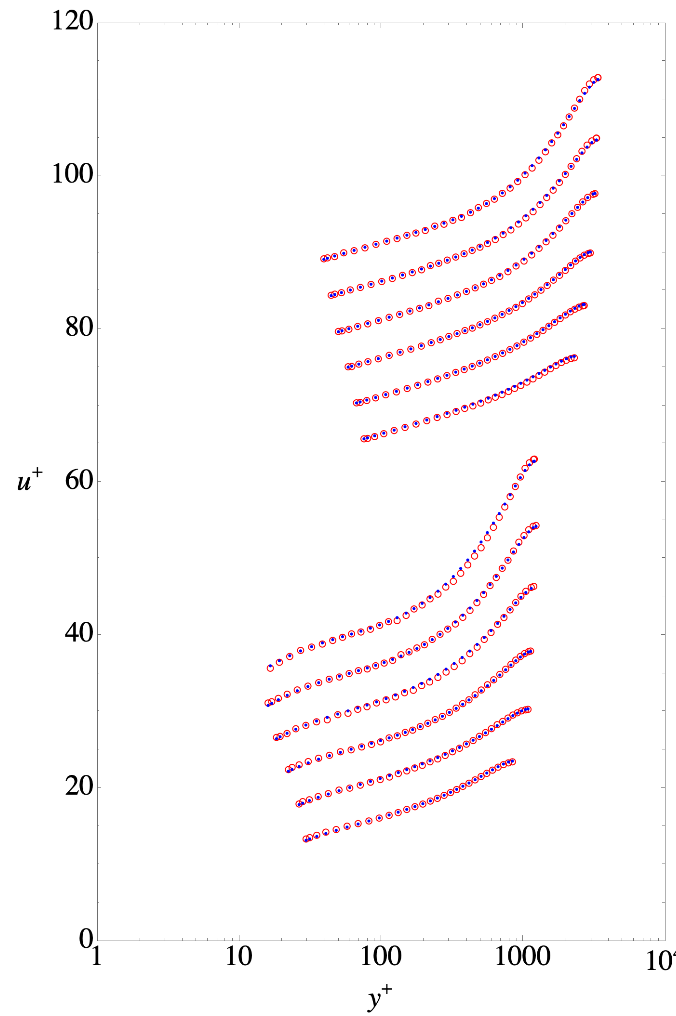

STANFORD AERONAUTICS & ASTRONAUTICS

R_τ	$\frac{u_e}{u_\tau}_{data}$	$\frac{u_e}{u_\tau}_{uvp}$	k	a	b	n	u^+_{rms}	u^+_{max}	u^+_{min}	$\frac{u_e}{U}$
429.39	20.1597	20.0852	0.4204	57.6329	0.4920	1.3805	0.0861	0.1577	-0.1210	0.995
666.20	20.7287	20.7431	0.4211	56.6151	0.5450	1.4265	0.0746	0.2021	-0.1149	0.995
696.78	20.8750	20.7386	0.4211	56.2556	0.5590	1.4445	0.0664	0.0913	-0.1364	0.995
837.26	21.1776	21.2092	0.4204	56.5069	0.5680	1.4405	0.0504	0.1764	-0.0847	0.995
937.18	21.3760	21.4448	0.4204	56.5698	0.5870	1.4315	0.0539	0.0900	-0.0906	0.995
1018.42	21.3920	21.4892	0.4214	57.2364	0.669	1.4125	0.0676	0.1057	-0.1350	0.995
546.03	21.1474	20.9520	0.4211	57.6327	0.4290	1.4025	0.0847	0.1585	-0.1954	0.995
783.15	21.6813	21.5114	0.4211	57.0318	0.4730	1.4125	0.0813	0.1599	-0.1699	0.995
940.33	21.8366	21.7718	0.4211	57.0327	0.4980	1.4225	0.0406	0.1033	-0.0648	0.995
1132.57	22.0424	22.1489	0.4208	57.2613	0.5450	1.4025	0.0499	0.1327	-0.0883	0.995
1273.59	22.2230	22.3037	0.4205	57.5810	0.6079	1.3825	0.0460	0.0982	-0.1190	0.995
1407.51	22.1511	22.2514	0.4197	57.5650	0.7447	1.3825	0.0500	0.1003	-0.0957	0.995
676.97	21.7204	21.6131	0.4213	57.0988	0.3915	1.4325	0.0880	0.2387	-0.1108	0.995
966.54	22.2435	22.1385	0.4213	56.6218	0.4360	1.4325	0.0667	0.1558	-0.1050	0.995
1144.22	22.4216	22.3211	0.4214	56.3373	0.4465	1.5025	0.0656	0.2158	-0.1005	0.995
1411.65	22.6737	22.7223	0.4210	57.0052	0.5263	1.4025	0.0426	0.0729	-0.0647	0.995
1533.96	22.9257	23.0538	0.4210	56.8663	0.5069	1.3725	0.0872	0.1769	-0.1126	0.995
1702.99	22.8822	23.0006	0.4200	56.9691	0.6029	1.3725	0.0921	0.1781	-0.1237	0.995

FavPGTBL

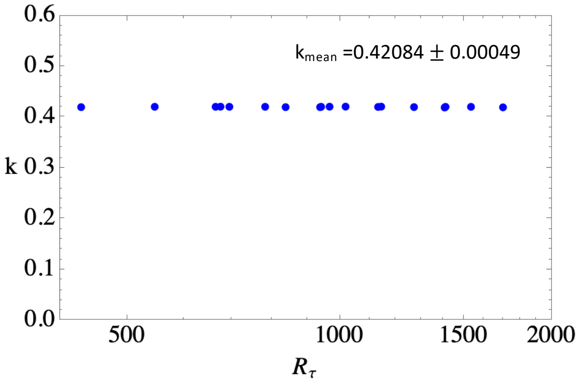

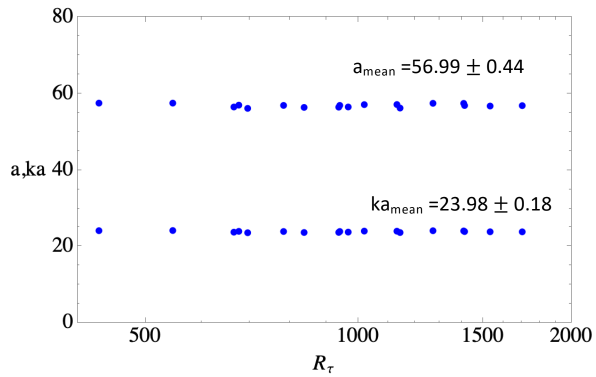

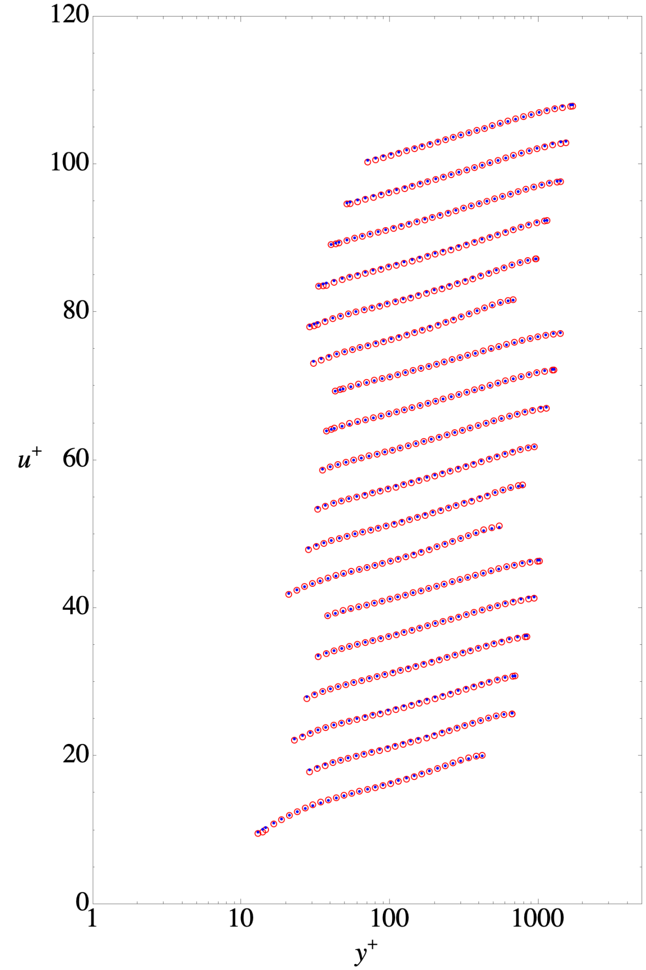

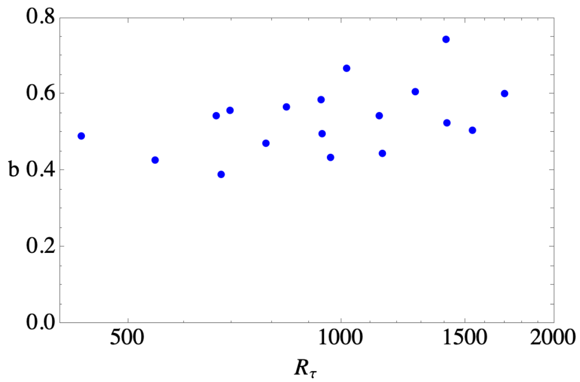

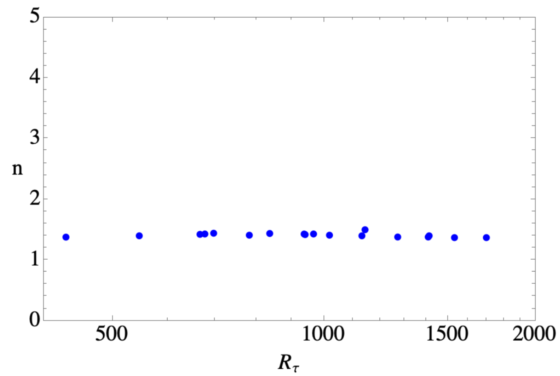

The boundary layer wall parameters *k* and *a* are approximately independent of Reynolds number and pressure gradient.

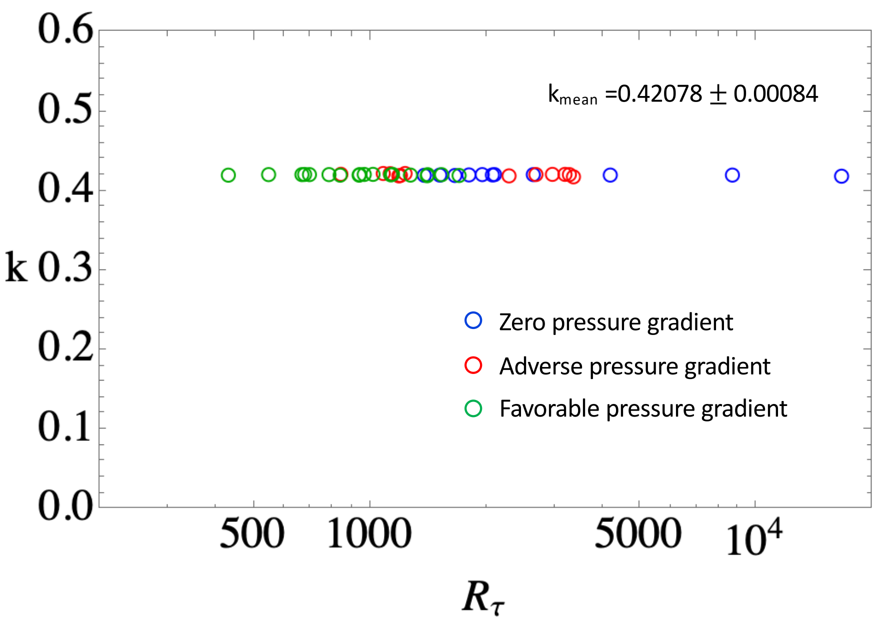

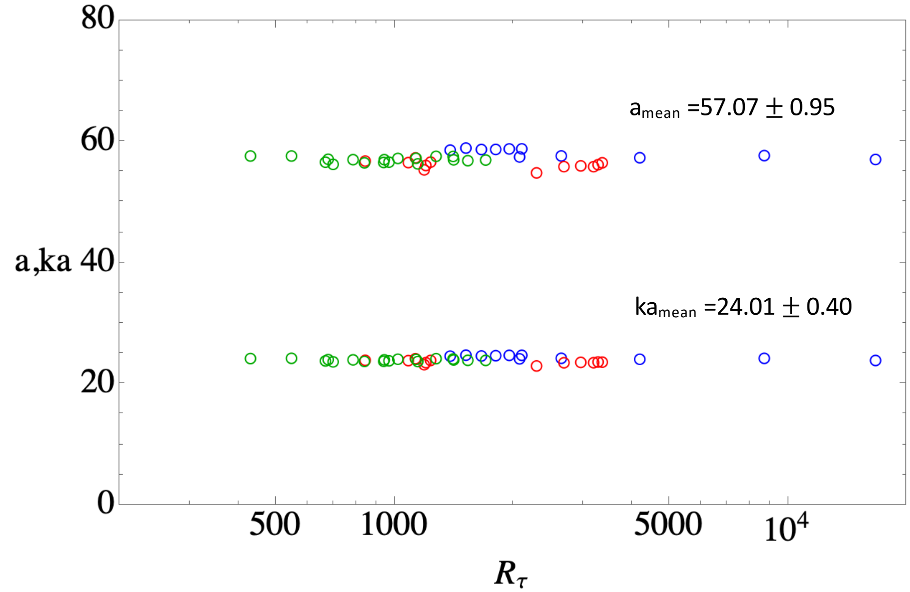

STANFORD
AERONAUTICS &
ASTRONAUTICS

A modified Clauser pressure gradient parameter

STANFORD
AERONAUTICS & ASTRONAUTICS

Begin with the von Kármán boundary layer integral equation

$$\frac{d\delta_2}{dx} + (2\delta_2 + \delta_1)\frac{1}{u_e}\frac{du_e}{dx} - \left(\frac{u_\tau}{u_e}\right)^2 = 0$$

The function $u_e(x)$ is the free stream velocity and the friction velocity is

$$u_\tau(x) \equiv \left(\frac{\tau_w}{\rho}\right)^{1/2}$$

The displacement thickness is defined as

$$\delta_1(x) = \int_0^\delta \left(1 - \frac{u}{u_e}\right) dy$$

The momentum thickness is

$$\delta_2(x) = \int_0^\delta \frac{u}{u_e}\left(1 - \frac{u}{u_e}\right) dy$$

Assume potential flow about a body in a free stream at a reference velocity U_∞.

$$U = \frac{u_e(x)}{U_\infty}$$

And a Reynolds number based on the distance x from the origin of the flow.

$$R_x = \frac{U_\infty x}{\nu}$$

STANFORD AERONAUTICS & ASTRONAUTICS

Express the Kármán equation in terms of displacement and momentum thickness Reynolds numbers

$$\frac{d\delta_2}{dx} + (2\delta_2 + \delta_1)\frac{1}{u_e}\frac{du_e}{dx} - \left(\frac{u_\tau}{u_e}\right)^2 = 0$$

$$\frac{d(\delta_2 u_e)}{dx} = u_e\frac{d\delta_2}{dx} + \delta_2\frac{du_e}{dx}$$

$$\frac{d(\delta_2 u_e)}{dx} + (\delta_2 + \delta_1)\frac{du_e}{dx} - u_e\left(\frac{u_\tau}{u_e}\right)^2 = 0$$

$$R_{\delta_1} = \frac{\delta_1 u_e}{\nu} \qquad R_{\delta_2} = \frac{\delta_2 u_e}{\nu} \qquad R_x = \frac{x u_\infty}{\nu} \qquad U = \frac{u_e}{U_\infty}$$

$$\frac{dR_{\delta_2}}{dR_x} + (R_{\delta_2} + R_{\delta_1})\frac{1}{U}\frac{dU}{dR_x} - U\left(\frac{u_\tau}{u_e}\right)^2 = 0$$

$$\frac{dR_{\delta_2}}{dR_x} = U\left(\frac{u_\tau}{u_e}\right)^2\left(1 - \frac{(R_{\delta_2} + R_{\delta_1})}{\left(\frac{u_\tau}{u_e}\right)^2}\frac{1}{U^2}\frac{dU}{dR_x}\right)$$

$$\frac{dR_\tau}{dR_x} = \frac{U}{dR_{\delta_2}/dR_\tau}\left(\frac{u_\tau}{u_e}\right)^2\left(1 - \frac{(R_{\delta_2} + R_{\delta_1})}{\left(\frac{u_\tau}{u_e}\right)^2}\frac{1}{U^2}\frac{dU}{dR_x}\right)$$

Define the following functions

The boundary layer friction law

$$\frac{u_e}{u_\tau} = \int_0^{R_\tau} \frac{2\left(1 - \frac{s}{R_\tau}\right)}{1 + \left(1 + 4\lambda^2\left(1 - \frac{s}{R_\tau}\right)\right)^{1/2}} ds \equiv F_0$$

Displacement thickness Reynolds number in wall units

$$R_{\delta_1} = \frac{u_e \delta_1}{\nu} = \frac{u_e}{u_\tau}\int_0^{R_\tau}\left(1 - \frac{u_\tau}{u_e}u^+\right) dy^+ \equiv F_1$$

Momentum thickness Reynolds number in wall units

$$R_{\delta_2} = \frac{u_e \delta_2}{\nu} = \int_0^{R_\tau} u^+\left(1 - \frac{u_\tau}{u_e}u^+\right) dy^+ \equiv F_2$$

Derivative of the momentum thickness Reynolds number in wall units

$$\frac{dF_2}{dR_\tau} \equiv F_3$$

STANFORD AERONAUTICS & ASTRONAUTICS

Express the Kármán equation as an equation for the friction Reynolds number as a function of streamwise Reynolds number.

$$\frac{dR_\tau}{dR_x} = \frac{U}{dR_{\delta_2}/dR_\tau}\left(\frac{u_\tau}{u_e}\right)^2\left(1 - \frac{(R_{\delta_2}+R_{\delta_1})}{\left(\frac{u_\tau}{u_e}\right)^2}\frac{1}{U^2}\frac{dU}{dR_x}\right)$$

$$\frac{dR_\tau}{dR_x} = \frac{U}{{F_0}^2 F_3}\left(1 - {F_0}^2(F_2+F_1)\frac{1}{U^2}\frac{dU}{dR_x}\right)$$

$$\frac{dF_2}{dR_\tau} \equiv F_3$$

The logical choice for the modified Clauser parameter is

$$\beta_c = -{F_0}^2(F_2+F_1)\frac{1}{U^2}\frac{dU}{dR_x}$$

STANFORD
AERONAUTICS &
ASTRONAUTICS

Deconstruct the modified Clauser parameter

$$\beta_c = -{F_0}^2(F_2 + F_1)\frac{1}{U^2}\frac{dU}{dR_x}$$

$$\beta_c = \left(\frac{u_e}{u_\tau}\right)^2 \frac{u_e}{\nu}\frac{U_\infty}{u_e}(\delta_2 + \delta_1)\frac{\nu}{U_\infty}\frac{1}{u_e}\frac{du_e}{dx}$$

$$\beta_c = \left(\frac{1}{u_\tau}\right)^2 (\delta_2 + \delta_1)u_e\frac{du_e}{dx}$$

$$\boxed{\beta_c = \rho\frac{(\delta_2 + \delta_1)}{\tau_w}\frac{dp_e}{dx}}$$

The usual definition is

$$\beta = \rho\frac{\delta_1}{\tau_w}\frac{dp_e}{dx}$$

STANFORD
AERONAUTICS &
ASTRONAUTICS

The boundary layer wake parameters b and n are approximately related through β_c

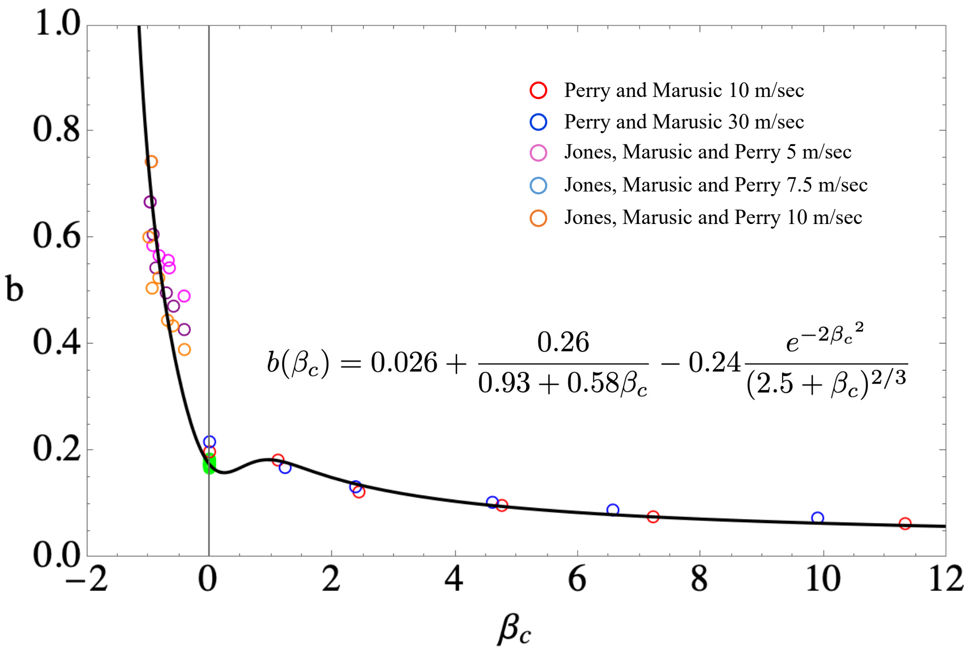

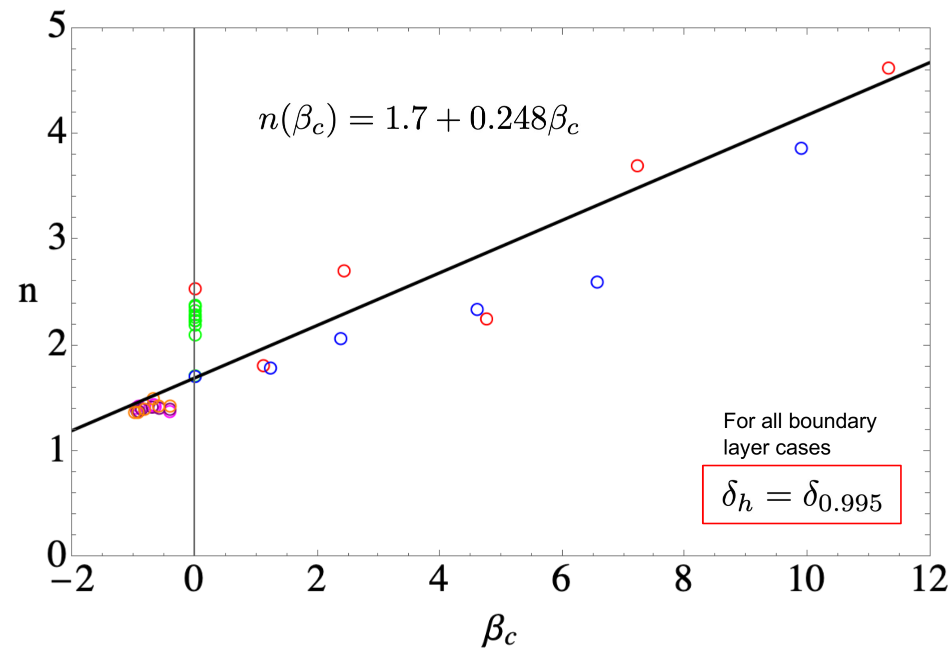

For $\beta_c = 0$, the parameter *b = 0.1760* which matches the correlation

For $\beta_c = 0$, the parameter *n = 2.217* which lies above the correlation

STANFORD
AERONAUTICS &
ASTRONAUTICS

High Reynolds number

Recall the UVP

$$u^+(y^+) = \int_0^{y^+} \left[\frac{2\left(1-\frac{s}{R_\tau}\right)}{1+\left(1+4\lambda^2\left(1-\frac{s}{R_\tau}\right)\right)^{1/2}} \right] ds$$

$$\lambda(k,a,b,n,R_\tau,y^+) = \frac{ky^+\left(1-\sigma(\frac{y^+}{a})\right)}{\left(1+\left(\frac{y^+}{bR_\tau}\right)^n\right)^{1/n}}$$

Carry out a scaling - Multiply and divide the damping and wake terms by *k*

Modified wall-wake mixing length function. The parameters *k* and *a* become one parameter *ka*.

$$\lambda(k,a,b,n,R_\tau,y^+) = \frac{ky^+\left(1-\sigma(\frac{y^+}{a})\right)}{\left(1+\left(\frac{y^+}{bR_\tau}\right)^n\right)^{1/n}} = \frac{ky^+\left(1-\sigma(\frac{ky^+}{ka})\right)}{\left(1+\left(\frac{ky^+}{bkR_\tau}\right)^n\right)^{1/n}} = \tilde{\lambda}(ka,b,n,kR_\tau,ky^+)$$

$y^+ \rightarrow ky^+$

$R_\tau \rightarrow kR_\tau$

Scaled velocity profile

$$ku^+(ka,b,n,kR_\tau,ky^+) = \int_0^{ky^+} \left[\frac{2\left(1-\frac{s}{kR_\tau}\right)}{1+\left(1+4\tilde{\lambda}^2\left(1-\frac{s}{kR_\tau}\right)\right)^{1/2}} \right] ds$$

$u/u_\tau \rightarrow ku/u_\tau$

STANFORD AERONAUTICS & ASTRONAUTICS

Define the shape function

$$\Phi(ka, b, n, kR_\tau, ky^+) = \int_0^{ky^+} \left[\frac{2\left(1 - \frac{s}{kR_\tau}\right)}{1 + \left(1 + 4\tilde{\lambda}^2\left(1 - \frac{s}{kR_\tau}\right)\right)^{1/2}} \right] ds - ln(ky^+)$$

where

$$\tilde{\lambda}(ka, b, n, kR_\tau, ky^+) = \frac{ky^+ \left(1 - \sigma(\frac{ky^+}{ka})\right)}{\left(1 + \left(\frac{ky^+}{bkR_\tau}\right)^n\right)^{1/n}}$$

Note

$$ky^+ = \left(\frac{y}{\delta_h}\right) kR_\tau$$

Plot Φ versus y/δ_h for various R_τ.

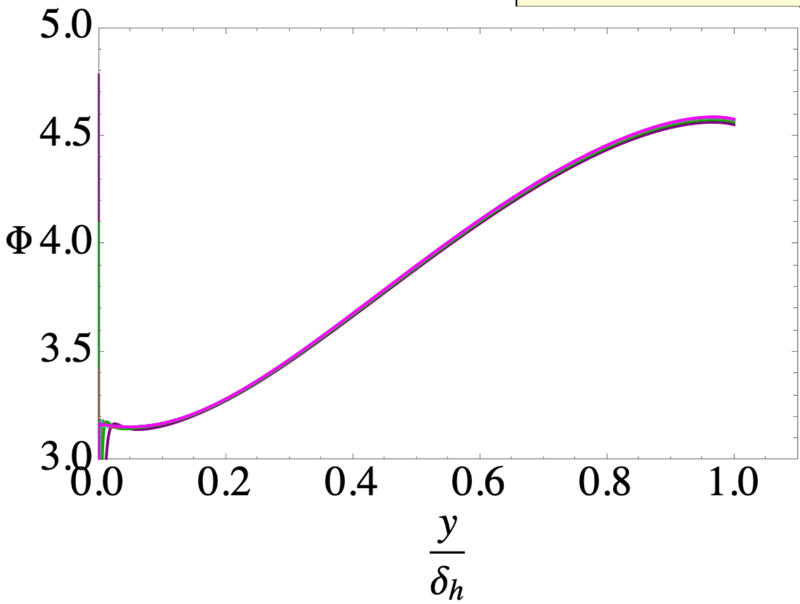

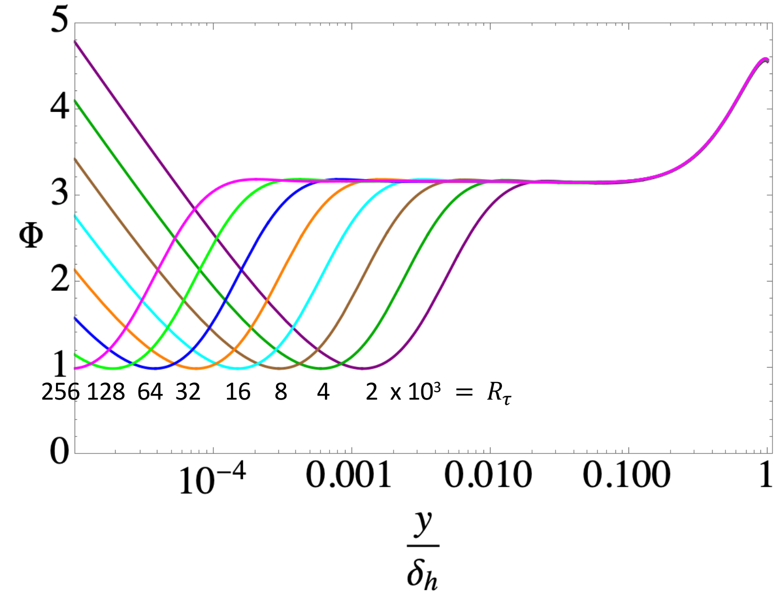

Above $kR_\tau \cong 2000,\ \Phi\ is\ independent\ of\ R_\tau$

$$\Phi(ka, b, n, kR_\tau, ky^+) = \phi(ka, b, n, \frac{y}{\delta_h})$$

For boundary layers, the wake parameters b and n are approximately related through β_c

$$\Phi(ka, b, n, kR_\tau, ky^+) = \phi(ka, \beta_c, \frac{y}{\delta_h})$$

ϕ versus y/δ_h for ZPGTBL, Pipe and Channel flow.

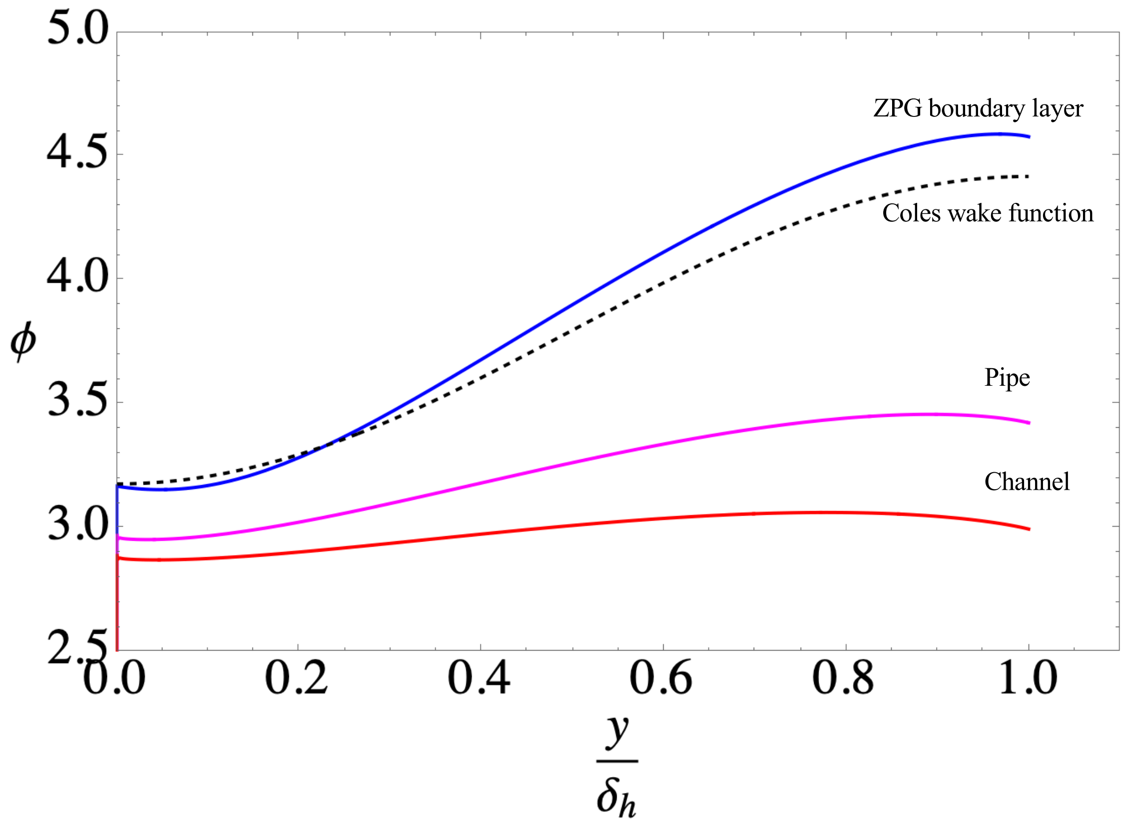

STANFORD AERONAUTICS & ASTRONAUTICS

Average parameters before and after the introduction of the new wall damping function

Flow	$\overline{k}$	σ_k	$\overline{a}$	σ_a	$\overline{m}$	σ_m	$\overline{b}$	σ_b	$\overline{n}$	σ_n
Pipe (21 profiles)	0.4092	0.0057	20.0950	0.381	1.6210	0.0379	0.3195	0.0157	1.6190	0.1204
Channel (7 profiles)	0.4086	0.0179	22.8673	1.599	1.2569	0.0292	0.4649	0.0485	1.3972	0.1213
ZPG Boundary Layer (11 profiles)	0.4233	0.0068	24.9583	0.663	1.1473	0.0373	0.1752	0.0060	2.1707	0.2238

Exponential damping

Flow	$\overline{k}$	σ_k	$\overline{a}$	σ_a	$\overline{m}$	σ_m	$\overline{b}$	σ_b	$\overline{n}$	σ_n
Pipe (21 profiles)	0.4082	0.0055	54.47	1.21	——	——	0.3315	0.0245	1.564	0.156
Channel (7 profiles)	0.3994	0.0030	53.56	1.53	——	——	0.4938	0.0406	1.414	0.095
ZPG Boundary Layer (11 profiles)	0.42050	0.00059	58.17	0.71	——	——	0.1760	0.0050	2.217	0.184

UWDF

Explicit high Reynolds number form of the UVP

$$u^+(k,a,b,n,R_\tau,y^+) = \int_0^{y^+} \left[\frac{2\left(1-\frac{s}{R_\tau}\right)}{1+\left(1+4\lambda^2\left(1-\frac{s}{R_\tau}\right)\right)^{1/2}} \right] ds$$

$0 < y^+ < R_\tau$

At Reynolds numbers larger than $kR_\tau \cong 2000$ the boundary layer velocity profile above $y^+ = 132$ is accurately approximated by

$$u^+ = \frac{1}{k} ln(ky^+) + \frac{1}{k}\phi\left(ka, b, n, \frac{y}{\delta_h}\right)$$

$y^+ > 132$

Evaluate at the boundary layer edge to determine the friction law.

$$u^+ = \frac{1}{k} ln(ky^+) + \frac{1}{k}\phi\left(ka, b, n, 1\right)$$

STANFORD AERONAUTICS & ASTRONAUTICS

The boundary layer shape function for various β_c

$$u^+ = \frac{1}{k} ln(ky^+) + \frac{1}{k}\phi\left(ka, \beta_c, \frac{y}{\delta_h}\right)$$

$y^+ > 132$
$kR_\tau > 2000$

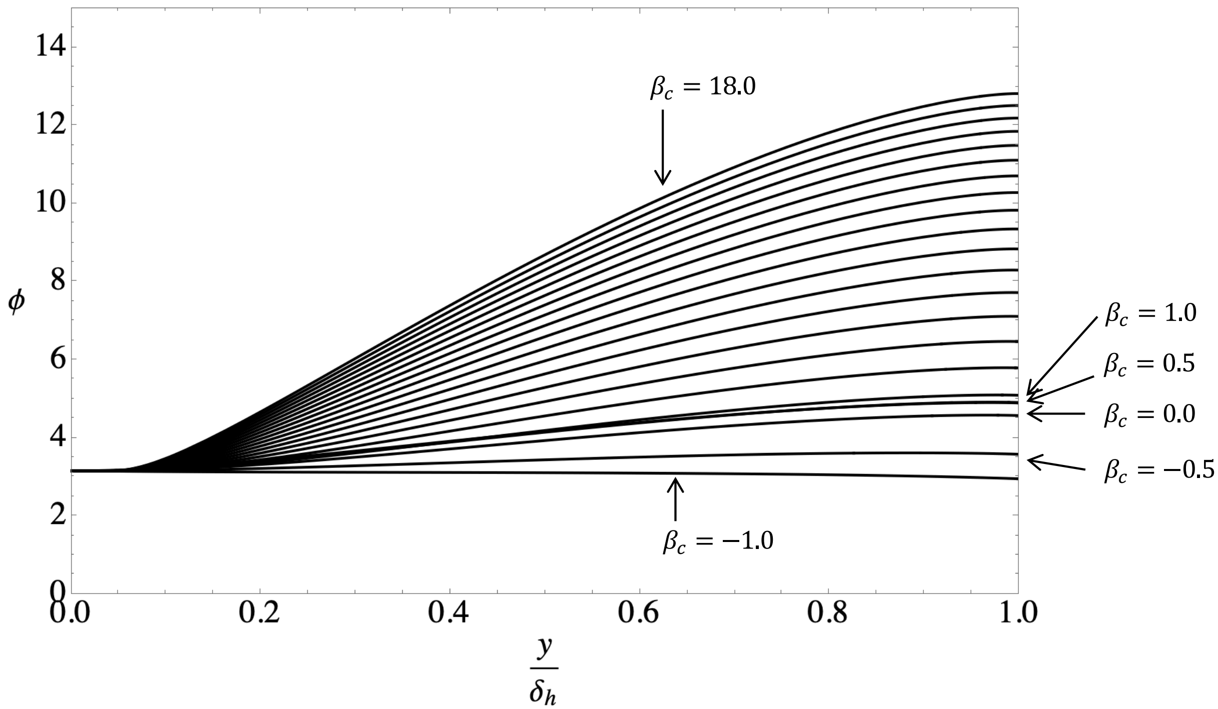

STANFORD
AERONAUTICS &
ASTRONAUTICS

The UVP can be used to create a new integral method for solving the von Kármán boundary layer integral equation

Viscous drag coefficient of the J0012 and NACA0012 airfoils

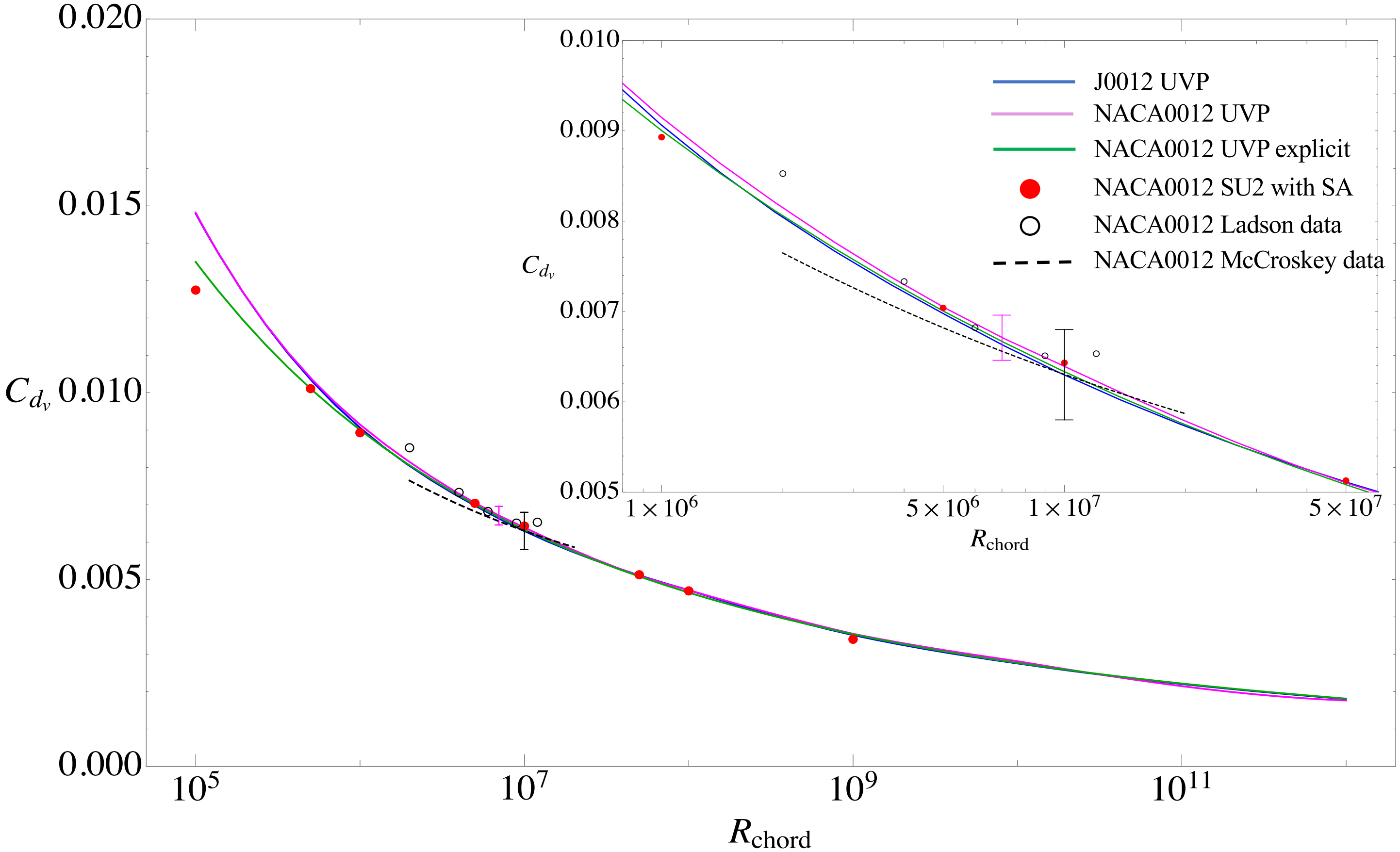

STANFORD
AERONAUTICS &
ASTRONAUTICS

The UVP can be applied to rough-wall pipe flow

STANFORD
AERONAUTICS & ASTRONAUTICS

Rough-wall pipe velocity profile

$$u_r^+(R_\tau, h^+, y^+) = u^+(R_\tau, y^+) - \Delta u_r^+(h^+)$$

Where $u^+(R_\tau, y^+)$ is the smooth-wall UVP.

The Clauser roughness velocity is

$$\Delta u_r^+(h^+) = \frac{1}{k} f(h^+) ln(1 + \alpha h^+)$$

Roughness height Reynolds number, roughness fraction

$$h^+ = \frac{h_s u_\tau}{\nu} \qquad \varepsilon = \frac{h_s}{R} = \frac{h^+}{R_\tau}$$

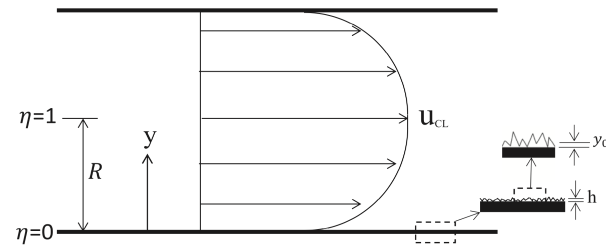

FIG. 1. Rough-wall pipe flow with nomenclature.

The roughness fraction of the smooth-wall Princeton Super Pipe is $\varepsilon = 6.96 \times 10^{-6}$.
At the highest PSP Reynolds number, h+ = 3.69 indicating that the entire data set is hydraulically smooth except possibly for a very small effect at the highest Reynolds number.

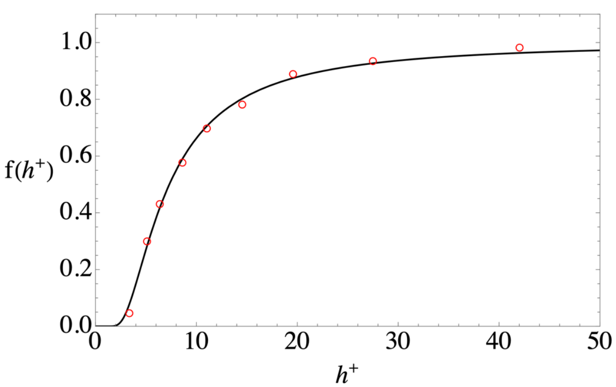

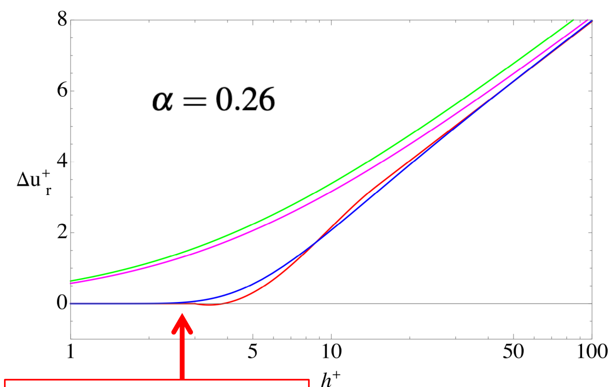

There is no roughness effect on pipe friction below h+ = 3.5

Comparison of UVP roughness function (blue) with other commonly used functions: Nikuradse (red), White (green) and Grigson (magenta).

STANFORD AERONAUTICS & ASTRONAUTICS

UVP fit to Rough-wall Princeton Super Pipe experimental data, $R_\tau = 28800\ to\ 361000$

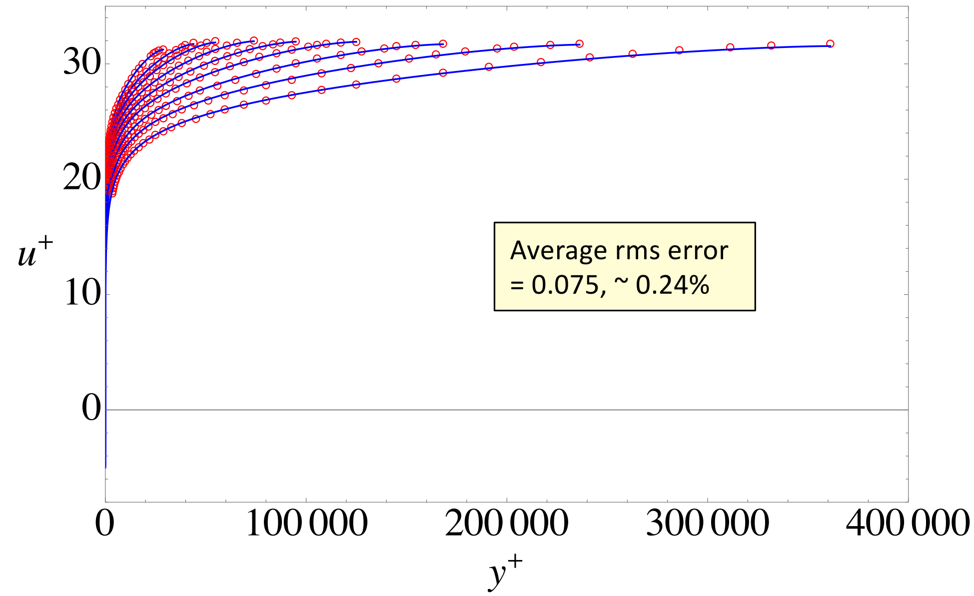

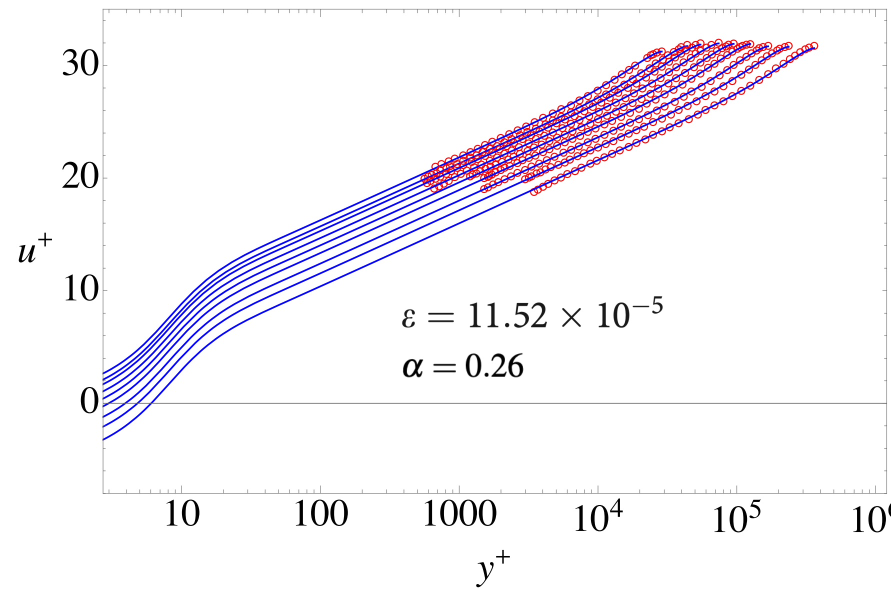

TABLE I. Average model parameters with standard deviation for basic wall flows. Ranges of R_τ for each flow are as follows: Pipe (3327–530 023), Channel (550–8016), ZPG boundary layer (1343–17 207).

Flow	$\bar{k}$	σ_k	$\bar{a}$	σ_a	$\bar{m}$	σ_m	$\bar{b}$	σ_b	$\bar{n}$	σ_n
Pipe (21 profiles)	0.4092	0.0057	20.0950	0.381	1.6210	0.0379	0.3195	0.0157	1.6190	0.1204
Channel (7 profiles)	0.4086	0.0179	22.8673	1.599	1.2569	0.0292	0.4649	0.0485	1.3972	0.1213
ZPG boundary layer (11 profiles)	0.4233	0.0068	24.9583	0.663	1.1473	0.0373	0.1752	0.0060	2.1707	0.2238

Revised pipe flow Moody diagram

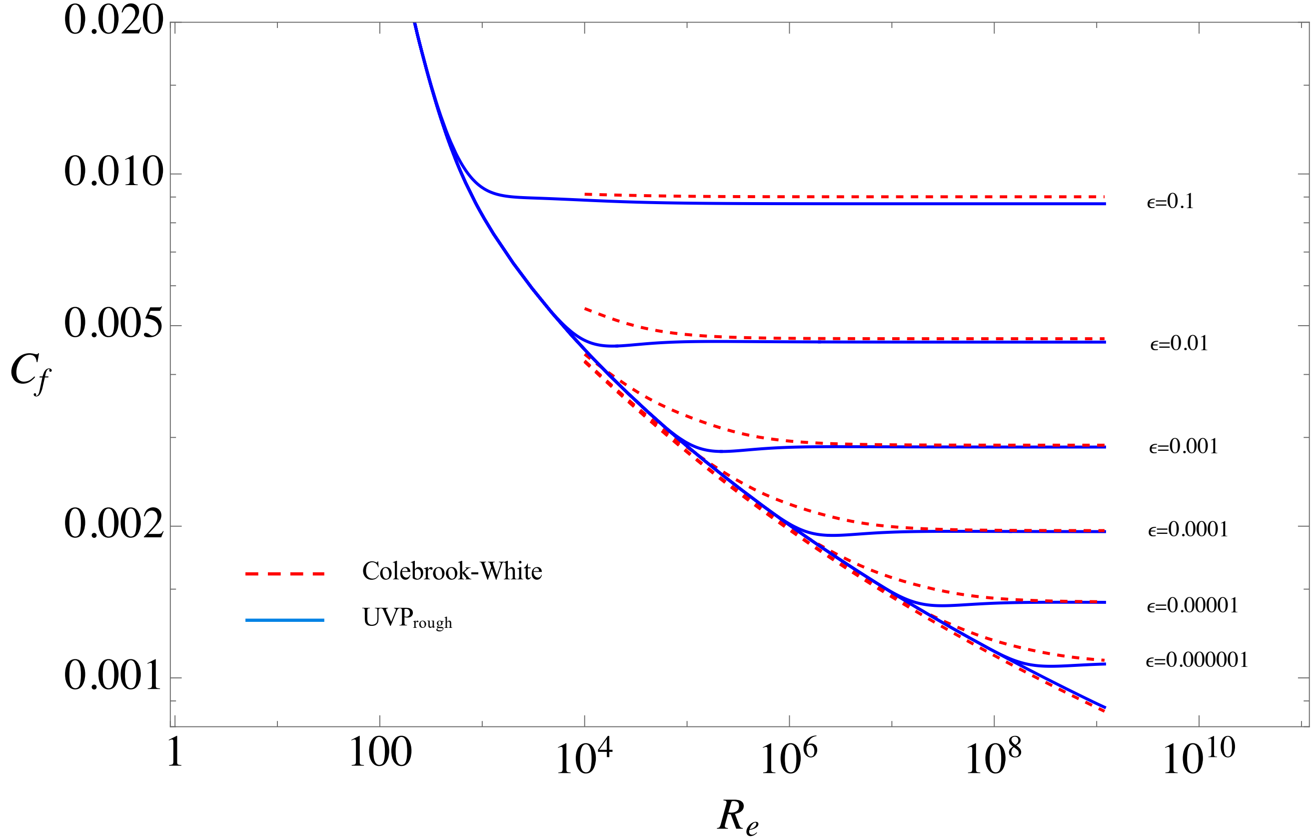

STANFORD
AERONAUTICS & ASTRONAUTICS

Conclusions

1)The UVP provides a useful replacement of the classical wall-wake profile and can be applied to a wide range of wall-bounded flows. The profile is uniformly valid from the wall to the free stream at all Reynolds numbers.

2) At Reynolds numbers larger than $kR_\tau \cong 2000$, above the buffer layer (about y+ = 132), the UVP accurately approximates an explicit form.

$$u^+ = \frac{1}{k} ln(ky^+) + \frac{1}{k}\phi\left(ka, \beta_c, \frac{y}{\delta_h}\right)$$

3) The inherent dependence of the UVP on Reynolds number, extended to include the effect of pressure gradient, enables it to be used as the basis of a new method for integrating the Karman equation for a wide variety of attached, wall bounded flows.

4) The minimization process is not convex. Alternate values of the model parameters, particularly k and a can lead to the same degree of accuracy. This is the case at low and moderate Reynolds numbers but at high Reynolds numbers alternate minima appear to be close together.

5) Over the past year, a new wall damping function has been derived for the UVP that improves the agreement with data while reducing the number of parameters in the UVP model from 5 to 4 for pipes and channels and from 4 to 3 for boundary layers. The variation in optimal model parameter values from case to case is reduced, especially for boundary layer flows.

6) The Kármán constant, k, and the wall length scale, a, cannot be thought of as independent parameters. They act together through the product, *ka*, that appears in the shape function. If ka is fixed, then changing the Karman constant applies a pure scaling to the velocity.

STANFORD
AERONAUTICS &
ASTRONAUTICS

Main References

Coles, D.E. 1956 The law of the wake in the turbulent boundary layer. *J. Fluid Mech.* 1 (2), 191–226.

Prandtl, L. 1934 *Aerodynamic Theory* (ed. W. F. Durand), vol III, chap. 21, p. 134. Julius Springer.

Cantwell, B.J. 2019 A universal velocity profile for smooth wall pipe flow. *J. Fluid Mech.* 878, 834–874.

Spalding, B.D. 1961 A single formula for the 'law of the wall'. *Trans. ASME J. Appl. Mech.* 0, 455–458.

Cantwell, B.J. 2021 Integral measures of the zero pressure gradient boundary layer over the Reynolds number range $0 \leq R_\tau < \infty$. *Phys. Fluids* 33, 085108.

M. A. Subrahmanyam, B. J. Cantwell, and J. J. Alonso, "A universal velocity profile for turbulent wall flows including adverse pressure gradient boundary layers,"JFM. 933, A16 (2022).

She, Z.-S., Chen X. & Hussain, F. 2017 Quantifying wall turbulence via a symmetry approach: a lie group theory. *J. Fluid Mech.* 827, 322–356.

Chen, X., Hussain, F. & She, Z. 2018 Quantifying wall turbulence via a symmetry approach. Part 2. Reynolds stresses. *J. Fluid Mech.* 405, 401–438.

Chen, X. &Sreenivasen, K.R. 2021 Reynolds number scaling of the peak turbulence intensity in wall flows. *J. Fluid Mech.* 908, R3.

van Driest, E.R. 1956 On turbulent flow near a wall. *J. Aeronaut. Sci.* 23 (11), 1007–1011.

Ramis, G.E.-A.Ö. & Schlatter, P. 2014 Simulation and validation of a spatially evolving turbulent boundary layer up to *Re* = 8300. *Intl J. Heat Fluid Flow* 47, 57–69.

Sillero, J.A., Jimenez, J. & Moser, R.D. 2013 One-point statistics for turbulent wall-bounded flows at Reynolds numbers up to $\delta^+ = 2000$. *Phys. Fluids* 25 (10), 105102.

Simens, M.P., Jimenez, J., Hoyas, S. & Mizuno, Y. 2009 A high-resolution code for turbulent boundary layers. *J. Comput. Phys.* 228 (11), 4218–4231.

Vinuesa, R., Bobke, A., Örlu, R. & Schlatter, P. 2016 On determining characteristic length scales in pressure-gradient turbulent boundary layers. *Phys. Fluids* 28, 055101.

Yamamoto, Y. & Tsuji, Y. 2018 Numerical evidence of logarithmic regions in channel flow at $R_\tau = 8000$. *Phys. Rev. Fluids* 3, 012602.

Zagarola, M.V. 1996 Mean-flow scaling of turbulent pipe flow. Doctoral dissertation, Princeton University.

Zagarola, M.V. & Smits, A.J. 1998 Mean-flow scaling of turbulent pipe flow. *J. Fluid Mech.* 373, 33–79.

McKeon, B.J. 2003 High Reynolds number turbulent pipe flow. Doctoral dissertation, Princeton University.

McKeon, B. J., Li, J., Jiang, W., Morrison, J. F. & Smits, A. J. 2003 Pitot probe corrections in fully developed turbulent pipe flow. *Meas. Sci. Technol.* 14, 1449–1458.

R. Baidya, J. Phillip, N. Hutchins, J. P. Monty, and I. Marusic, "Distance from the wall scaling of turbulent motions in wall-bounded flows," Phys. Fluids 29, 020712 (2017).

A. E. Perry and I. Marusic, "A wall-wake model for the turbulence structure of boundary layers. Part 2. Further experimental support," J. Fluid Mech. 298, 361–407 (1995).

M. Jones, I. Marusic, and A. E. Perry, "Evolution and structure of sink-flow turbulent boundary layers," J. Fluid Mech. 428, 1–27 (2001).

STANFORD
AERONAUTICS &
ASTRONAUTICS